UNIVERSITÀ DI PARMA

UNIVERSITA' DEGLI STUDI DI PARMA

"Scienze del Farmaco, delle Biomolecole e dei Prodotti per la Salute"

CICLO XXXII

Protein therapeutics for clinical applications: Hemoglobin-based oxygen carriers and modulation of their oxygen-binding properties

Coordinator: Chair.mo Prof. Marco Mor

Tutor: Chair.mo Prof. Stefano Bruno

Dottoranda: Esra'a Ali Mohammad Alomari

Anni 2016-2019

Index

Summary

Protein therapeutics are proteins used as drugs, purified from natural sources or produced recombinantly – either in the wild-type form or as non-natural mutants. The history of protein therapeutics started in 1922 with the purification of insulin from dog pancreases. Insulin preparations from animal tissues were later used for the treatment of diabetes mellitus, but they were initially very costly, their supply was limited by tissue availability, and immunological reactions were recorded in many patients. More recently, the recombinant DNA techniques have opened up a new era in drug discovery and development. In the last decade alone, the U.S. Food and Drug Administration has approved more than 65 protein therapeutics for different indications, covering around 150 diseases (Frokjaer & Otzen, 2005).

Several potential problems had to be addressed over time to use proteins as therapeutics. In the beginning, proteins were obtained from human or animal natural sources. In a few cases, the natural source is still the first choice, particularly when the endogenous protein is naturally produced at high concentrations. Serum albumin and several clotting factors, for example, are still purified from human plasma. For proteins that are endogenously produced at low concentrations, the advances in molecular biology proved crucial, allowing the expression of virtually all proteins in host organisms where they are not naturally produced. To obtain high yields in these recombinant systems, host organisms, expression vectors, and fermentation protocols had to be optimized.

Another issue associated with protein therapeutics in comparison to small-molecule drugs is their potential instability. Indeed, many factors, such as pH, temperature, solubility, and storage conditions can impact their conformation, which is strictly associated to their bioactivity. Indeed, unlike small-molecule drugs, proteins can lose their pharmacological activity even if they retain their chemical integrity. Therefore, activity needs to be checked at every step of the formulation to make sure that denaturation has not occurred.

A further issue regarding protein therapeutics is their half-life in vivo. Once proteins have been administered, they can undergo rapid degradation by endogenous proteases or rapid excretion by the kidneys. Protein engineering and chemical modifications have both been used to tackle this potential problem.

In my Ph.D. work, I focused on two groups of protein therapeutics for which the aforementioned issues were tackled:

1) Hemoglobin-based oxygen carriers (Part I) are a group of genetically or chemically modified derivatives of hemoglobin used to provide oxygen in various therapeutic applications. Chapter 1 will offer an introduction to the field, focusing on the modulation of their oxygen-binding properties; Chapter 2 will deal with the production of two chemically modified human hemoglobins endowed with different oxygen affinity and their experimentation in a Guinea Pig model; Chapter 3 will focus on engineered fetal hemoglobin derivatives in which both genetic

and chemical modifications have been introduced to improve the properties of the product; in chapter 4, the preparation of an acellular perfusion solution for organs is described.

2) Alpha 1-antitrypsin (Part II) is a serpin used as an irreversible inhibitor of trypsin in the treatment of some genetic conditions. For this work, the goal was i) to produce the protein in high yields using a fermentation system; ii) to formulate the protein as powder for nasal administration; iii) to improve the half-life of the protein through a chemical modification (PEGylation), and iv) to evaluate protein stability and activity at all steps of the formulation process.

Part I: Hemoglobin-based oxygen carriers

Chapter 1: Introduction

1.1 Hemoglobin-based oxygen carriers

Several biotechnological products collectively known as oxygen carriers have been developed over the years to address the clinical needs not currently met by transfusions with donated red blood cells. Indeed, blood transfusions pose several problems, including shortages of blood, the risk of bloodborne diseases, and the high costs associated with storage (Dolgin, 2017).

Most oxygen carriers take advantage of hemoglobins (Hbs), the proteins that naturally evolved to transport oxygen, and that can be chemically or genetically modified to produce HBOCs. These HBOCs are known as hemoglobin-based oxygen carriers (HBOCs) (2011; Bobofchak et al, 2003; Inayat et al, 2006; Jahr et al, 2012; Kocian & Spahn, 2008; Meng et al, 2018; Mozzarelli et al, 2010; Winslow, 2006).

The first attempts at administering acellular Hb – a natural candidate as a substitute for red blood cells (RBCs) – resulted in serious side effects, mainly on the kidneys and on the cardiovascular system (Cardenas et al, 2017). It is now known that these effects are associated with the significantly different conditions that acellular Hb is exposed to in the plasma in comparison to that inside RBCs, particularly in terms of i) concentration, which is high inside RBC and low in plasma, where tetramer dissociation can occur; ii) pH, which affects the oxygen-binding properties through the Bohr effect iii) presence and concentration of allosteric effectors and iv) presence and concentration of reducing

agents. These differences alter several biochemical properties of acellular Hb, particularly with respect to tetramer stability, oxygen binding properties, and redox state. Therefore, the non-natural plasma environment can prevent HBOCs from efficiently distributing oxygen from the lungs to the tissues.

The first HBOCs were designed to closely mimic human Hb A (HbA) inside RBCs in terms of oxygen binding properties. Subsequently, a wider range of products has been made available, with oxygen affinities ranging from that of free dimers and quaternary R-state Hb (around 1 torr in p50) to that of Hb complexed with allosteric effectors (around 26 torr). However, all of these products have performed poorly in clinical trials, with several toxic effects (Estep et al, 2008; Natanson et al, 2008; Simons et al, 2018), calling for a more in-depth definition of the relationship between oxygen binding properties, redox properties, and toxicity.

1.2 Hemoglobin as oxygen carriers, regulation, and reactivity

HbA constitutes around 97% of the protein content of human RBCs and is one of the most abundant proteins expressed overall in the human body, with around 750 g in circulation at any given time. HbA at normal concentrations increases the solubility of oxygen by about 70-fold in comparison to plasma alone.

The oxygen-binding properties of Hb are mainly associated with the heme group bound at each subunit of Hb, a tetramer consisting of two $\alpha\beta$ dimers - with α and β being homologous - in a $\alpha_2\beta_2$ stoichiometry. The heme iron - stabilized in the ferrous form by the heme-binding pocket - is

coordinated by the four porphyrin nitrogen atoms of the protophorphyrine IX ring and by a histidine residue known as proximal histidine (Perutz, 1970). On the distal side, the free coordination position can be occupied by molecular oxygen:

$$\text{Heme-Fe(II)} + O_2 \leftrightarrows \text{Heme-Fe(II)-}O_2$$

The oxygen dissociation curves of HbA exhibit a typical sigmoidal shape, as represented in Figure 1.1, indicating a cooperative binding.

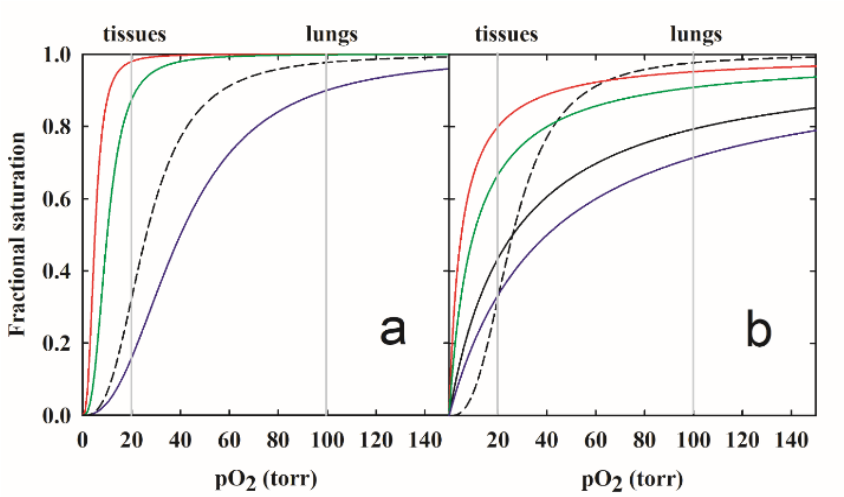

Figure 1.1: (a) Oxygen binding curve of human RBCs at physiological pH (7.4) and temperature (37 °C), with a p50 of 26 mmHg and a Hill coefficient of 2.8 (dash line); simulation of the oxygen-binding curves for HBOCs endowed with a p50 of 5 (red line), 10 (green line) and 40 mmHg (blue line) and normal cooperativity (n=2.8). The typical pO_2 of lungs and peripheral tissues are indicated (gray), **(b)** Oxygen binding curve of human RBCs at physiological pH (7.4) and temperature (37°C), with a the p50 of 26 mmHg and Hill n=2.8 (dash line); simulation of the oxygen-binding curves for HBOCs endowed with a p50 of 5 (red line), 10 (green line) and 40 mmHg (blue line) and no cooperativity (n=1). The typical pO_2 of lungs and peripheral tissues are indicated (gray).

The affinity for oxygen is normally expressed as p50, i.e. the oxygen partial pressure at which half of the heme sites are occupied by oxygen. Inside RBC, at physiological pH (7.4) and 37 °C, the p50 is around 26 mmHg (Antonini & Brunori, 1971).

The oxygen binding curves can be analyzed using the Hill equation:

$$log\frac{Y}{1-Y} = n \cdot log\left(\frac{pO2}{p50}\right)$$

The Hill coefficient (n), provides an indication of the cooperativity. The Hill coeffcient of human RBC ranges between 2.8 and 3. In Figure 1.1, simulations of oxygen off-loading for HBOCs different p50 and n are reported.

From a functional point of view, cooperativity optimizes oxygen release in the pO_2 range between 100 mmHg and 20 mmHg, at which Hb is 97% and 30% saturated, respectively. Myoglobin, a non-cooperative oxygen-binding protein, would be equally saturated in the lungs, but it would unload only 5% of oxygen in the peripheral tissues as its affinity remains high at low oxygen partial pressures.

From a structural point of view, cooperativity is associated to a conformational equilibrium between at least two forms endowed with different oxygen affinity, the T and the R states (Eaton et al, 1999). The equilibrium between these conformations depends on oxygen occupancy, which, in turn, depends on the oxygen partial pressure to which Hb is exposed (pO_2). The conformations of the T and R states, as

well as the transition between the T and R state upon oxygen binding, has been described in molecular details: oxygen binding to the heme on the distal side pulls the iron into the plane of the porphyrin ring (Perutz, 1970), resulting in the F helix and FG corner of the first monomer binding oxygen (usually a α subunit) to move closer to the opposite subunit. The overall allosteric transition results in the rotation and translation of the $\alpha_1\alpha_1$ dimer by ~14° and ~1 Å relative to the $\beta_2\beta_2$ dimer (Baldwin & Chothia, 1979).

1.2.1 In vivo effectors that regulate oxygen affinity in red blood cells

Inside RBCs, hemoglobin binds to several allosteric effectors at sites other than heme. These bonds result in a modulation of the equilibrium between the T and R states, significantly affecting oxygen affinity. The stabilization of the relaxed state shifts the oxygen equilibrium curve to the left, resulting in a high-affinity Hb conformation. A shift of the equilibrium toward the T state results in the stabilization of the low-affinity conformation. These effectors, particularly organic phosphates, are not present in plasma.

The most relevant allosteric effector of mammalian RBC is 2,3-bisphosphoglycerate (2,3-DPG), which binds Hb in a 1:1 stoichiometry. The compound was reported in 1967 by Reinhold (Benesch & Benesch, 1967) and its mechanism was elucidated by Arnone (Arnone, 1972). The structure of the complex between deoxygenated Hb and 2,3-DPG shows that it binds at the β-cleft through ionic bonds, linking the two β-subunits together, and, therefore, hindering the T-R transition. Overall, the

preferential binding of 2,3-DPG to deoxygenated Hb stabilizes the T state in comparison to the R state, producing an increase in overall p50 from 12 to 26 mmHg at physiological temperature, carbon dioxide concentration, and pH. The lack of 2,3-DPG not only alters the oxygen-binding properties of acellular HBOCs, but also those of RBCs, which, when stored, experience a decrease in p50 due to the depletion of 2,3-DPG. However, upon transfusion, their metabolism recovers and 2,3-DPG production resumes – with the recovery of the original p50 in about three days (Scott et al, 2016).

Carbon dioxide is anther allosteric effector inside RBCs, in which the carbonic anhydrase is particularly active and catalyzes the conversion of carbonate to carbon dioxide. CO_2 reacts with the N-terminal amino groups of the chains of Hb to form carbaminoHb:

$$R\text{-}NH + CO_2 \leftrightarrows R\text{-}NH\text{-}CO_2^- + H^+$$

The newly formed negative charge forms intersubunit salt bridges that stabilize the T state, thus contributing to the release of more oxygen to the venous blood, where CO_2 if formed. The increase in O_2 affinity at decreasing pH values in the range 6-9 is known as alkaline Bohr effect and is considered physiologically relevant as it favors O_2 unloading in venous blood, where the pH is slightly lower with respect to oxygenated blood (7.2 vs 7.4). From a structural point of view, the alkaline Bohr effect is associated with the protonation\deprotonation of several amino acid residues, particularly histidine residues β146 and α122. Overall, the

decrease in pH and the direct allosteric effect of CO_2 are synergistically responsible for a marked increase in oxygen off-loading in the venous system. As carbonic anhydrase is only intracellular and pH is also modulated by the metabolism of RBCs, acellular Hb and HBOCs oxygen affinities are not fine-tuned at the capillary level by these allosteric effectors in the same way as intracellular Hb. A crosslinked covalent polymer containing polyHb, superoxide dismutase, catalase, and carbonic anhydrase was prepared to confer HBOCs the capability to process carbon dioxide. The conjugation of the antioxidant enzymes with polyHb proved an effective therapeutic agent in several conditions where their concentration within RBCs are not high enough, as in ischemia-reperfusion injuries (Bian et al, 2011).

As acellular Hb tend to exhibit high affinities due to the lack of allosteric effectors in plasma and because of tetramer dissociation when diluted, HBOCs might not be capable to efficiently transport oxygen from the lungs to peripheral tissues, with only a small amount of oxygen being unloaded. Figure 1.1 reports simulated oxygen binding curves to HBOCs endowed with different theoretical p50 and Hill's coefficients in the ranges described in the literature.

1.2.2 Tetramer-dimer equilibrium

Oxygen affinity and cooperativity significantly depend on the integrity of the Hb tetramer. Indeed, Hb tetramers can be described as αβ heterodimers capable of forming $(\alpha\beta)_2$ tetramers, the prevalent form at physiological Hb concentration inside RBCs (around 5 mM). However, at

when Hb concentrations reaches the low micromolar range, the tetramer dissociation becomes significant

$$\alpha_2 \beta_2 \leftrightarrows 2\alpha\beta$$

The dissociation constant of the equilibrium (K_D=[dimer]^2/[tetramer]) is much higher in the R state of Hb in comparison to the T state. Depending on the individual HBOC and its protocols of administration, the final HBOC concentration in plasma reaches levels where tetramer dissociation is significant. Chemical modifications to obtain HBOCs can further promote tetramer dissociation (Caccia et al, 2009). In these cases, dimeric Hb or dimeric HBOCs usually exhibit low p50s (1-5 mmHg) and completely lose cooperativity, regardless of the chemical modifications (Caccia et al, 2009).

Dimeric hemoglobin binds haptoglobin to form a complex exposed to macrophage scavenging and endocytosis. Moreover, dimeric Hb is filtered by kidneys and excreted in the urine. As a result of excess Hb dimers filtered, severe nephrotoxicity occurs in pathological anemic conditions where hemoglobin is released in the plasma, or upon administration of Hb for experimental purposes (Alayash, 2011).

1.2.3 Reactivity of the heme group

The center heme prosthetic group presented within Hb is reactive with many molecules, producing uncontrollable reactions outside the RBCs, where they are kept under control or reversed by a complex

enzymatic system and by small-molecule reducing agents. The heme iron tends to undergo oxidation to form ferric ions, which triggers the formation of reactive oxygen species (ROS) and nitrogen species (NOS) involved in oxidative stress (Buehler & Alayash, 2004; Rifkind et al, 2014).

In plasma, acellular Hb spontaneously autoxidizes, as the antioxidant protective enzymes which reverse oxidation in RBCs are not present, generating methemoglobin and superoxide ions. These species promote oxidative stress, leading to deleterious effects on DNA, proteins, and lipids (Cardenas et al, 2017).

Hb also binds nitric oxide (NO) and, in the presence of oxygen, is oxidized to met-Hb. This reaction is relevant from a toxicological point of view, as both free hemoglobin and HBOCs tend to scavenge NO, leading to vasoconstriction due to NO depletion (Cardenas et al, 2017).

1.3 Are RBCs-like affinities necessary for therapeutic efficacy?

The first HBOCs were originally designed to act as "blood substitutes", and were intended to exhibit similar behavior as RBCs in terms of oxygen-binding properties. More recently, HBOCs are seen as "oxygen therapeutics" and are intended to be used in an emergency. It is still debated whether HBOCs need to have the same functional properties as RBCs, especially in terms of oxygen affinity. Particularly, high-affinity HBOCs have been suggested for the oxygenation of severely hypoxic tissues (Belcher et al, 2018; Mozzarelli et al, 2010), and for the treatment of sickle cell disease (Keipert, 2016; Nugent et al, 2019). Moreover, HBOCs can be used to increase tissue oxygenation in solid tumors – which are

highly hypoxic - to improve sensitivity to radiations (Belcher et al, 2018), and for the reperfusion of organs (Aburawi et al, 2019; Ferenz & Steinbicker, 2019; Laing et al, 2017). Some applications of high-affinity HBOCs as plasma expanders seem to be altogether independent of the capability to bind oxygen (Olofsson et al, 2008; Smani, 2008; Wang et al, 2017). Nevertheless, the modulation of the oxygen-binding properties is still an attractive prospect for the design of HBOCs, in view of designing different products for different clinical needs.

1.4 Strategies to modify Hb

Different strategies have been explored to chemically modify HBOCs, to obtain products endowed with different oxygen-binding properties, differently sensitive to allosteric effectors, and with different autoxidation rates. The first generations of chemically modified HBOCs were based on non-specific modifications, mostly obtained through cross-linking chemistries to stabilize tetramers (Alayash et al, 2007). Most of these products had undesirable properties, such as a very low oxygen binding, a higher rate of auto-oxidation and marked NO scavenging activity (Alayash, 2019). Hb polymerization and PEGylation chemistry have been introduced to produce more homogeneous products.

1.4.1 PEGylated HBOCs and affinity modulation

PEGylated HBOCS take advantage of the well-established use of polyethylene glycol (PEG) for the decoration of protein therapeutics (Roberts et al, 2002), particularly to increase their half-life. Indeed, PEG

creates a shell around the protein molecules, hindering the proteolytic action of proteases, masking proteins from antibodies and preventing receptor-mediated cellular uptake. Moreover, PEG-protein conjugation increases the hydrodynamic volume of the protein complex, which is much greater than the simple sum of the molecular weights (MWs) of the components. For example, hemoglobin (MW of 64000 Da) conjugated with 6 PEG molecules of MW 5000 Da each exhibits a hydrodynamic volume comparable to a molecule of 130000 Da, whereas the actual MW is about 94000 Da. As a result, PEGylated proteins undergo limited extravasation and renal ultrafiltration. Because of their high colloid osmotic pressure, PEGylated HBOCs can act as plasma expanders (Olofsson et al, 2008; Smani, 2008).

PEGylated HBOCs, depending on the chemistry of conjugation and on the residues involved in the reaction, are endowed with significantly different properties, particularly with respect to oxygen binding. Several groups have worked on the production of stable PEG-Hb derivatives suitable for the delivery in the circulation as oxygen therapeutics, particularly Acharya and coworkers (Li et al, 2006; Manjula et al, 2000; Manjula et al, 2005), Winslow and coworkers (Winslow, 2004; Young et al, 2005), Perrella and coworkers (Caccia et al, 2009; Iafelice et al, 2007; Portoro et al, 2008), and Kluger and coworkers (Lui et al, 2008; Lui & Kluger, 2009). Particularly, the investigation of PEGylation chemistry on Hb has led to identification of residues that are hotspots for the allosteric transition of Hb. Figure 1.2 represents some residues shown to be involved in the PEGylation of human Hb, the modification of which

produced different outcomes in terms of oxygen-binding properties.

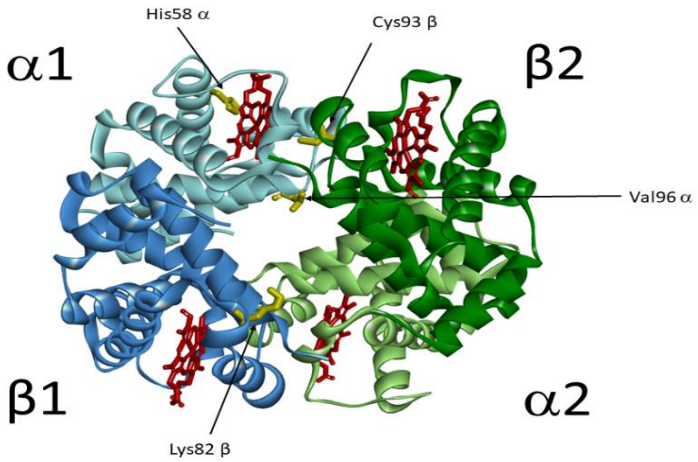

Figure 2.1: Structure of HbA (PDB: 1GZX). The residues that proved crucial to modulate oxygen affinity are indicated.

The experimental conditions of the PEGylation reaction and the conformational structure of Hb at the time of the reaction strongly affect the oxygen-binding affinity and cooperativity of the HBOCs. For example, the PEGylation of HbA can give different HBOCs endowed with different oxygen-binding properties depending on the presence of oxygen. PEGylation of HbA under aerobic conditions yields high-affinity products, such as MP4 and PEG-Hb^{oxy} (Portoro et al, 2008, Vandegriff et al, 2003). These products have a p50 close to R-state Hb (p50 5-6 mmHg) with abolished cooperativity. If the PEGylation is carried out under anaerobic conditions, or in the presence of inositol hypophosphate, which stabilizes the T state, low-affinity products are obtained. An example is PEG-Hb^{deoxy} (p50= 14.13 ± 0.36 mmHg) with partial cooperativity (n= 1.32 ± 0.06)

(Caccia et al, 2009).

1.4.2 Polymerized HBOCs and their affinity modulation

The need to increase the size of HbA to reduce extravasation and renal filtration was also tackled by polymerizing HbA with bifunctional reagents, particularly glutaraldehyde. Glutaraldehyde reacts reversibly with Hb lysine residues, forming carbinolamines, unstable products that react to produce a more stable imine (Schiff's base). At the end of the chemical reaction, the product must be stabilized by reducing the imine to an amine. Sodium borohydride was used in this respect (Gasthuys et al, 2005; Habeeb & Hiramoto, 1968; Lopez-Gallego et al, 2005). The final solution of glutaraldehyde-polymerized HBOCs contains a heterogeneous mixture in terms of size.

A product called PolyHeme was developed by Northfield laboratories (Evanston, Illinois, USA) and consisted of human Hb polymerized with glutaraldehyde and then pyridoxylated to decrease the oxygen affinity, with a p50 that resulted to be 28-30 mmHg under physiological conditions (Gould et al, 1998). The product has an average molecular weight of 150 kDa, ranging from 64 to 400 kDa. It was discontinued in 2009 following evidence that it elicited significant hypertension *in vivo*. These disappointing results called for the investigation of the modulation of the oxygen-binding properties of polymerized Hbs. As for PEGylated HbA, the conditions of the reaction, as well as the ligation state of HbA, were investigated as possible variables (Zhang et al, 2011). It was shown that polymerization of T state HbA yielded an HBOC endowed with high p50,

which further increased when glutaraldehyde was increased from a 40:1 ratio (37 mmHg) to a 50:1 ratio (48.8 mmHg). In both cases, cooperativity was abolished (n<1). When HbA was polymerized under aerobic conditions, the p50 decreased significantly to values around 1 mmHg. Cooperativity was also abolished. The mixture of low affinity and high-affinity glutaraldehyde-cross-linked Hb was suggested as a possible HBOC with tunable oxygen affinity (Belcher et al, 2017).

1.4.3 Non-human hemoglobins and their derivatives as HBOCs

Chemical modifications of HbA were explored to stabilize tetramers and preserve cooperativity. However, the lack of allosteric effectors – and particularly 2,3-BPG – in plasma prevented the development of HbA-based HBOCs with properties close to those of RBCs. For this reason, several researchers focused their attention on non-human Hbs.

Bovine Hb (bHb) was a natural choice for the design of HBOCs, not only because it is very abundant as a byproduct of the meat industry, but also because of intrinsically exhibit a low affinity for oxygen and a high sensitivity to chloride ions. Indeed, bovine Hb has a p50 of about 29 mmHg in the stripped form, comparable to that of human RBCs. The low oxygen affinity is due to the N terminus shifting toward the central water cavity resulting from His-2(β) deletion (Smith et al, 1979). The p50 is further increased by chloride ions, which are present in plasma at a concentration of around 100 mM (98-107 mM) . Therefore, several approaches applied to HbA have been applied also to bHb. However, it should be considered that PEGylation of bHb could produce HBOCs

endowed with different properties in comparison with those derived from HbA. For instance, PEGylation of bHb in comparison to HbA gives products with a higher viscosity and hydrodynamic volume (Wang et al, 2017).

An example of glutaraldehyde-polymerized bovine Hb is Hemopure® (HBOC-201), developed by Biopure (now OPKbiotech). It has a p50 of around 40 mmHg, lower than human RBCs. Oxygen affinity of glutaraldehyde-polymerized bHb was shown to depend on the ligation state of Hb (i.e. the ligand of the heme at the sixth coordination position) during the chemical reaction. PolybHbs were prepared at different glutaraldehyde:bHb ratios, with Hb either in the oxy or deoxy state (Buehler et al, 2010b; Zhou et al, 2011). When bHb is under anaerobic conditions, the resulting p50 was higher than that of human RBCs and tended to increase at higher ratios, from 29.7 mmHg (10:1) to 41 mmHg (30:1). Cooperativity decreased in all cases ($n<1.4$). When the reaction was carried out on oxy bHb, the p50 was much lower (<5 mmHg) and the cooperativity was lost (Zhou et al, 2011). The optimal ratio of glutaraldehyde:protein to minimize hypertension and autoxidation was investigated in a Guinea pig model (Baek et al, 2012).

1.4.4 Mutant HBOCs and affinity modulation

HBOCs based on natural Hbs are limited by blood supplies and by the naturally occurring variants, which are evolutionary optimized to work inside red blood cells rather than in plasma. As an alternative, it was suggested to produce recombinant hemoglobins (rHbs), which allow for

mutations that modulate the oxygen-binding properties, as well as other properties, such as the reactivity with NO, the auto-oxidation rate and the heme affinity. Several strategies have been explored (Ronda et al, 2008a): i) the selective stabilization of high or low affinity conformations, ii) the alteration of functionally relevant interactions between oxygen and specific aminoacidic side chains in the heme pocket (e.g. the distal histidine), and iii) the modification of heme accessibility (Birukou et al, 2010). Many naturally occurring variants exhibit reduced oxygen affinity because of the loss of interactions stabilizing the R state (such as that between Asn102(β) and Asp94(α)) or the stabilization of the interdimeric interface. Mutations causing an increase of oxygen affinity either prevent the formation of salt bridges stabilizing the T state, like those of Arg141(α) or His146(β), or of $\alpha_1\beta_2$ interactions stabilizing the T state (e.g. mutations of Trp37(β) as in Hb Rothschild).

As for the modulation of the NO scavenging properties, some mutations were shown to decrease the NO deoxygenase activity of Hb up to 30-fold. Particularly, mutants L29F(α) and V67W(β) Hbs were developed by Olson's group at Rice University. A recombinant Hb containing these mutations, alongside others (rHb 3011), showed reduced NO scavenging rates once administered to rats (Varnado et al, 2013).

A series of human Hb tyrosine mutants have been expressed and PEGylated to identify the mutations that minimize Hb pro-oxidant activity, maintaining a p50 in a range compatible with oxygen delivery to tissues (Cooper et al, 2019).

In recent years, protocols to produce recombinant Hbs and their mutants have been particularly developed in *Escherichia coli* (Fronticelli & Koehler, 2009; Frost et al, 2018; Graves et al, 2008).

1.4.5 Recombinant fetal HBOCs

HbF is the primary oxygen carrier in fetuses. Structurally, HbF contains two α subunits (as HbA) and two γ subunits. Researchers have recently tested HbF as a starting material for HBOCs because it is more stable and less prone to oxidation than HbA. Notably, the γ chain in HbF lacks one cysteine residue in comparison to βHbA that contributes to the irreversible oxidation of Hb (Chakane et al, 2017; Ratanasopa et al, 2016; Ratanasopa et al, 2015). On the other hand, HbF has a higher oxygen affinity in comparison to HbA. One strategy toward HBOCs development was, therefore, to introduce mutations in the β subunits of HbA to make it more similar to γ HbF subunits (Ratanasopa et al, 2016). Recombinant human fetal Hb has been prepared and PEGylated as a possible recombinant HBOC and evaluated in view of its oxidative stress effect. The p50 shifted from 3.8 ± 0.2 mmHg of HbA to 1.2 ± 0.1 mmHg under the same experimental conditions (pH 7.0, 25 °C) (Simons et al, 2018).

Chapter 2: Differential oxidative stress and organ damage in a Guinea pig transfusion model: High- and low-affinity PEGylated hemoglobin-based oxygen carriers

This work was published in:

E. Alomari *et al*. High- and low-affinity PEGylated hemoglobin-based oxygen carriers: Differential oxidative stress in a Guinea pig transfusion model, *Free Radic Biol Med.* 18 (2018) 299–310. DOI:org/10.1016/j. freeradbiomed.2018.06.018.

Part of this work was published in:

Alomari *et al*, Protein carbonylation detection methods: a comparison, *Data in Brief.* 19 (2018) 2215–2220. DOI: 10.1016/j.dib.2018.06.088

2.1 Introduction

As mentioned in Chapter 1, one of the causes of HBOCs toxicity *in vivo* is associated with their autoxidation, which triggers the production of reactive oxygen species (ROS), which, in turn, produce damages to biomolecules, such as DNA, lipids, and proteins. Cells, tissues, and whole organs suffer from damages as a consequence (Buehler et al, 2010a; Cardenas et al, 2017; Rifkind et al, 2014). Some studies have correlated the extent of HBOC-induced oxidative stress to the oxygen-binding properties of HBOCs (Benitez Cardenas et al, 2019) and HBOCs with different biochemical properties were associated with different toxic effects. However, these effects *in vivo* cannot be easily predicted only from the biochemical properties of HBOCs, also in consideration of the lack of validated animal models to assess oxidative stress (Alayash, 2017; Alayash et al, 2007). It is therefore important to evaluate oxidative stress in the organs of animal models where these products are tested.

In this work, our goal was to provide an *in vivo* experimental approach to investigate the association between different oxygen-binding properties, HBOCs oxidation, and oxidative stress. The experiment was carried out by using two PEGylated HBOCs, PEG-Hb^{deoxy} and PEG-Hb^{oxy}, which are chemically very similar (both are PEGylated with the same reagents) but exhibit different oxygen-binding properties because they were prepared under anaerobic and aerobic conditions, respectively (see Chapter 1).

To examine HBOCs toxicity, a Guinea pig transfusion model was designed. Guinea pigs were chosen because they have an antioxidant

capacity similar to that of humans. Particularly, like humans but unlike mice and rats, they cannot produce ascorbic acid, a plasma reducing agent. Moreover, like humans, they have abundant antioxidant enzymes in comparison to other species (Alayash, 2014, Buehler et al. 2007).

Our work was focused on the identification of oxidative stress biomarkers related to inflammation, tissue damage, and organ dysfunction, in order to assess the relationship between HBOCs-induced oxidative stress and HBOCs' oxygen-binding properties. Plasma, hearts, and kidneys from animals transfused with HBOCs were used to investigate different common oxidative stress markers such as protein carbonyl content, protein S-nitrosylation, protein S-glutathionylation, protein adducts with 4-hydroxynonenal and protein adducts with malondialdehyde.

2.2 Material and methods

2.2.1 Materials

High-quality chemicals were purchased from Sigma-Aldrich (St. Louis, MO, USA); MAL-PEG was purchased from Iris Biotech GmbH (Marktredwitz, Germany). Immunochemical assays were purchased from Cell Biolabs (San Diego, CA, USA), Merck Millipore (Darmstadt, Germany) or Cayman Chemical (Ann Arbor, MI, USA), as specified for each marker. The HRP substrate CheLuminate-HRP PicoDetect was purchased from AppliChem (Darmstadt, Germany).

2.2.2 Human hemoglobin preparation

50 mL of packed human red blood cells (RBCs) were resuspended in 100 mL of endotoxin-free water to induce cell lysis. NaCl (5% w/v) was then added and the suspension was centrifuged at 3800 rpm for 1 h to remove RBC membranes and intact RBCs. The supernatant solution containing hemoglobin was sterilized using a 0.2 µm filter then dialyzed against a solution containing 50 mM sodium phosphate, 100 mM KCl, 0.5 mM EDTA, pH 7.0 for PEG-Hb^{deoxy} and against a phosphate buffer saline solution (PBS) for PEG-Hb^{oxy}. The solutions were then concentrated to 2.5 mM (on a heme basis) by using a 50 kDa cutoff tangential flow system. All equipment and tubes were previously flushed with 5% sodium hydroxide to remove lipopolysaccharides and then washed with sterilized water. The powders used for the preparations were dissolved in sterilized water for parental use.

2.2.3 Hemoglobin PEGylation

To prepare PEG-Hb^{deoxy}, the reaction was carried out in the absence of oxygen at 20 °C. Hb solutions were deoxygenated in nitrogen flux in 1 L bottles under gentle shaking. All the reagents were deoxygenated. Inositol hexaphosphate (IHP) – an allosteric effector of Hb that strongly stabilizes the T state – was added to the Hb solution (0.6 mM based on tetramer) in slight excess (1.2 mol/tetramer mol). To produce PEGylation; iminothiolane (IMT) (80 mol/tetramer mol) was added, followed by 5 kDa MAL-PEG after 1.5 min (12 mol/tetramer mol). To stop the reaction between MAL-PEG and IMT, a lysine solution (20 mol/ MAL-PEG mol) was

added after 25 min, followed by the addition of a cysteine solution (6 mol/ MAL-PEG mol) after 5 min. The reacted solution was dialyzed against PBS to remove the residual reagents. The solution was then concentrated by using a 50 kDa cutoff tangential flow system. In the end, the solution was sterilized using a 0.2 µm membrane filter. To remove endotoxins, the PEGylated Hb solution was spun in Proteus NOEndo columns (Charles River Laboratories, Wilmington, MA, USA). The final PEG-Hb^{deoxy} concentration was 1.64 mM, and it was stored at -80 ^{0}C.

For PEG-Hb^{oxy}, the same reaction was carried out in the presence of oxygen, in a 1 L bottle at 4–5 °C under continuous shaking. Hb (3 mM on heme basis) was reacted with IMT (10 mol/tetramer mol) in PBS buffer, pH 7.4 for 4 h. 5 kDa MAL-PEG (20 mol/tetramer mol) was reacted with Hb for 2 h. The PEGylation reaction was terminated by the addition of a cysteine solution (6 mol/MAL-PEG mol). The reacted solution was then dialyzed against PBS and concentrated using a 50 kDa cutoff tangential flow system to eliminate unreacted MAL-PEG and other reagents. In the end, the PEG-Hb solution was sterilized by passing it through a 0.2 µm syringe filter and spun in Proteus NoEndo spin columns to remove endotoxins. The final concentration of PEG-Hb^{oxy} was 1.69 mM, and it was stored at -80 ^{0}C.

2.2.4 Hb concentration measurements

To determine the Hb concentration and to check its oxidation state, absorption spectra were collected in the range 450-700 nm using a Cary 4000 UV-Vis spectrophotometer at all steps. Purity was assessed by

densitometry analysis of SDS-PAGE gels. The average ratio of PEG moieties per Hb tetramer was assessed by electrophoresis using a protocol already described (Caccia et al, 2009).

2.2.5 PEG-Hb^{deoxy} and PEG-Hb^{oxy} characterization

For each PEG-Hb, the oxygen-binding properties were determined using a Cary 4000 UV-Vis spectrophotometer coupled with a gas-mixing system. Samples were diluted in a buffered solution containing 100 mM HEPES, 1 mM EDTA, pH 7.0 to reach a final concentration of 200 μM. To slow down met-Hb formation during the experiment, the Hayashi enzymatic mixture (glucose-6-phosphate, G-6-P dehydrogenase, nicotinamide adenine dinucleotide phosphate, ferredoxin, ferredoxin NADP reductase, and catalase) was added. The experiments were carried out using a 2 mm cuvette fused to a reservoir for gas equilibration. Helium\oxygen mixtures with a total flow of 50 mL/ min were produced using an Environics 4000 gas mixer. The sample in every titration experiment was thermostatted in a water bath at 15°C under continuous shaking. For every fractional oxygen saturation at a defined pressure, the spectra were collected in the range 450-750 nm. At the end of every titration, the spectra of the 100% oxygen-saturated sample and that of the sodium dithionite (DTO)- reduced sample were collected and used as a reference for data analysis. The fractional saturation was calculated by analyzing the spectra as a linear combination of oxy-, deoxy and met-spectra using the software Sigmaplot.

2.2.6 Endotoxin quantification

The endotoxin content – a crucial parameter to be evaluated before in vivo administration and possibly resulting from bacterial contamination and lipopolysaccharide release – was assessed in the final preparations by using a sensitive limulus amebocyte lysate (LAL) kit (Endochrome-K, Wilmington, MA, USA). Standard dilutions of lipopolysaccharides and preparation samples were incubated at 37°C with LAL. Endotoxins activate the LAL reagent to cleave chromogenic peptides that absorb at a 550 nm. A standard curve was used to quantify endotoxins in the PEG-Hb^{oxy} and PEG-Hb^{deoxy} preparations.

2.2.7 Animals preparation and HBOCs administration

HOBCs transfusion procedures involving animals were carried out in collaboration with the Istituto di Ricerche "Mario Negri", Milan, in accordance with institutional guidelines and in compliance with national and international laws regarding animal care. Twenty-four Guinea pigs (458 ± 134 g) were housed in suitable conditions. After one week of acclimatization, Guinea pigs were randomized into three groups: i) control (auto-transfusion, AT), ii) transfusion with PEG-Hb^{oxy}, iii) transfusion with PEG-Hb^{deoxy}.

Baseline physiological parameters were monitored before transfusion. Isovolemic transfusion was achieved by withdrawal of 9 mL of whole blood from the carotid, with the concomitant administration of either PEG-Hb^{oxy} or PEG-Hb^{deoxy} through the jugular vein. In the control group, animals were subjected to auto-transfusion. The vital signs of the

animals were monitored before, during and after transfusion.

2.2.8 Blood pressure and gas analysis

A high sensitivity transducer connected to a data system supported by CODAS hardware and software (DataQ, Akron, OH, USA) was used to monitor aortic pressure and ECG. Arterial blood gases and hematocrit were assessed before transfusion and after 2 h by using an I-STAT System (Abbott Laboratories, Princeton, NJ, USA).

2.2.9 Blood and organs collections

Blood samples were collected before transfusion, as a baseline measurement, after 2 h and after 7 days. Plasma samples were collected after centrifugation to separate RBCs, then stored at -80°C for further analysis. After 7 days, the animals were sacrificed, and their kidneys and hearts were collected and stored directly at -80°C.

2.2.10 Determination of residual PEG-Hb^{deoxy} and PEG-Hb^{oxy} in plasma

To determine the residual concentration of HBOCs, plasma withdrawn before transfusion, after 2 h and after 7 days were used. Samples from the same group (1 μL from each) were pooled together. Aliquots of 2 μL of pooled plasma samples were loaded in a 12% SDS-PAGE gel, which was then blotted onto a nitrocellulose membrane. A 2% (w/v) bovine serum albumin solution (BSA) was used to block the membrane, which was then incubated with anti-Hb antibodies conjugated with horseradish peroxidase (HRP) (Abcam, Cambridge, UK).

The chemiluminescence signals were collected with a ChemiDoc™ system (Bio-Rad Laboratories, Inc., Hercules, California, U.S.A.) after the addition of the HRP substrate CheLuminate-HRP PicoDetect (PanReac AppliChem, Darmstadt, Germany). The experiment was carried out in triplicate.

2.2.11 Plasma biochemical analysis

L-Lactate

L-Lactate levels in plasma samples were measured before transfusion, after 2 h and after 7 days from transfusion through the conversion of lactate to pyruvate by lactate dehydrogenase in the presence of NAD^+ (lithium salt). In the presence of hydrazine, which reacts with the newly formed pyruvate, the equilibrium is shifted toward the products. A Cary 4000 UV-Vis spectrophotometer was used to monitor the formation of NADH at 340 nm.

8-hydroxy-2'-deoxyguanosine (8-OHdG)

8-OHdG is a ubiquitous marker of oxidative stress derived from the oxidation of DNA. 8-OHdG levels in plasma samples after 7 days from transfusion were assessed through a competitive enzyme immunoassay (DNA Damage ELISA Kit - 8-OHdG Quantitation, Cell Biolabs, San Diego, CA, USA). The assay was performed in a 96-wells plate. Each well was coated with 100 μL of 1 μg/mL 8-OHdG conjugate solution provided in the kit and incubated overnight at 4°C. On the second day, the plate was washed with water and then 200 μL of assay diluent was added to each well and blocked for 1 h at room temperature on an orbital shaker. Plasma

samples were centrifuged at 3000 x g for 10 min at 4°C and were diluted seven times. A dilution series of 8-OHdG standard was prepared. Then 50 μL of diluted plasma samples and 8-OHdG standards were added to the 8-OHdG-coated plate for 10 min and followed by an anti-8-OHdG antibody (1:500 dilution). The plate was incubated at room temperature for 1 h, washed 3 times and dried. Then 100 μL of a secondary antibody conjugated with HRP (1:1000 dilution) was added to each well for 1 h of incubation at room temperature. The HRP substrate solution was added after washing the plate and incubated for 15 min. The enzymatic reaction was stopped and the absorbance was immediately read at 450 nm using a microplate reader (Halo LED 96-Dynamic Scientific Ltd., Newton Pagnell, UK).

Allantoin

Allantoin, a biomarker of oxidative stress, was measured by fluorometric assay. Briefly, plasma samples were spiked by adding different concentrations of racemic allantoin, then they were incubated with allantoinase, which converts S-allantoin to allantoate. The same samples were then incubated with 10 mM resorcinol and 4.7 HCl at 100°C for 5 min to hydrolize allantoate to glyoxylate. Glyoxylate was detected by fluorescence using a TECAN Spark 10 M reader (Tecan, Switzerland).

High sensitivity cardiac protein T (cTNT)

The cTNT concentration in the plasma samples was measured by using an electrochemiluminescence immunoassay (ECLIA) (ECLIA, Elecsys

2010 analyzer, Roche Diagnostic, Germany). cTNT concentrations in plasma samples at baseline, after 2h and 7 days from transfusion were compared to a calibration curve.

Other plasma analytes

Creatinine, Na^+, Cl^-, K^+, bilirubin, urea, lactate dehydrogenase (LDH), total protein, glutamic oxaloacetic transaminase (GOT), glutamate pyruvate transaminase (GPT) and amylase were measured using a Roche Cobas ITEGRA 400 analyzer, using commercial reagents supplied from Roche diagnostics (Mannheim, Germany).

2.2.12 Protein extraction from tissues

Hearts and kidneys were thawed in ice, rinsed with deionized water, weighed, cut into small pieces and ground cryogenically with mortar and pestle in the presence of liquid nitrogen. The resulting powders were divided into aliquots of 50 mg, frozen directly in liquid nitrogen and stored at -80°C before protein extraction. Aliquots of 50 mg were thawed and suspended in phosphate buffer 50 mM, pH 7.4, sonicated in the presence of 1% DTT and a protease inhibitor cocktail mixture (Sigma-Aldrich, St. Louis, MO, USA). The sonicated homogenate was centrifuged at 1500 xg at 4°C for 20 min; the supernatant was collected and stored at -80°C for further analysis. The total extracted protein content was assessed by Bradford assays (Bio-Rad Laboratories, Inc., Hercules, CA, USA) and SDS-PAGE analysis. The quantity of soluble protein after each extraction was around 1.2 ±0.3 mg/mL.

2.2.13 Protein and lipid oxidation markers of heart and kidney tissue

Protein carbonylation

The carbonyl content is a very common marker of oxidative stress and was assessed by using 4 different methods.

Levine spectrophotometric method:

Carbonylated proteins were reacted with 2,4-dinitrophenylhydrazine (DNPH) to produce a chromophoric adduct with an extinction coefficient of 22,000 M^{-1} cm^{-1} at 366 nm (Reznick & Packer, 1994; Weber et al, 2015). To avoid nucleic acid interference, protein samples were preliminarily treated with streptomycin sulfate (1% final concentration). Samples were then incubated for 15 min at room temperature and centrifuged at 8000 xg for 15 min. The supernatant protein solution was derivatized by the addition of 500 µL of 10 mM DNPH to reach 5 mM final concentration and incubated for 1 h in the dark, with strong agitation every 15 min. The derivatized carbonylated proteins were precipitated with trichloroacetic acid (TCA, 10% final concentration) and were recovered by centrifugation for 20 min at 10000 xg. To remove the excess of DNPH, extensive washing was performed with a 10% TCA solution, followed by two washing steps with ethanol/ethyl acetate (1:1) (v/v). The pellet was then solubilized in 1 mL of a solution containing 6 M guanidinium hydrochloride, incubated at 37°C for 1 h and centrifuged at the end to remove any insoluble particle. The spectra were collected in the range 250-600 nm, and the protein concentration in every sample was assessed at 280 nm and the DNPH derivatives were assessed at 366 nm. The carbonyl content in every sample was normalized to the total protein concentration assessed by

absorbance at 280 nm, assuming that one unit of absorbance corresponds to 1 mg/mL. For every protein sample, a control spectrum before derivatization was measured to take into account the contribution of heme groups and other chromophoric groups. For kidney protein extracts, which contained a significant amount of hemoglobin, additional precipitation and washing steps with HCl-acetone (3:100) (v/v) were applied before the addition of DNPH.

ELISA assay:

The OxiSelect Protein Carbonyl ELISA kit (Cell Biolabs, San Diego, CA, USA) was applied to protein samples from individual heart protein extracts after treatment with streptomycin sulfate (1% final concentration). The reaction of protein extract and BSA-based calibrants with DNPH was carried out in 96- wells plates. The products were then probed with an anti-DNPH antibody and a secondary antibody conjugated with horseradish peroxidase (HRP). The chromogenic reaction between HRP and its substrate was stopped when the color started to change. The absorbance in each well was registered at 450 nm using a plate reader (Halo LED 96-Dynamic Scientific Ltd., Newton Pagnell, UK). Fully reduced BSA was used as blank and the carbonyl contents were calculated from the standard curve using the calibrants provided by the manufacturer.

Western blot detection method:

The same protein samples that were used for the Levine and ELISA assays were also immunoblotted for an alternative immunochemical detection. The derivatization reaction of 2 μg aliquots with DNPH was performed before electrophoresis. The resulting gels were blotted onto a

nitrocellulose membrane by using a Trans-Blot Turbo Blotting System (Bio-Rad Laboratories, Inc., Hercules, California, USA). The membrane was then blocked with 2% BSA overnight at 4 °C. After that, it was incubated with an anti-DNPH antibody (OxyBlot™ Protein Oxidation Detection Kit, Merk Millipore, Darmstadt, Germany). The anti-DNPH antibodies were then probed with a goat anti-rabbit secondary antibody conjugated with HRP. After extensive washing steps, the carbonylated protein bands were detected by adding the Chemiluminate HRP PicoDetect substrate (PanReac AppliChem, Darmstadt, Germany). The chemiluminescence signals were collected with a ChemiDoc™ system (Bio-Rad Laboratories, Inc., Hercules, California, U.S.A). The chemiluminescence signals were normalized to the protein content measured on the same gel stained with Coomassie blue.

Fluorescein-5-thiosemicarbazide (FTC) detection method:

Carbonylated proteins were labeled with FTC, which reacts with the carbonyl groups, through a specific reaction reported in (Chaudhuri et al, 2006) Protein samples (1 mg/mL) prepared as indicated above were reacted with FTC 1 mM in a ratio 1:4 (v/v) and incubated at room temperature in the dark for 150 min. The derivatized proteins were precipitated with an equal volume of chilled 20% TCA (v/v), incubated for 10 min in ice in the dark and centrifuged at 15000 xg at 4°C. To remove unreacted FTC, the pellets were suspended and washed four times with ethanol/ethyl acetate (1:1 v/v) solutions. The pellets were finally dissolved in 80 µl of a buffered solution containing 100 mM Tris-HCl, 5 mM $MgCl_2$, 1 mM EDTA, 8 mM urea and 150 mM NaCl, pH 8.0. They were

then loaded in a 12% SDS-PAGE gel. The gel of the fluorescent proteins was acquired by using a ChemiDoc™ system (Bio-Rad Laboratories, Inc., Hercules, California, U.S.A), with an excitation at 492 nm and an emission at 516 nm. Finally, the same gel was stained with Coomassie blue and the intensity of the FTC signals were normalized to the intensity of the protein content.

Protein S–nitrosylation

To detect protein S-nitrosylation, the biotin-switch method was used (S-nitrosylated Protein Detection Kit - Cayman Chemical, Ann Arbor, MI, USA). Briefly, the free thiol groups were blocked with a blocking reagent supplied in the kit, then the S-NO groups were reduced with a reducing agent for 15 min at 37°C and then reacted with the labeling reagent containing biotin-maleimide. The treated protein samples were loaded in two separate 12 % SDS-PAGE gels. One of the gels was stained in Coomassie blue, the other was electroblotted to a nitrocellulose membrane, which was then incubated with an avidin-HRP conjugate. The images of the gel and the membrane were acquired using a ChemiDoc™ system (Bio-Rad Laboratories, Inc., Hercules, California, U.S.A). The analysis was expressed in arbitrary units by calculating the ratio of the chemiluminescence signal and the Coomassie blue signal (proportional to protein concentration) after normalizing it for the total protein content in every sample.

Protein S–glutathionylation

S-glutathionylation was detected by using a biotin-avidin switch method and Western blot analysis using an avidin-HRP conjugate. (S-Glutathionylated Protein Detection Assay, Cayman Chemical, Ann Arbor, MI, USA) was used according to the manufacturer's instructions. Briefly, the free thiol groups of the protein extract were blocked with a blocking reagent provided in the kit. Then protein-S-glutathione bonds were then reduced by a reducing reagent supplied in the kit. The free thiols were then labeled with biotin-maleimide. The labeled proteins were loaded in two 12 % SDS-PAGE gels. One of the gels was electroblotted onto a nitrocellulose membrane, the other gel was stained in Coomassie blue. The biotinylated proteins were then probed by incubating the membrane with an avidin-HRP conjugate (1:75 dilution). The detection was carried out using the chemiluminescent substrate CheLuminate-HRP PicoDetect (PanReac AppliChem, Darmstadt, Germany). SDS-PAGE and Western blots analysis was done as described for the S-nitrosylated proteins.

Protein-4-hydroxynonenal (HNE) adducts

HNE adducts of proteins were quantified by using a competitive ELISA assay (Protein OxiSelect™ HNE Adduct, Cell Biolabs, San Diego, CA, USA). The assay was performed in a 96-wells plate. The plat was coated overnight at 4°C with HNE conjugate solution provided in the kit. Dilution series of HNE-derivatized BSA standards were prepared, then the protein samples and HNE-BSA standards were added to the wells of the HNE conjugate coated plate. The plate was incubated for 10 min at room

temperature on an orbital shaker. An anti-HNE antibody for 1 h incubation. The stripped wells were then washed three times, followed by the addition of a secondary antibody conjugated with HRP. After 1 h, the plate was washed and the HRP substrate was added for 5 min. The detection was carried out at 450 nm in a microplate reader (Halo LED 96-Dynamic Scientific Ltd., Newton Pagnell, UK). The quantity of HNE-adducts in protein extracts was calculated using the calibration curve obtained with BSA-HNE calibrants.

Protein-malondialdehyde (MDA) adducts

The MDA adducts were determined using a competitive ELISA system (OxiSelect™ MDA Adduct Competitive ELISA Kit, Cell Biolabs, San Diego, CA, USA). The assay was performed in a 96-wells plate, coated overnight at 4°C with MDA conjugate solution provided in the kit. Dilution series of MDA-derivatized BSA standards were prepared, then the protein samples and MDA-BSA standards were added to wells of the MDA conjugate coated plate for 10 min. An anti-MDA antibody was added to each well, incubated at room temperature for 1 h. The plate was washed three times, dried and then a secondary antibody conjugated with HRP was added to each well for 1 hr. After that, the plate was washed well and followed by adding HRP substrate solution for 10 min. The absorbance was measured at 450 nm using a microplate reader (Halo LED 96-Dynamic Scientific Ltd., Newton Pagnell, UK).

Lipid hydroperoxide determination

The lipid hydroperoxide content in heart and kidney tissues was determined with the Lipid Hydroperoxide Assay Kit (CaymanChemicals, Ann Arbor, Michigan, USA). Briefly, fresh samples were prepared for both heart and kidneys tissues, lipids were carefully extracted from the samples with cold chloroform. The lipid extract was used directly in the assay plate according to the manufacturer's instructions. The assay is based on the redox reaction between ferrous ions and the highly unstable hydroperoxide derivatives in the extract to produce ferric ions, which could then react with thiocyanate. The absorbance of the product was registered quickly before solvent evaporation at 500 nm using a microplate reader (Halo LED 96-Dynamic Scientific Ltd., Newton Pagnell, UK). Standard curves using calibrants provided by the manufacturer were used to calculate the lipid hydroperoxide content.

Superoxide dismutase (SOD)

SOD levels in 1 mg/mL protein solutions of heart and kidney tissue extracts were measured using the OxiSelect™ Superoxide Dismutase Activity Assay (Cell Biolabs, San Diego, CA, USA). Firstly, dilution series of SOD standards were prepared. Then, master mixture solutions were prepared directly in the wells by adding 5 μL of the sample or standard diluents, 5 μL of xanthine solution, 5 μL of chromogenic solution, 10 μL assay buffer, and 60 μL of water. In the end, 10 μL of a xanthine oxidase solution were added to the mixture in every well. The absorbance was registered at 490 nm using a microplate reader (Halo LED 96-Dynamic

Scientific Ltd., Newton Pagnell, UK).

Catalase

The activity of catalase was assessed by using the OxiSelect™ Catalase Activity Assay (Cell Biolabs, San Diego, CA, USA). Catalase levels were measured in 1 mg/mL protein extracts of heart; catalase activity could not be assessed in the tissue extracts from kidneys because of heme interference. The assay is based on the decomposition of hydrogen peroxide into water and oxygen by catalase. The rate of this conversion is proportional to the amount of catalase present in the samples. Catalase standard dilutions were prepared. 20 μL of each sample (catalase standards or heart protein solutions) were added into individual plate wells, followed by the addition of 50 μL of 12 mM H_2O_2 for just 1 min. The reaction was quenched with sodium azide. Residual H_2O_2, inversely proportional to catalase concentration, was reacted with a chromogenic solution containing benzenesulfonic acid and HRP. The colorimetric signals were registered at 520 nm using a microplate reader (Halo LED 96-Dynamic Scientific Ltd., Newton Pagnell, UK).

Hydrogen peroxide

The fluorimetric Oxiselect™ Hydrogen peroxide assay kit (Cell Biolabs, San Diego, CA, USA) was used to measure H_2O_2 concentration in heart and kidneys tissue extracts. The measurements were based on the reaction of 10-acytyl-3, 7-dihydroxyphenoxazine with H_2O_2 in samples or standard diluents in 1:1 stoichiometry in the presence of HRP to produce

a fluorescent compound, resorufin. Fluorescence was read in a Spark 10 M (Tecan, Switzerland) microplate reader. Excitation was at 550 nm and emission at 590 nm.

2.2.14 Image analysis

Coomassie-stained SDS-PAGE gel and Western blots were acquired by using a ChemiDoc™ system (Bio-Rad Laboratories, Inc., Hercules, CA, USA) and analyzed with the Image Lab™ software (Bio-Rad Laboratories, Inc., Hercules, CA, USA). The signal intensity of lanes or individual bands of Western blots (expressed as arbitrary units) were normalized by dividing them by the total protein content of the corresponding lane, as quantified by densitometry of the SDS-PAGE gel. For each measurement, three technical replicates were performed.

2.2.15 Statistical analysis

Statistically significant differences were assessed, as appropriate depending on the data, by one-way analysis of variance (ANOVA), Kruskal-Wallis test or two-way ANOVA, followed by Tukey's Test, Dunn's test or Sidak's test, respectively. In all analyses, a value $p < 0.05$ was taken as the level of statistical significance. In all plots, values are represented as mean ± standard deviation (SD). Parameters resulting from data regression are represented as coefficient ± standard error of the regression (SE). Graphs and statistical analyses were performed with Sigma Plot (Systat Software, San Jose, CA, USA).

2.3 Results and discussion

2.3.1 Preparation of HBOCs

The oxygen binding parameters of PEG-Hb^{deoxy} and PEG-Hb^{oxy} are summarized in Table 2.1. PEG-Hb^{deoxy} exhibited an oxygen affinity lower than unmodified HbA and maintained cooperativity. On the other hand, PEG-Hb^{oxy} exhibited higher oxygen affinity and lost all cooperativity. As described in the introduction, there is an ongoing debate about the relevance of oxygen affinity in bringing about therapeutic. Therefore, both products were tested in vivo.

	p50 (torr)	Hill coefficient (n)	PEG/ tetramer	Endotoxin concentration (EU/mL)
HbA	2.61 ± 0.05	2.36 ± 0.06	-	-
PEG-Hb^{deoxy}	3.18 ± 0.08	2.5 ± 0.2	5.7	21
PEG-Hb^{oxy}	0.85 ± 0.02	1.34 ± 0.04	6.6	14

Table 2.1: p50s and Hill coefficients ± S.E. for HbA, PEG-Hb^{deoxy} and PEG-Hb^{oxy}, in a solution containing 100 mM HEPES, 1 mM EDTA, at 15 °C, pH 7.0. The hemoglobin concentration was 110-200 μM.

2.3.2 Animal survival after transfusion

After seven days from the transfusion, the survival rate was 71.4% (5/7) in the auto-transfusion group, 66.7% (6/9) in the PEG-Hb^{deoxy} group and 37.5% (3/8) in the PEG-Hb^{oxy} group. Statistical analysis of the survival rate by using a long-rank (Mantel-Cox) test did not show a significant

difference among groups.

2.3.3 Hemodynamics and oxygen saturation analysis

During the transfusion experiment, the heart rate was increased in both HBOCs-treated groups in comparison to the auto transfused animals (190 ± 18 beats/ min for the autotransfused animals, 227 ± 22 beats/ min for the animals treated with PEG-Hb^{oxy} and 210 ± 6 beats/ min for those treated with and PEG-Hb^{deoxy}). A trend towards a decrease in the heart rate after 120 minutes from transfusion was observed in animals treated with PEG-Hb^{deoxy} (Figure 2.1a). The mean arterial blood pressure values were in the normal physiological range, but a significant increase in both PEG-Hb^{deoxy} and PEG-Hb^{oxy} groups was detected after 60 min from the end of transfusion (Figure 2.1b).

Hb concentration and hematocrit showed a significant decrease after 2 h from transfusion compared to the baseline values. Both analytes were expected to decrease, as around 26% of the animals' blood was withdrawn and substituted with HBOCs solutions (Figure 2.1c and d). Regardless of RBCs loss, both treatment groups were able to maintain oxygen saturation to the optimum level, even with a moderate increase in oxygen saturation (sO_2) levels compared to baseline, suggesting that HBOCs could improve oxygen saturation (Figure 2.1e).

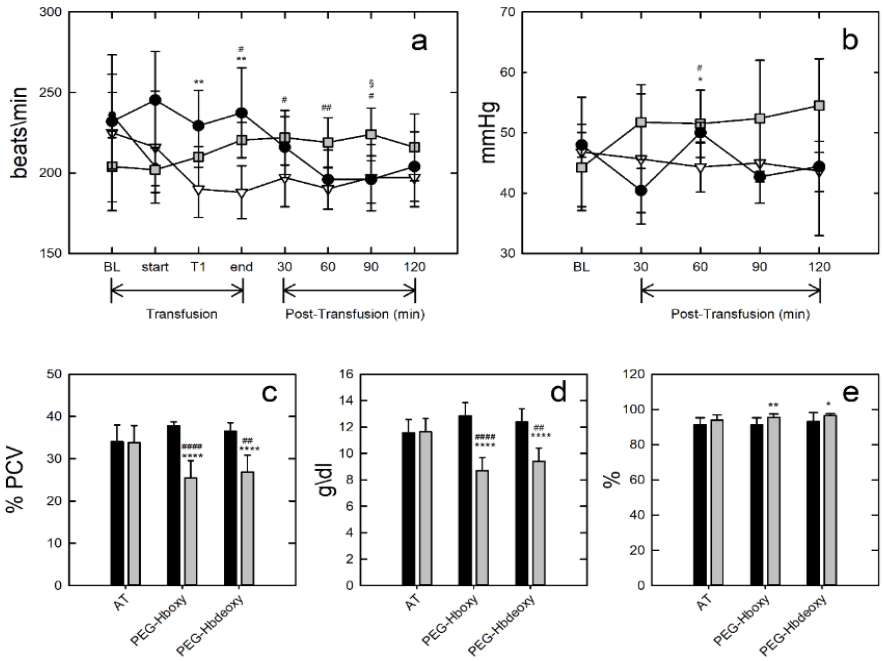

Figure 2.1: (a) Heart rates before and after transfusion with PEG-Hb^{deoxy} (closed circles) or PEG-Hb^{oxy} (gray squares), compared with the control group (open triangles). Data are shown as mean ± SD. Statistical analysis: Ordinary one-way ANOVA followed by Tukey's multiple comparisons test, comparison among groups at the same time point, * ctrl vs PEG-Hb^{deoxy}, # ctrl vs PEG-Hb^{oxy}, § PEG-Hb^{oxy} vs PEG-Hb^{deoxy}. CTRL n=7, PEG-Hb^{oxy} n=8, PEG-Hb^{deoxy} n=9 (** p<0.01, # p<0.05, ## p<0.01, (§ p<0.05). **(b)** Mean Arterial Pressure before and after transfusion with PEG-Hb^{deoxy} (closed circles) or PEG-Hb^{oxy} (gray squares) in comparison with the control group (open triangles). Statistical analysis: Ordinary one-way ANOVA followed by Tukey's multiple comparisons test, comparison among groups at the same time point, * ctrl vs PEG-Hb^{deoxy}, # ctrl vs PEG-Hb^{oxy}, § PEG-Hb^{oxy} vs PEG-Hb^{deoxy}(* p<0.05, # p<0.05). Hematocrit **(c)**, Hb content **(d)** and sO_2 **(e)** before transfusion (black bars) and after 2 hours (gray bars). Data are shown as mean ± SD. Statistical analysis: Two-way ANOVA followed by Sidak's multiple comparisons test, * vs own baseline, # vs 2h ctrl (* p<0.05, ** p<0.01, **** p<0.0001, # p<0.05, ## p<0.01, #### p<0.0001). In all measurements, Auto-transfusion n=7, PEG-Hb^{oxy} n=8, PEG-Hb^{deoxy} n=9.

2.3.4 HBOCs content in plasma

The residual content of HBOCs was assessed in plasma samples pooled from all animals within each group before transfusion, after 2 h and after 7 days by using an HRP-conjugated anti-HbA monoclonal antibody (Figure 2.2). The band around 25 kDa, corresponding to mono-PEGylated Hb subunits, was evaluated through densitometric analysis. After 7 days of HBOCs transfusion, plasma levels of PEG-Hb^{oxy} and PEG-Hb^{deoxy} were 13% and 4% of that measured after 2 h from transfusion, respectively. Western blot of plasma samples withdrawn before HBOCs treatment and plasma samples collected from the autotransfusion group showed that the anti-Hb monoclonal antibody did not cross-react with any Guinea pig plasma protein nor with its free hemoglobin.

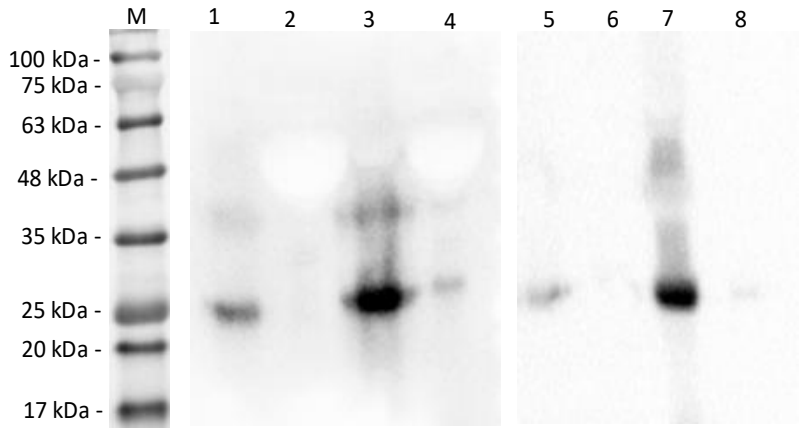

Figure 2.2: Western blot of plasma samples compared with purified HBOCs. **M:** molecular weight marker; **1:** purified PEG-Hb^{oxy}; **2:** plasma pool of animals before transfusion with PEG-Hb^{oxy}; **3:** plasma pool of animals after 2 hours from transfusion of PEG-Hb^{oxy}'; **4:** plasma pool of animals after 7 days from transfusion of PEG-Hb^{oxy}; **5:** purified PEG-Hb^{deoxy}; **6:** plasma pool of animals before transfusion of PEG-Hb^{deoxy}; **7:** plasma pool of animals after 2 hours from transfusion of PEG-Hb^{deoxy}; **8:** plasma pool of animals after 7 days from the transfusion of PEG-Hb^{deoxy}.

2.3.5 Plasma analytes

L-lactate

L-lactate is a biomarker of tissue oxygenation and was evaluated in all animals. Interestingly, a significant decrease in L-lactate levels was observed in PEG-Hb^{oxy}-treated animals, both after 2 h and after 7 days from treatment. The autotransfusion group and PEG-Hb^{deoxy}- treated group did not exhibit any significant difference in L-lactate levels after transfusion in comparison to their baseline levels (Figure 2.3). A similar result was noticed in another experimental animal model treated with MP4, a bioequivalent of PEG-Hb^{oxy} (Tsai et al, 2003). Unlike HBOCs with low affinity, PEG-Hb^{oxy} delivers oxygen at the capillary levels, thus increasing the peripheral oxygen partial pressure.

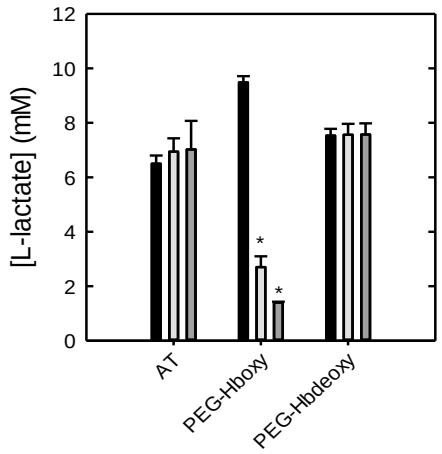

Figure 2.3: L-lactate concentration for the autotransfusion group (AT) and animals transfused with PEG-Hb^{oxy} and PEG-Hb^{deoxy}. Samples were collected and analyzed before treatment (BL, black bars), after 2 hours from transfusion (light gray bars), and after 7 days (dark gray bars). Data are shown as mean ± SD. Statistical analysis: Ordinary one-way ANOVA followed by Tukey's multiple comparisons test. * $p<0.05$, BL vs own PT. AT=6/5/5, PEG-Hb^{oxy} n=8/8/3, PEG-Hb^{deoxy} n= 9/5/5.

Plasma oxidation markers

8-OHdG

8-OHdG is a common biomarker used to assess DNA oxidation (Pilger & Rudiger, 2006). 8-OHdG concentration was measured in all plasma samples after 7 days from transfusion. A significant elevation was found in the treated groups in comparison with the control group. No significant difference among PEG-Hb^{oxy} and PEG-Hb^{deoxy} groups was observed, although the 8-OHdG concentration was slightly higher in the PEG-Hb^{oxy} group (Figure 2.4). A significant elevation in 8-OHdG levels was also seen in guinea pig brains transfused with polymerized HBOCs (Butt et al, 2011).

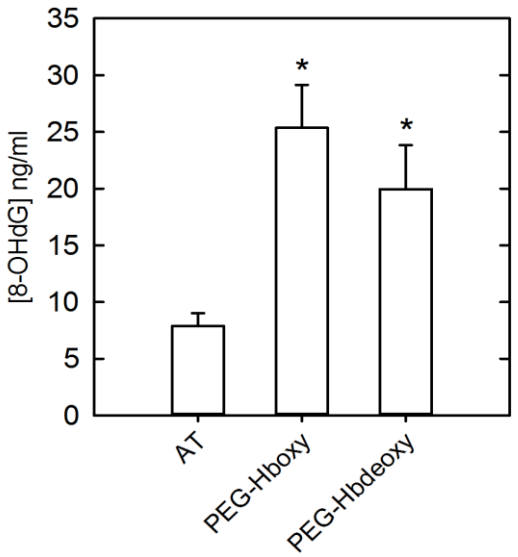

Figure 2.4: Plasma levels of 8-OHdG after 7 days from transfusion. Data are shown as mean ±SD. Statistical analysis: Ordinary one-way ANOVA followed by Tukey's multiple comparisons test. * $p < 0.05$ vs AT.

Allantoin

Allantoin is a biomarker of oxidative stress. Allantoin concentration was assessed in all plasma samples before treatment, and after 2 and after 7 days from transfusion. Allantoin levels increased after 2 h in all groups, but after 7 days the values returned to normal (Figure 2.5), suggesting that the increase of urate oxidation alteration was a consequence of the transfusion procedure. Guinea pigs, like humans, lost the ability to produce ascorbate as an antioxidant defense system, but they maintained the uricolytic enzyme pathway. Guinea pigs are more sensitive than humans to oxidating agents at least at the plasma level, because it has less amount of circulating urate, a scavenger of oxidants (Marchetti et al, 2016; Marchetti et al, 2018).

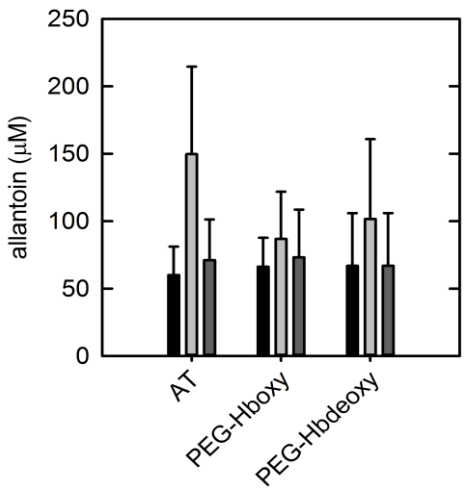

Figure 2.5: Allantoin concentration in the plasma of the autotransfusion group (AT) and for animals transfused with PEG-Hb^{oxy} and PEG-Hb^{deoxy}. Samples were collected before treatment (BL, black bars), after 2 hours from transfusion (light gray bars) and after 7 days (dark gray bars). Data are shown as mean ± SD. Statistical analysis: Ordinary one-way ANOVA followed by Tukey's multiple comparisons. AT=6/5/5, PEG-Hb^{oxy} n=8/8/3, PEG-Hb^{deoxy} n= 9/5/5.

Biomarkers associated with renal function

Urea and creatinine levels are considered as indicators of renal function, which is deteriorated if the kidney is exposed to injury or oxidative stress (Walker et al, 2001). Creatinine and urea concentrations in all plasma samples were evaluated at baseline, after 2 h and after 7 days from transfusion. A general increase for both analytes occurred after 7 days in all groups. A statistical significance was noticed only in animal groups treated with PEG-Hb^{oxy} (Figure 2.6).

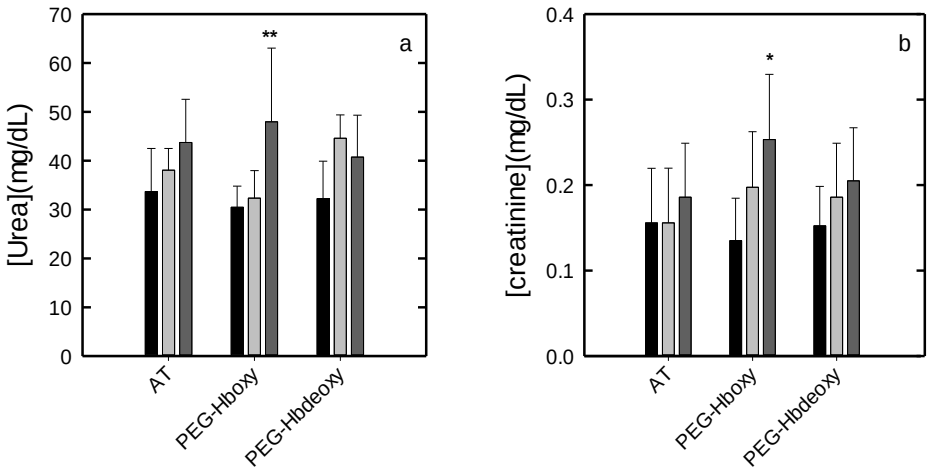

Figure 2.6: (a) Urea concentration, **(b)** Creatinine concentration for the autotransfusion group (AT) and for animals transfused with PEG-Hb^{oxy} and PEG-Hb^{deoxy}. Before treatment (BL, black bars), after 2 hours from transfusion (light gray bars) and after 7 days (dark gray bars). Data are shown as mean ± SD. Statistical analysis: Ordinary one-way ANOVA followed by Tukey's multiple comparisons. * $p<0.05$, ** $p<0.01$ BL vs own PT. AT=6/5/5, PEG-Hb^{oxy} n=8/8/3, PEG-Hb^{deoxy} n= 9/5/5.

Electrolytes

Electrolytes imbalance is related to acute kidney dysfunction (Rabe, 2011). K^+, Na^+ and Cl^- levels were measured in all plasma samples. K^+ elevation, which might be associated with renal dysfunction, were 2-3 fold higher in comparison with the baseline and well outside the reference values for healthy Guinea pigs for all groups, ruling out toxicity related to the HBOCs.The causes for this elevation are not known but it can be speculated that they are a consequence of renal dysfunction following transfusion. Unfortunately, blood transfusion in Guinea pig is poorly described in the literature and it is difficult to conclude the reason for this effect, particularly for autotransfused animals. Marginally higher levels of K^+, albeit not statistically significant, were observed for PEG-Hb^{oxy}-treated animals in comparison with those transfused with PEG-Hb^{deoxy} (Figure 2.7a). Na^+ and Cl^- did not exhibit any increase neither immediately after transfusion nor after 7 days.

Total protein content

The total protein content was significantly increased after 7 days for all three groups. The values after 2 h remained similar to the pre-treatment baseline, thus ruling out an effect of hemodilution. The higher total protein content is generally associated with a general inflammation state. However, uniformly high levels in all three groups rule out a specific response to HBOCs derivatives (Figure 2.7b).

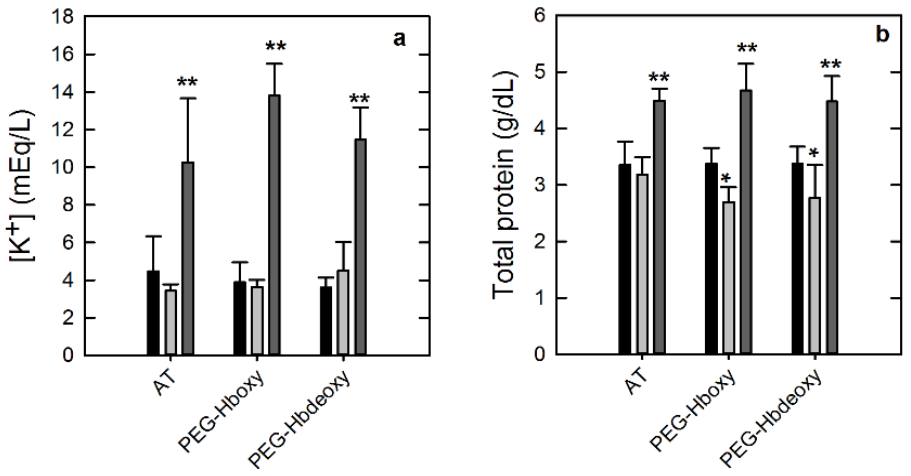

Figure 2. 7: (a) Potassium concentration, **(b)** total protein content in plasma for the autotransfusion group (AT) and for animals transfused with PEG-Hb^{oxy} and PEG-Hb^{deoxy}. Before treatment (BL, black bars), after 2 hours from transfusion (light gray bars) and after 7 days (dark gray bars). Data are shown as mean ± SD. Statistical analysis: Ordinary one-way ANOVA followed by Tukey's multiple comparisons. * $p<0.05$, ** $p<0.01$ BL vs own PT. AT=6/5/5, PEG-Hb^{oxy} n=8/8/3, PEG-Hb^{deoxy} n= 9/5/5.

Biomarkers associated with heart function

LDH activity

LDH is a late biomarker commonly used to assess heart damage. After ruling out any interference from the LDH contained in the HBOCs solutions (data not shown), LDH activity was investigated in all plasma samples at baseline, after 2 h and after 7 days from transfusion. After transfusion with HBOCs, the LDH activity increased 10 times compared with baseline in both groups and remained elevated after 7 days. The auto-transfusion group did not exhibit any increase in LDH activity (Figure 2.8a).

GOT

GOT is a biomarker detected in plasma associated with liver and heart injury (Nigam, 2007). A significant increase was observed after 2 h from transfusion for animals treated with PEGylated hemoglobins. For both groups, however, GOT levels after 7 days were not statistically different from the pre-treatment ones (Figure 2.8b). GPT and amylase did not exhibit any elevation, suggesting that GOT levels were not from the liver.

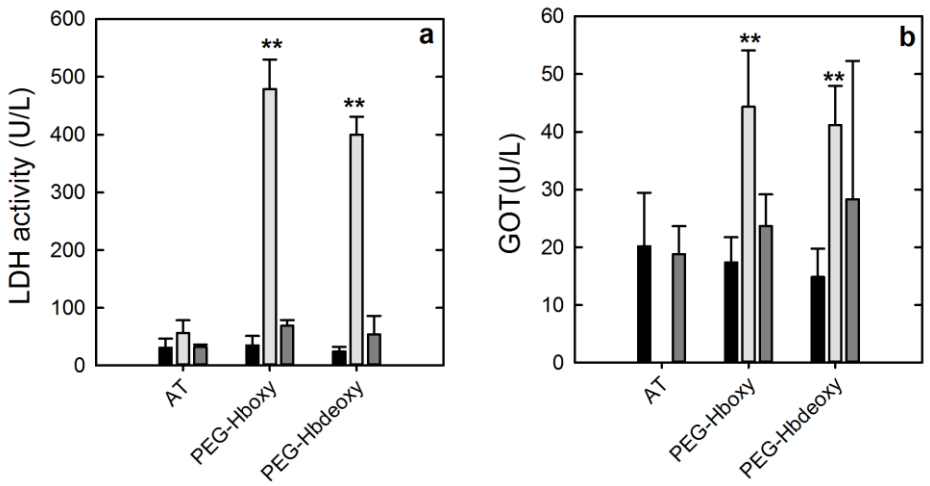

Figure 2.8: (a) LDH activity and (b) GOT activity for the autotransfusion group (AT) and for animals transfused with PEG-Hb^{oxy} and PEG-Hb^{deoxy}. Samples were collected before treatment (BL, black bars), after 2 hours from transfusion (light gray bars) and after 7 days (dark gray bars). Data are shown as mean ± SD**.** Statistical analysis: Ordinary one-way ANOVA followed by Tukey's multiple comparisons test(a)or Kruskal-Wallis test followed by Dunn's test(b). * $p<0.05$, **$p<0.01$ BL vs own PT, # $p<0.05$, ## $p<0.01$ PT PEG-Hb^{deoxy} vs PT PEG-Hb^{oxy} (at the same time point). AT=6/5/5, PEG-Hb^{oxy} n=8/8/3, PEG-Hb^{deoxy} n= 9/5/5.

Creatine kinase

Creatine kinase, a cardiac enzyme, is secreted in the circulation when the myocardial tissue is damaged. Creatine kinase concentrations were measured in all plasma samples. An increase was found after 2 h of transfusion in PEG-Hb^{oxy} and PEG-Hb^{deoxy} groups and auto-transfusion once compared to their baseline, but it was not statistically significant. After 7 days from treatment, the creatine kinase values returned to the baselines (Figure 2.9a).

cTnT

For further assessment of a possible heart tissue damage, plasma levels of cTnT were measured before transfusion (BL), after 2 hours and after 7 days. cTnT increased after 2 hours in animals treated with PEG-Hb^{deoxy}, but not in other groups (Figure 2.9b). After 7 days, cTnT levels were back to normal. cTnT is known to transiently increase as a consequence of ischemia–reperfusion injury, tissue damage produced when blood supply returns to the tissue after a period of ischemia. The elevation was in agreement with tachycardia in PEG-Hb^{deoxy} group.

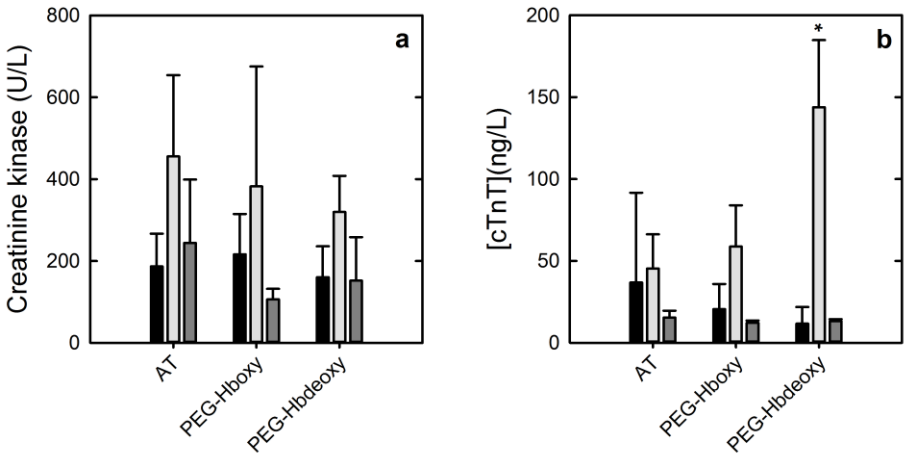

Figure 2.9: **(a)** Creatine kinase activity, **(b)** cTnT concentrations for the autotransfusion group (AT) and for animals transfused with PEG-Hb^{oxy} and PEG-Hb^{deoxy}. Before treatment (BL, black bars), after 2 hours from transfusion (light gray bars) and after 7 days (dark gray bars). Data are shown as mean ± SD**.** Statistical analysis: Ordinary one-way ANOVA followed by Tukey's multiple comparisons test(a)or Kruskal-Wallis test followed by Dunn's test(b). * $p<0.05$, BL vs own PT. (at the same time point). AT=6/5/5, PEG-Hb^{oxy} n=8/8/3, PEG-Hb^{deoxy} n= 9/5/5.

2.3.6 Oxidation markers in heart proteins and lipids

Carbonylation

The protein carbonyl content is a validated marker of oxidative stress and was measured in heart protein extracts (Weber D et al, 2015). Two quantitative assays were used to measure the carbonyl content, the Levine spectrophotometric method and a commercial ELISA assay based on an anti-DNPH antibody. Neither Levine nor ELISA showed significant differences among treated groups compared to the auto-transfusion group (Figure 2.12a and b). Both methods gave very similar values. The electrophoretic gel detection approach with fluorescein-5-thiosemicarbazide (Chaudhuri et al, 2006) and Oxy-blot of samples

probed with DNPH allowed for the identifications of individual carbonylated protein (Chaudhuri et al, 2006). Neither method showed any difference among groups (Figure 2.10, Figure 2.11). Data from densitometry analysis were expressed as arbitrary units, without any significant difference (Figure 2.12 c. and d).

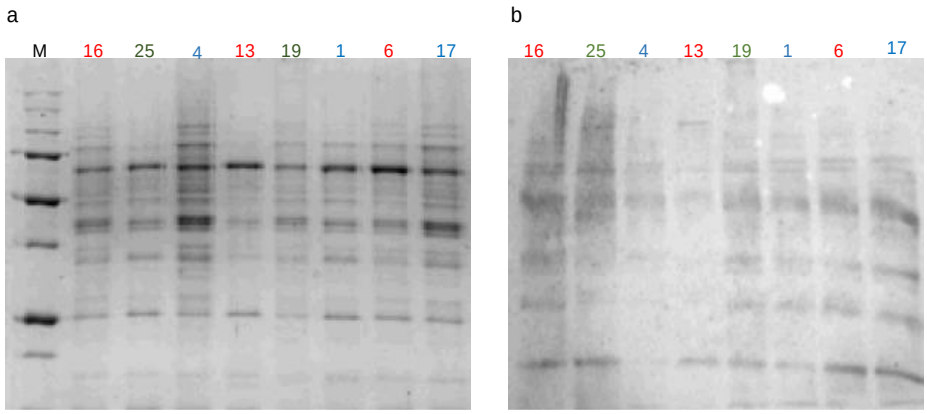

Figure 2.10: Carbonylated proteins in heart tissue extracts separated by SDS-PAGE gel. **(a)** SDS-PAGE gel of the whole extract and **(b)** the corresponding western blot. The numbers in blue, green and red refer to samples from AT, PEG-Hb^{oxy} and PEG-Hb^{deoxy}-treated animals, respectively.

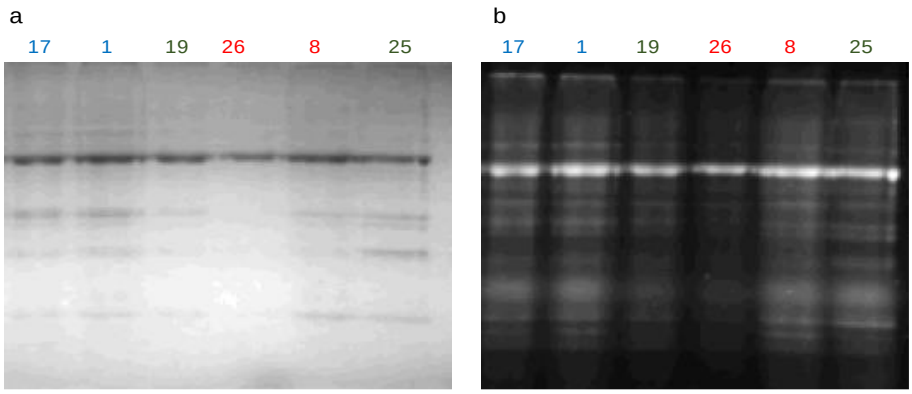

Figure 2.11: Carbonylated proteins in heart tissue extracts. **(a)** SDS-page stained with Coomassie blue, **(b)** fluorescein-5-thiosemicarbazide gel before Coomassie blue staining. Numbers in blue, green and red are related to samples from AT, PEG-Hb^{oxy} and PEG-Hb^{deoxy}, respectively.

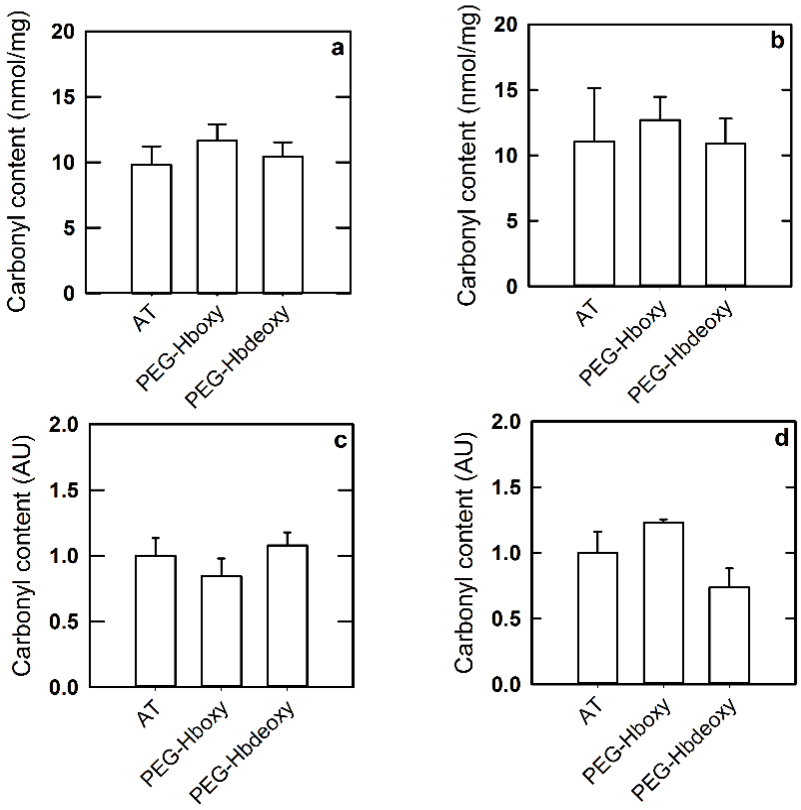

Figure 2.12: Carbonylation of heart proteins measure using **(a)** the Levine spectrophotometric method **(b)** an ELISA method **(c)** a fluorescein-5-thiosemicarbazide-based method and **(d)** the Oxy-blot method. Data are shown as mean ± SD. Statistical analysis: Ordinary one-way ANOVA followed by Tukey's multiple comparisons test.

Protein S-nitrosylation

Protein S-nitrosylation is an oxidative protein modification formed in cardiomyocytes as a mechanism of protection against oxidative and nitrosative stress (Sun et al, 2006). Western blot signals from the biotin switch detection method did not show any difference between bands. The data did not show any significant difference among groups (Figure 2.13a and b).

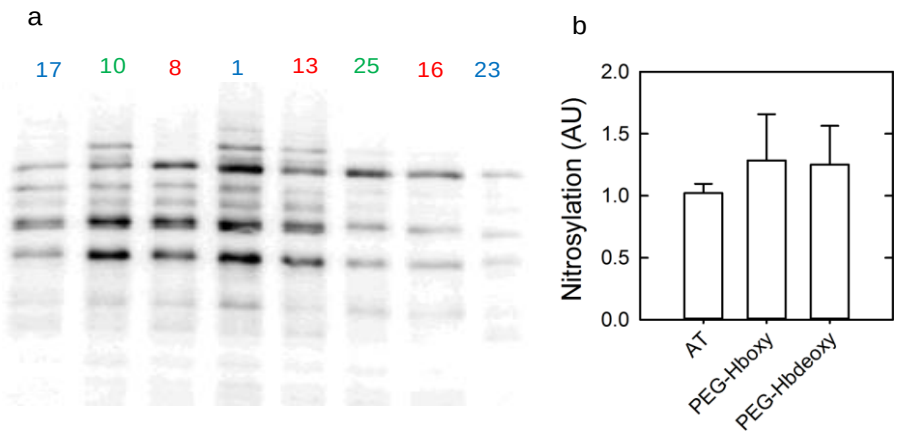

Figure 2.13: Nitrosylated protein in heart tissue extract. **(a)** Western blot of nitrosylated protein and **(b)** content of nitrosylated protein. Data are shown as mean ± SD. Statistical analysis: Ordinary one-way ANOVA followed by Tukey's multiple comparisons test. Numbers in blue, green and red are related to samples from AT, PEG-Hb^{oxy} and PEG-Hb^{deoxy}, respectively.

S-glutathionylation

S-glutathionylation is a biomarker of oxidative stress (Lind et al, 2002). Glutathionylated proteins were investigated in heart protein extracts from all animals. Western blots analysis did not show a significant difference among groups (Figure 2.14a and b).

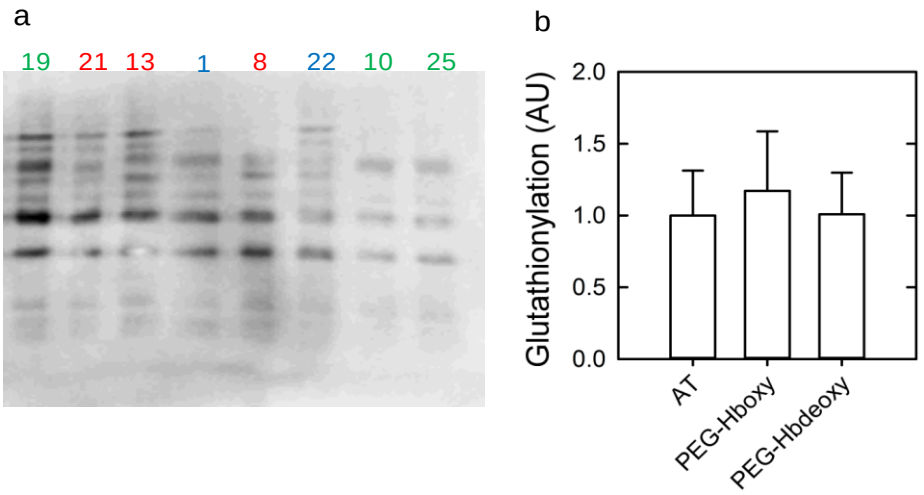

Figure 2.14: Glutathionylated proteins in heart extract. **(a)** Western blot of glutathionylated proteins and **(b)** content of nitrosylated protein. Data are shown as mean ± SD. Statistical analysis: Ordinary one-way ANOVA followed by Tukey's multiple comparisons test. Numbers in blue, green and red related to samples from AT, PEG-Hb^{oxy} and PEG-Hb^{deoxy}, respectively.

MDA and HNE adducts

Lipid peroxidation of polyunsaturated fatty acids generates HNE and MDA products which form adducts with the proteins side chains (Ayala et al, 2014, Weber et al, 2013). MDA and HNE adducts were investigated in heart tissue protein extracts from all animals. MDA did not exhibit any significant difference among groups (Figure 2.15a). However, HNE adducts measurements showed a significant increase in both groups transfused with HBOCs. The PEG-Hb^{oxy} group exhibited a higher elevation compared to PEG-Hb^{deoxy} (Figure 2.15b). HNE modified adducts were detected already as a reliable marker in Guinea pigs brains after HBOCs treatment (Butt et al, 2011, Babusiak, et al. 2005).

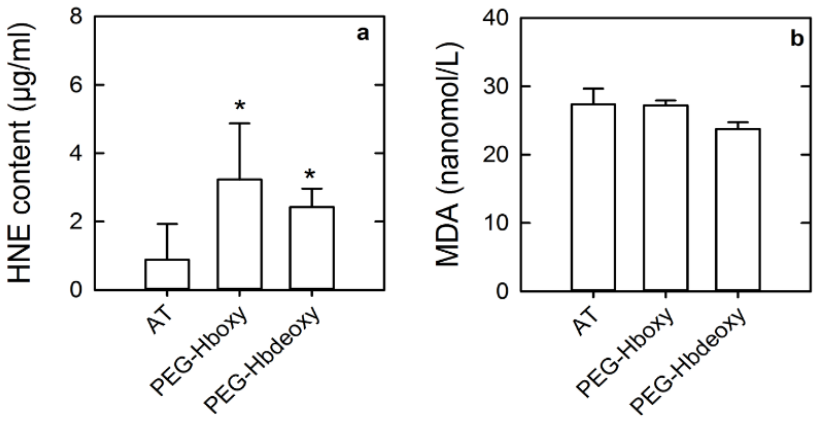

Figure 2.15: (a) Content of HNE adducts and **(b)** content of MDA adducts in heart protein extracts. Data are shown as mean ± SD. Statistical analysis: Ordinary one-way ANOVA followed by Tukey's multiple comparisons test. * vs AT. # vs other treatment groups. * $p<0.05$ treatment groups vs AT.

Lipid hydroperoxide

Lipid peroxidation was assessed in heart tissue lipid extracts from all animals. No significant difference was detected (Figure 2.16).

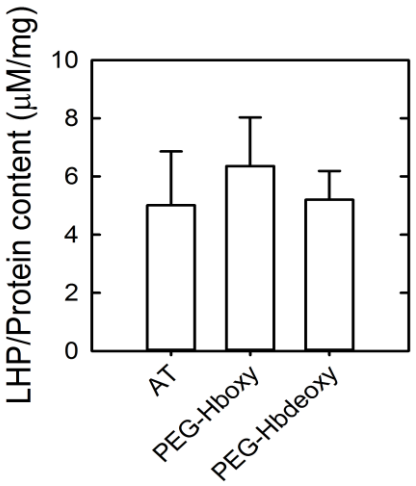

Figure 2.16: LHP content in heart protein extracts. Data are shown as mean ± SD. Statistical analysis: Ordinary one-way ANOVA followed by Tukey's multiple comparisons test.

Antioxidant enzymes and H_2O_2 in heart tissue extracts

Total SOD and catalase activities were evaluated in heart extracts. The catalase activity significantly decreased in the group transfused with PEG-Hb^{deoxy} in comparison to AT and the PEG-Hb^{oxy}-treated group (Figure 2.17a). The concentration of H_2O_2 exhibited a significant decrease in the group treated with PEG-Hb^{deoxy} compared to others (Figure 2.17b). SOD activity did not show any significant difference among groups (Figure 2.17c). A decrease in catalase activity was already observed in Guinea pigs exposed to HBOCs (Rentsendorj et al, 2016). The loss of catalase activity may be due to the enzyme down-regulation resulting from ROS production and inflammations (Venkatesan et al, 2007).

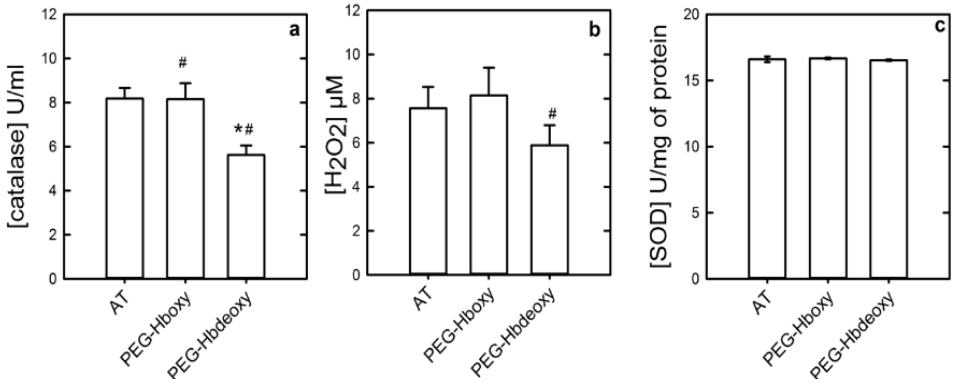

Figure 2.17: Antioxidant enzymes in heart extracts. **(a)** Concentrations of catalase, **(b)** H_2O_2 and **(c)** SOD in heart extracts. Data are shown as mean ±SD. Statistical analysis: Ordinary one-way ANOVA followed by Tukey's multiple comparisons test. * $p<0.05$ vs AT; # $p<0.05$ PEG-Hb^{oxy} vs PEG-Hb^{deoxy}.

2.3.7 Oxidation markers in kidney proteins and lipids

Carbonylation

The carbonyl protein content in kidney extracts was measured using a modified Levine method after an additional step for heme removal, which proved crucial to correctly assess the absorption of DNPH (Figure 2.18). No difference was detected among groups neither from the Levine method nor the electrophoretic gel detection approach with fluorophore analog (Figure 2.19a and b).

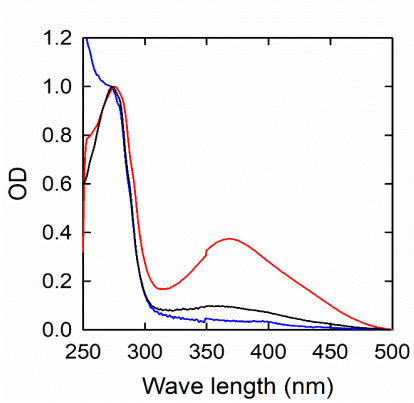

Figure 2.18: Spectra of a renal tissue extract. The red line is the spectrum of a sample that underwent all modifications without heme removal and DNPH reaction. The blue line is the same sample upon the introduction of a heme-removing step. The black line is the sample treated for heme removal and reacted with DNPH.

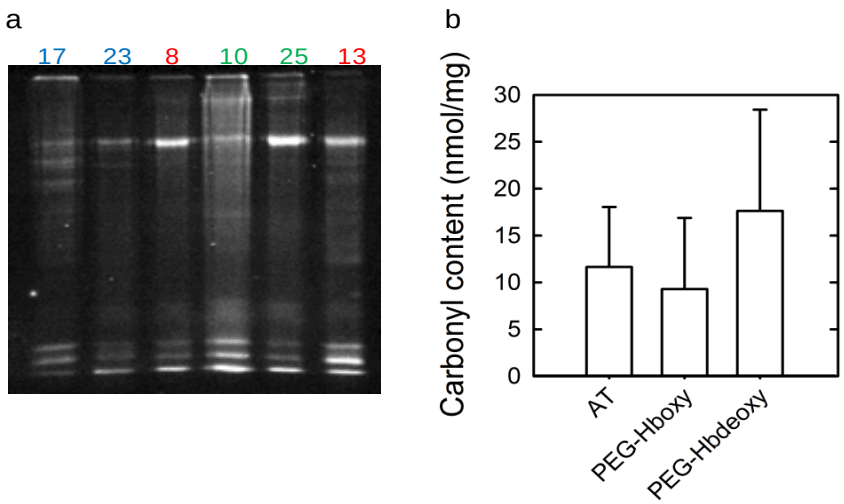

Figure 2.19: **(a)** SDS-PAGE from kidney proteins treated with fluorescein-5-thiosemicarbazide, **(b)** Carbonyl contents in kidney extract by applying the modified Levine method**.** Data are shown as mean ±SD. Statistical analysis: Ordinary one-way ANOVA followed by Tukey's multiple comparisons test. Numbers in blue, green and red are related to samples from AT, PEG-Hb^{oxy} and PEG-Hb^{deoxy}, respectively.

S-nitrosylation in kidney proteins

Nitrosylted proteins were assessed in all renal protein extracts. The data from Western blot and densitometric analysis of bands did not show any significant difference between the three groups (Figure 2.20).

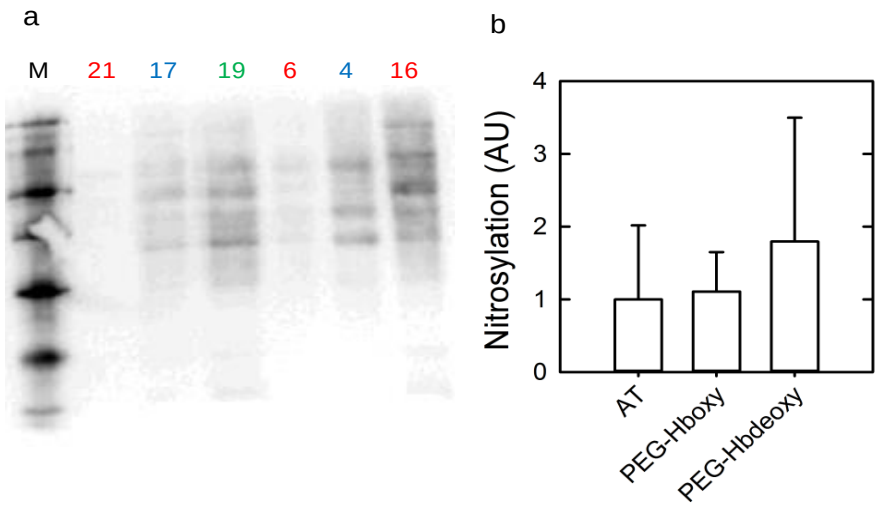

Figure 2.20: Nitrosylated protein content in kidney extracts. **(a)** Western blot of nitrosylated proteins in individual plasma samples; M is a biotinylated molecular weight marker(Sigma Aldrich), numbers in blue, green and red are related to samples from AT, PEG-Hb^{oxy} and PEG-Hb^{deoxy}, respectively. **(b)** Densitometric analysis of the Western blots, grouped by treatment group. Data are shown as mean ± SD. Statistical analysis: Ordinary one-way ANOVA followed by Tukey's multiple comparisons test.

S-glutathionylation

Protein glutathionylation is a reversible protein modification that was validated as an oxidative stress biomarker. The data from Western blot and densitometric analysis of kidney extracts did not show any significant difference between the three groups (Figure 20 a and b).

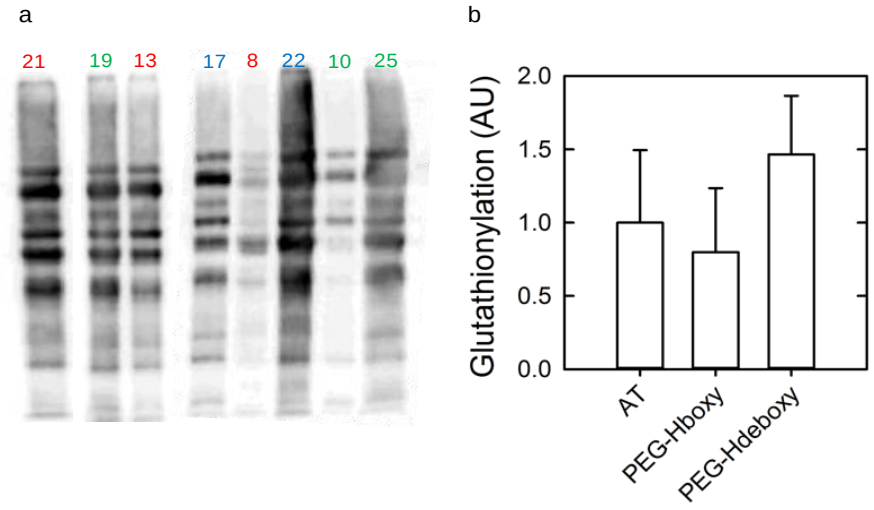

Figure 2.20: Glutathionylated proteins in kidney extracts. **(a)** Representative Western blot of glutathionylated protein in individual protein extracts; **(b)** Analysis of the Western blot. Data are shown as mean ± SD. Statistical analysis: Ordinary one-way ANOVA followed by Tukey's multiple comparisons test. Numbers in blue, green and red are related to samples from AT, PEG-Hb^{oxy} and PEG-Hb^{deoxy}, respectively.

MDA and HNE adducts

MDA and HNE adducts in kidney protein extracts were investigated as oxidative stress biomarkers. HNE adducts showed an elevation only in the group transfused with PEG-Hb^{oxy} (Figure 2.22a). MDA adducts exhibited a significant increase also in PEG-Hb^{oxy} group compared to the others. The result from this assay confirmed the results of plasma analytes related to kidney function (Figure 2.22b). MDA and HNE adducts were already identified as markers of oxidative stress in other experiment carried out on Guinea pigs transfused with HBOCs to assess the role of haptoglobin – a protein binds the free hemoglobin in the plasma to inhibit

its oxidative activity – in decreasing the cellular Hb toxicity (Boretti et al, 2009).

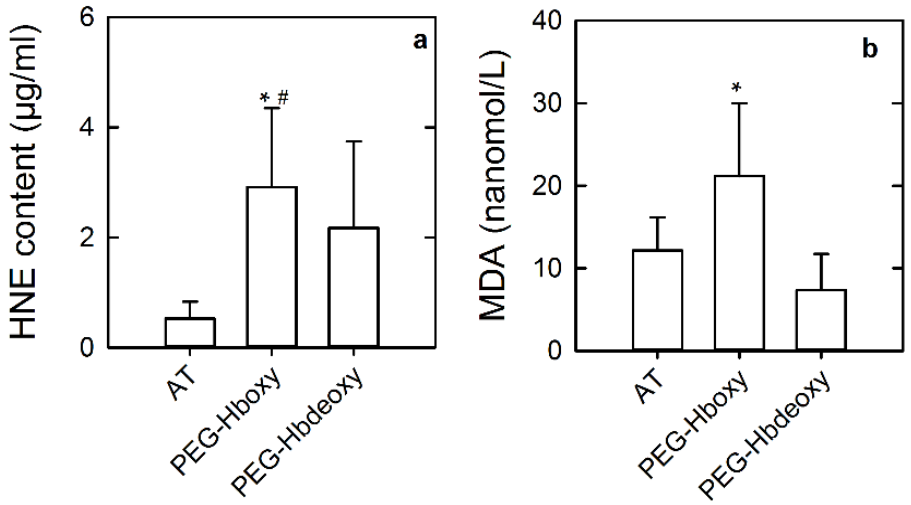

Figure 2.22: (a) HNE adducts and **(b)** MDA adducts in kidney protein extracts. Data are shown as mean ± SD. Statistical analysis: Ordinary one-way ANOVA followed by Tukey's multiple comparisons test. * $p<0.05$ vs AT; # $p<0.05$ PEG-Hb^{oxy} vs PEG-Hb^{deoxy}.

Lipid hydroperoxide

Lipid hydroperoxide content in the kidney lipid extracts was measured, but no significant difference was found among groups (Figure 2.23).

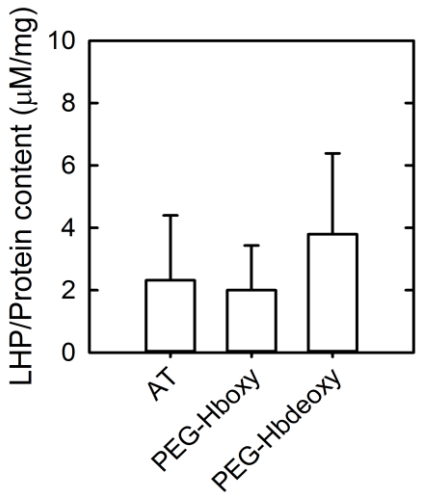

Figure 2.23: LHP content in heart protein extracts. Data are shown as mean ± SD. Statistical analysis: Ordinary one-way ANOVA followed by Tukey's multiple comparisons test.

Antioxidant enzymes and H_2O_2 in kidney tissue extracts

The concentration of hydrogen peroxide was measured in samples from all groups and no difference was found (Figure 24a). Antioxidant enzyme activities were assessed in kidneys proteins extracts and the SOD activity did not exhibit any significant difference among groups. The catalase activity could not be measured because of the interference of heme groups (Figure 24b).

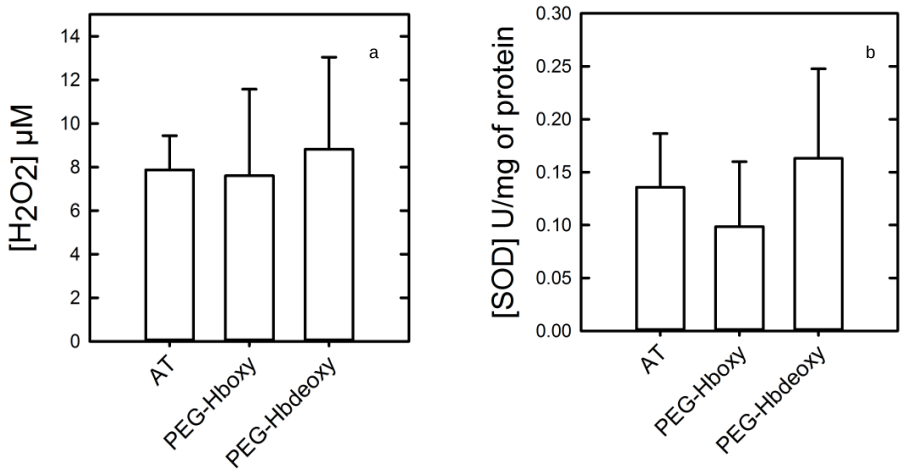

Figure 2.24: Antioxidant enzymes in kidneys extracts. **(a)** Concentrations of H_2O_2 and **(b)** SOD. Data are shown as mean ±SD. Statistical analysis: Ordinary one-way ANOVA followed by Tukey's multiple comparisons test.

2.4 Conclusions

An exchange transfusion model in Guinea pigs was designed to assess the differential oxidative stress levels induced by two HBOCs, modified with the same PEGylation chemistry but endowed with different oxygen-binding properties. After 7 days of transfusion, the concentration of HBOCs decreased to 90%. The experimental results showed some differences among groups. L-lactate level decreased in animals treated with PEG-Hb^{oxy}, showing that HBOCs with higher oxygen affinity can increase the oxygen partial pressure at the capillary level and reduce the anaerobic metabolism. Plasma levels of creatinine and urea were elevated in the group transfused with PEG-Hb^{oxy}, pointing to a kidney function deterioration. The measured biomarkers in kidney tissue extracts confirmed the plasma results. MDA adducts were elevated in

PEG-Hb^{oxy} and the HNE adducts were elevated in both treatment groups. These results suggested that PEG-Hb^{oxy}, with higher oxygen affinity, could lead to higher nephrotoxicity in comparison to PEG-Hb^{deoxy}. This effect could be related to a higher concentration of dimers in PEG-Hb^{oxy}, which is more prone to renal filtration. DNA oxidative stress biomarkers showed an increase in both PEG-Hb^{oxy} and PEG-Hb^{deoxy} groups. All plasma biomarkers related to heart function showed a transient elevation after 2 h and returned to the normal physiological values after 7 days, suggesting short-term toxicity. Biomarkers from heart tissue extracts did not show any difference between groups. HNE was the only marker that was elevated in both PEG-Hb^{oxy} and PEG-Hb^{deoxy} compared to auto-transfusion.

Overall, these results indicate that differences in oxygen affinity in two otherwise very similar products are responsible for a different response both in terms of therapeutic effect and oxidative stress. We found that PEG-Hb^{oxy} with higher affinity produced higher tissue oxygenation in comparison to PEG-Hb^{deoxy}, which is possibly correlating with the higher oxidative stress it induced. Moreover, this work strongly contributes to the ongoing debate on the requirements that blood substitutes should have in terms of oxygen binding parameters.

Chapter 3: PEGylation of engineered fetal recombinant hemoglobin

3.1 Introduction

As mentioned in Chapter 1, fetal hemoglobin exhibits potential advantages over HbA as a precursor for HBOCs, although, unlike HbA, it needs to be produced in a recombinant system due to the obvious limitation of its natural source. Several approaches have been attempted: i) to express recombinant HbF ii) to introduce in HbA mutations inspired by HbF to reduce oxidation and heme loss and to increase stability iii) to design chemical modifications of either HbF or mutated HbA to further improve the oxygen-binding properties.

This project was focused on the characterization and chemical modification of a recombinant mutant fetal hemoglobin, from now on indicated as F45, expressed in *E. coli* and carrying three mutations: i) L96Y at the γ subunit ii) V67F on the γ subunits and iii) L29F on the α subunits. Mutations L29F(α) and V67F(γ) - to decrease the autoxidation rate and to decrease NO reactivity - are covered in John Olson's / Somatogen's patent WO1998050430A2 (as already described in the introduction chapter 1.4.4). Mutation L96Y(γ) - to introduce an electron transfer pathway to donate electrons and reduce the non-functional ferric met-Hb form - has been patented by the University of Essex, United Kingdom (WO2018167469A1).

My role in this project consisted in the characterization of the HbF mutant in terms of oxygen affinity and cooperativity. Additionally, I

PEGylated the protein on a large-scale to be used as a transfusion solution for *in vivo* experiments at the University of Essex, United Kingdom.

3.2 Materials and methods

3.2.1 Materials

High-quality chemicals were purchased from Sigma-Aldrich (St. Louis, MO, USA); MAL-PEG was obtained from Iris Biotech GmbH (Marktredwitz, Germany). Anti-Hb antibodies conjugated with horseradish peroxidase (HRP) for Western blots were from Abcam (Cambridge, UK), the HRP substrate CheLuminate-HRP PicoDetect was from PanReac AppliChem (Darmstadt, Germany). Sartobind Q ® STIC PA endotoxin removal capsules 4 were from Sartorius. Lysine and cysteine were from Fluka. The Vacuum 0.2 µm filters were purchased from Sarstead. All plasticware, glasswares, and tubes were washed with NaOH and rinsed with endotoxin-free water.

3.2.2 Recombinant fetal hemoglobin preparation

The fetal hemoglobin F45 mutant was expressed in *E. coli*. To improve stability, the recombinant protein was exposed to CO, as the carboxy form is less prone to oxidation. The protein at 3.5 mM concentration was stored at -80°C. Aliquots were thawed one day before the experiments and centrifuged at 10000 x g for 30 minutes at 4°C to remove any precipitated protein. The hemoglobin solution was then filtered with 0.2 µm vacuum filters and its concentration was brought to 2.5 mM with a

buffered solution containing 50 mM sodium phosphate, 100 mM KCl, 0.5 mM EDTA, pH 7.0. The final hemoglobin solution volume was 154 mL.

3.2.3 PEGylation

Inositol hexaphosphate (IHP) was added as a powder to the hemoglobin solution (1.2 mol/Hb tetramer mol) and deoxygenated in nitrogen flux in a 1 L bottle. CO was removed by photolysis by overnight illumination at 20°C under gentle shaking. All the reagents were added in the absence of oxygen to keep Hb under anaerobic conditions. On the second day, the Hb solution was reacted with iminothiolane (IMT) (80 mol/tetramer mol). After 1.5 min, 5 KDa MAL-PEG was added (12 mol/tetramer mol) and incubated in the dark for 25 min. To stop the reaction, 14 mL of lysine solution (4.8-5 M) was added, followed by 8 mL of a cysteine solution (0.9 M) after 5 min.

The solution of PEGylated F45 was collected and centrifugated at 10000 g for 30 minutes at 4°C to remove any precipitated Hb. A phosphate buffer saline solution (PBS) was used for dialysis to remove the unreacted chemicals. The Hb solution was concentrated by using a 50 kDa cut-off tangential flow membrane and then sterilized using a 0.2 µm vacuum filter. Finally, endotoxins were removed and the concentration was brought to 2.5 mM by using sterilized, endotoxin-free PBS. The final PEGylated Hb solution was aliquoted into separate Falcon tubes, flashed-frozen in liquid nitrogen and shipped to be used for the *in vivo* experiment.

3.2.4 SDS-PAGE, iodine stain gel and western blot

The purity and yield of PEGylated hemoglobin were assessed by image analysis of Western blots and SDS-PAGE gels, stained with either Commassie blue or a specific iodine-based stain that binds selectively to PEG groups. For the Western blot analysis, bovine serum albumin was used to block the membrane, which was then probed with an anti-Hb antibody conjugated with horseradish peroxidase (HRP). The PEG-specific staining solution consisted of 50 mL of 5% (w/v) $BaCl_2$ and 2.5 mL of 0.05 M iodine. Images of gels and Western blots were collected with a ChemiDoc™ system (Bio-Rad Laboratories, Inc., Hercules, California, U.S.A.).

3.2.5 Hemoglobin Concentration determination

Hb concentration and redox state were determined at every step by collecting absorption spectra in the range 450-700 nm using a Cary 4000 UV-Vis spectrophotometer. The mutant spectra were compared with purified HbA spectra, which were used as a reference.

3.2.6 Oxygen binding measurements

The oxygen binding properties were determined by using a Cary 4000 UV-Vis spectrophotometer for both F45 and PEG-F45. Samples were diluted in a buffer containing 100 mM HEPES, 100 mM sodium chloride, 1.2 mM sodium phosphate, 1 mM EDTA, pH 7.0 to reach a final concentration of 100 μM. To slow down met-Hb formation during the experiment, the Hayashi enzymatic mixture (glucose-6-phosphate, G-6-P

dehydrogenase, nicotinamide adenine dinucleotide phosphate, ferredoxin, ferredoxin NADP reductase, and catalase) was added. The samples were loaded in a 2 mm cuvette fused to a reservoir for gas equilibration (Ronda et al, 2008a). Helium\oxygen mixtures with a total flow of 50 ml/min were produced by an Environics 4000 gas mixer. Samples were thermostatted at 25°C under continuous shaking. At every oxygen partial pressure, after a 30 min equilibration time, spectra were collected in the range 450-750 nm. At the end of every titration, the spectra of the 100% oxygen-saturated sample and DTO-reduced sample were collected and used as a reference for data analysis. The fractional saturation was calculated by analyzing the spectra as a linear combination of oxy-, deoxy and met- spectra.

3.3 Results and discussion

3.3.1 Characterization of engineered HbF (F45)

Spectra of oxy F45 showed an anomalous peak at 620 nm (Figure 3.1). Moreover, neither deoxygenation in helium, nor reduction with sodium dithionite led to the formation of the typical peak centered at 555 nm of deoxy-Hbs (Figure 3.1). The band centered at 620 nm did not disappear in either condition. It can be hypothesized that these spectral features are associated with a heme derivative different from met-Hb. It has been reported in the literature that some bacterial expression systems lead to the formation of modified heme groups with different characteristics (Lloyd & Mauk, 1994). Particularly, the peak at 620 nm could be related

to the formation of sulfhemoglobin, which is formed once inorganic sulfide ions react with the heme iron (Varnado et al, 2013).

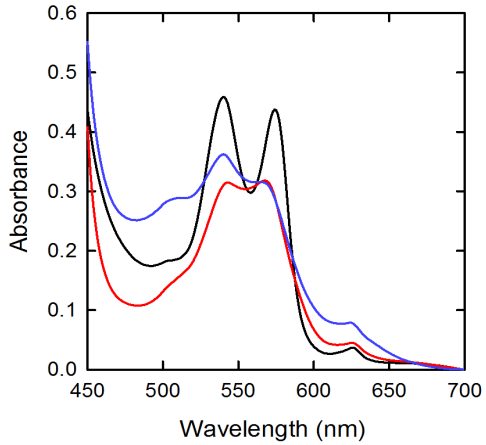

Figure 3.1: The spectra of F45 mutant in the presence of oxygen (black), upon deoxygenation in helium (red) and after reduction with sodium dithionite (blue).

3.3.2 PEGylation of recombinant HbF

The PEGylation yield was assessed by SDS-page and compared in the same gel with PEGylated HbA (Figure 3.2a). PEGylated HbF was also investigated by using a special iodine staining solution which reacts only with proteins conjugated with PEG (Figure 3.2b). The yield of PEGylation was assessed by densitometric analysis of the gel (Figure 3.2). The band around 10 kDa corresponds to the unmodified monomer; the expected MW is around 16 kDa but it was shown to have an anomalous electrophoretic migration. The bands at 32, 37 and 50 kDa are the PEGylated derivatives. Their identity as Hb derivatives was confirmed by Western blotting using specific anti-hemoglobin antibodies (data not shown).

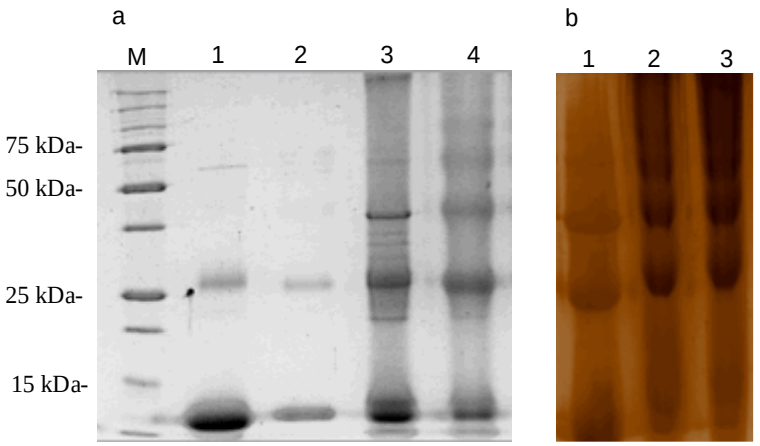

Figure 3.2: (a) Coomassie-stained SDS-PAGE, (1): HbA; (2): PEG-HbA, (3): F45 mutant, (4): PEG-F45. **(b)** Iodine-staining of an SDS-PAGE gel, (1): F45, (2,3): PEG-F45, bands in the darker color are related to PEG-F45 in comparsion to lane 1.

3.3.3 Characterization of PEGylated F45

The spectrum of the PEGylated mutant was collected in the oxygenated form after DTO addition (Figure 3.3). Similarly to unmodified F45, the spectra of PEG-F45 showed a band at 560 nm not observed in the spectra of wt HbF. It is possible that PEGylation affected the coordination of the heme. Indeed, the peak at 560 nm in the DTO-treated form is reminiscent of bis-histidyl hexacoordinated globins, in which the distal histidine, normally not bound to the heme iron in HbF or HbA, forms a coordination bond similar to that of the proximal histidine. This ligation state, in the Fe^{2+} deoxy form typically exhibits a band centered at 560 (Merlino et al, 2011).

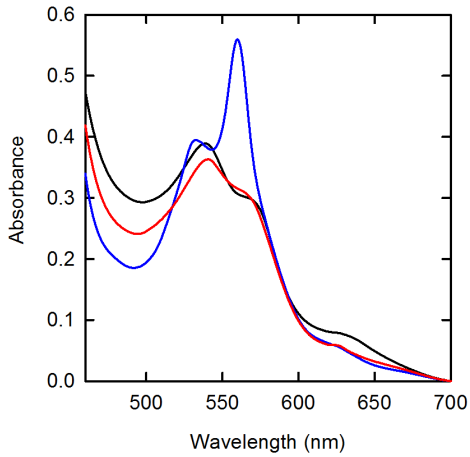

Figure 3.3: Spectra of PEG-F45 mutant in the presence of oxygen (black), upon deoxygenation in helium (red) and after reduction with sodium dithionite (blue).

3.3.4 Oxygen binding curve of F45 and PEG-F45

The oxygen binding curves were investigated for both F45 and PEGylated F45 under similar experimental conditions. The data are shown in Figure 3.4 and Table 1. Mutant F45 exhibited a high affinity for oxygen, with a measured p50 of 1.47 torr and low cooperativity compared to HbA. Although the PEGylation reaction was carried out in the T state, PEGylated F45 had a higher affinity for oxygen than F45, and no cooperativity. The same increase in oxygen binding affinity was observed once HbA was PEGylated in the presence of oxygen, as we obtained in (chapter2) from PEG-Hb^{OXY}, but not in its absence (Caccia et al, 2009). The higher oxygen affinity could be related to the dissociation to dimers.

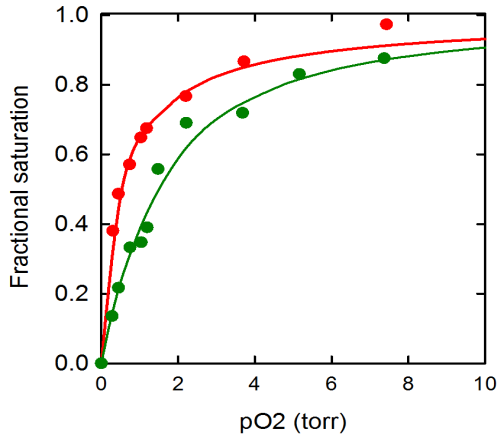

Figure 3.4: Oxygen binding curves of F45 (in green) and PEG-F45 (in red). The dots represent the experimental data and the solid lines in the same color represent the curve fit to the Hill equation. The curves were measured at 25 °C in the presence of the Hayashi reducing system.

	HbA	F45	PEG-F45
p50 (Torr)	2.61 ± 0.05	1.5 ± 0.1	0.52 ± 0.04
n	2.36 ± 0.06	1.2 ± 0.1	0.89 ± 0.07

Table 3.1. Oxygen binding parameters for the F45 mutant, PEGylated F45 and HbA.

3.4 Conclusions

Recombinant fetal hemoglobin was suggested to have advantages over recombinant HbA as a starting material for the production of HBOCs. In this project, genetic manipulation was used to engineer HBOCs with enhanced properties by introducing three mutations at different sites to decrease NO scavenging and to reduce methemoglobin formation. The oxygen affinity of the F45 mutant was high in comparison to HbA. Spectra of F45 indicated the presence of a heterogeneous mixture of ligation forms, conformations, or heme derivatives. The purified large scale Hb solution was modified by PEGylation to increase the size and the protein retention time in the circulation. The PEGylation reaction resulted in a product with a higher affinity for oxygen in comparison to F45, with no cooperativity. The PEGylated solution served as an HBOCs for *in vivo* experiments at Essex University, United Kingdom. Based on preliminary data from *in vivo* administration, this study might demonstrate that PEGylated Hb, once proper mutations will be introduced, may allow overcoming the main limitations that have hinder so far the development of safe and effective HBCOCs, such as autooxidation and vasoconstriction.

Chapter 4: Polymerized HBOCs as perfusion solution for organs

4. 1 Introduction

Organ allotransplantation is often the only medical procedure available for many conditions resulting in organ failure. Globally, the lack of organs suitable for transplantation is one of the main challenges in medicine. As the difference between the number of cases requiring transplantations and the number of donated organs increases, the expansion of the pool of available organs is crucial. One strategy consists in the use of marginal organs, i.e. those from older donors or those who died from cerebrovascular accidents (Saidi & Hejazii Kenari, 2014; Schütte-Nütgen et al, 2019).

The primary option to preserve organs before transplantation is cold static preservation (CSP), which reduces their metabolism. However, this method has many drawbacks, including the risk of early graft dysfunction. Recently, to tackle CSP limitations, an innovative strategy has been adapted by using *ex vivo* normothermic perfusion, providing sufficient oxygenation and nutrients at 37 °C, thus giving the organ the possibility to recuperate under pseudo-physiological conditions (Ceresa et al, 2018; Eshmuminov et al, 2018). Organs preservation in a normothermic perfusion machine requires an extracorporeal oxygenation method to maintain active cellular metabolism, not only to sustain organ viability, but also to maximize the success of repairing and using marginal organs - which is not appropriate for transplantation. Therefore, the perfusion

solution must be able to provide sufficient oxygenation to sustain active ATP production. In general, red blood cells (RBCs) suspensions are typically used to perfuse allografts at 37 °C. However, it has been found that RBCs have many drawbacks. Particularly, the oxygen-carrying capacity decreases with time as a result of haemolysis due to the mechanical effect of rotary blood pumps (Sakota et al, 2008).

As a more efficient alternative to RBCs, artificial oxygen carriers have been suggested. HBOCs have given results comparable to RBCs in many studies and do not undergo mechanical alteration (Aburawi et al, 2019; Laing et al, 2017; Matton et al, 2018). A comparison of kidney perfusion with RBCs and HBOCs under normothermic conditions showed a higher degree of tubular injury with RBCs, whereas no histological damage was noticed in tissues perfused with HBOCs. A significant improvement of lactate levels in kidneys perfused with HBOCs was also observed (Aburawi et al, 2019). HBOCs perfusion also resulted in improved vascular flow and ATP production. A decrease in reactive oxygen species was found in organs perfused with polymerized HBOCs in comparison to RBCs (Laing et al, 2017; Matton et al, 2018). Pigs that were transplanted with livers perfused with HBOCs under subnormothermic (20°C) conditions achieved 100% survival rates. An interesting result is that improved HBOCs oxygenation of liver grafts oxygenation triggered cell regeneration (Fontes et al, 2015). It should also be pointed out that the side effects observed in HBOCs administration in vivo are not expected in organ perfusion, as the quantity of HBOCs reaching the circulation of the

recipient of the graft is not detectable, as organs are extensively washed before transplantation (Laing et al, 2017).

Among the possible HBOCs available for the aforementioned application, polymerized HBOCs proved particularly useful, as they are less costly than PEGylated HBOCs and less viscous. General aspects of polymerized hemoglobins were described in chapter 1. As the required oxygen-binding properties of HBOCs to be perfused should be similar to those of RBCs, bovine Hb (bHb) has been suggested as a starting point, as it exhibits an intrinsically higher p50 in comparison to HbA, around 29 mmHg. The p50 of its polymerized derivatives can be further modulated depending on the polymerization protocol. For example, Hemopure is a product based on polymerized bHb with a p50 of 36 mmHg (Zhou et al, 2011).

As a part of my Ph.D. work, I prepared and characterized a polymerized bHb produced in large amounts, optimizing the purification and formulation protocols. This product is currently being used by collaborators at the S. Orsola Hospital in Bologna in preliminary experiments on human kidneys. The perfused organ will be analyzed histologically and biochemically.

4.2 Materials and methods

4.2.1 Materials

Glutaraldhyde (25%), $NaBH_4$, NaOH and other chemicals were purchased from Sigma-Aldrich (St. Louis, MO, USA). $K_3[Fe(CN)_6]$ was brought from Merk (Darmstadt, Germany). Sterile plasticware, glassware, and tubes used were washed with NaOH and rinsed with sterilized water.

4.2.2 Bovine hemoglobin preparation

Fresh bovine blood (8 L) was collected using EDTA as an anticoagulant (1.5 mg/mL of blood). The plasma fraction was separated by centrifugation at 15000 xg for 10 minutes to pellet red blood cells (RBCs). RBCs were washed three times using three volumes of isotonic saline solution (0.9% NaCl) and were centrifuged at every washing step at 10000 xg for 30 minutes at 4°C. To induce RBCs lysis, the homogenizer PandaPlus 200 (GEA ®) was used, applying a 500 torr pressure for one cycle. The RBCs lysate was centrifuged to remove cell debris at 10000 xg for 1 h at 4°C. The solution containing bHb was recovered and kept at 4°C.

4.2.3 Bovine hemoglobin polymerization

The polymerization reaction between bHb and glutaraldehyde as the cross-linking agent was carried out according to a previous protocol developed by the Buehler group (Zhou et al, 2011). Oxygenated bHb was reacted with 25% glutaraldehyde using a 10:1 molar ratio of glutaraldehyde:Hb. The reaction was carried out in the dark at 37 °C for 3 h under continuous stirring. The reaction was then quenched by using

$NaBH_4$, in a 1:2 molar ratio of glutaraldehyde: $NaBH_4$. The quenching solution was prepared in 20 mM PBS, pH 8. The quenching reaction was carried at 4°C with stirring for 30 min. The polymerized hemoglobin solution was then passed through a tangential flow filter to remove unreacted glutaraldehyde at 4°C for 24 h by using 5 L Ringer's solution (7.2 g/L NaCl, 0.017 g/L $CaCl_2$ and KCl 0.37 g/L, pH 7.4) as exchange buffer. The same solution was used to dilute polymerized Hb to the concentration of 3.5 g/dL for final use. The HBOC solution was frozen and stored at -80°C.

In another preparation, the reaction was quenched with 0.1 M glycine in 50 mM Tris-HCl.

4.2.4 Hemoglobin concentration and metHb level determinations

The bHb concentration and met-bHb were determined before and after polymerization by collecting absorption spectra in the range 450-700 using a Cary 4000 UV-Vis spectrophotometer. $K_3[Fe(CN)_6]$ was used to get a cyanomet-Hb spectrum to determine the metHb ratio.

4.2.5 SDS-PAGE of bHb and polymerized bHb

Coomassie-stained SDS-PAGE gel was used to evaluate the polymerization reaction of bHb and to compare it to the non-reacted bHb sample. The gel image was acquired with a ChemiDoc™ system (Bio-Rad Laboratories, Inc., Hercules, CA, USA) and analyzed with the Image Lab™ software (Bio-Rad Laboratories, Inc., Hercules, CA, USA).

4.2.6 Oxygen binding measurements

The polymerized bHb oxygen-binding properties were measured and compared to those of bHb under the same experimental condition. A Cary 4000 UV-Vis spectrophotometer was used to carry out the measurements. Samples were diluted in a buffered solution containing 100 mM HEPES, 1 mM EDTA, pH 7.0 to reach a final concentration of 200 μM. To slow down met-Hb formation during the experiment, the Hayashi enzymatic mixture (glucose-6-phosphate, G-6-P dehydrogenase, nicotinamide adenine dinucleotide phosphate, ferredoxin, ferredoxin NADP reductase, and catalase) was added. The experiments were carried out using a 2 mm cuvette fused to a reservoir for gas equilibration (Ronda et al, 2008). Helium\oxygen mixtures with a total flow of 50 mL/min were produced by an Environics 4000 gas mixer. The sample in every titration experiment was thermostatted in a water bath at 25°C under continuous shaking. For every fractional oxygen saturation at a defined pressure, the spectra were collected in the range 450-750 nm. At the end of every titration, the spectra of the 100% oxygen-saturated sample and DTO-reduced sample were collected and used as a reference for data analysis. The fractional saturation was calculated by analyzing the spectra as a linear combination of oxy-, deoxy and met- spectra.

4.3 Results and discussion

4.3.1 Polymerized Hb preparation

bHb (4 L) at a concentration of 4.5 mM (7.2 g/dL) was obtained from 8 L of blood and was used as a starting point for the polymerization.

4.3.2 Polymerized bHb characterization

SDS-PAGE of polymerized bHb

SDS-PAGE of bHb and polymerized bHb was used to assess the degree of polymerization. The polymerized Hb distribution in SDS-PAGE was assessed by densitometric analysis. The band around 10 kDa corresponds to the unmodified monomer; the expected MW is around 16 kDa but it was shown to have an anomalous electrophoretic migration. 37% of Hb was in the unmodified monomer. 40.3%, 14% and 7.5 % of monomers were polymerized – to a different extent – giving bands of apparent molecular weight of around 32, 37 and 250 kDa, respectively (Figure 4.1).

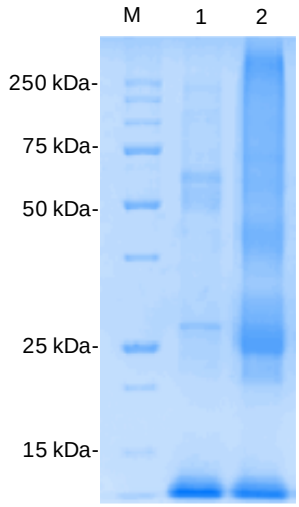

Figure 4.1: Coomassie blue-stained SDS-PAGE, M: molecular wight marker, (1): bovine hemoglobin, (2): a glutaraldehyde polymerized bHb by using 1:10 ratio (bHb:G).

Methemoglobin levels in the Polymerized bHb

Spectra of polymerized bHb were acquired at the end of dialysis and data were analyzed as a linear combination of three reference spectra of pure deoxy, oxy, and met bHb (Figure 4.2) to retrieve - at the same time - the fractional saturation and the metHb content for samples exposed to different oxygen pressures. Initially, the bovine hemoglobin solution exhibited a MetHb level of 3%. The polymerized solution exhibited a metHb level of 12.9%.

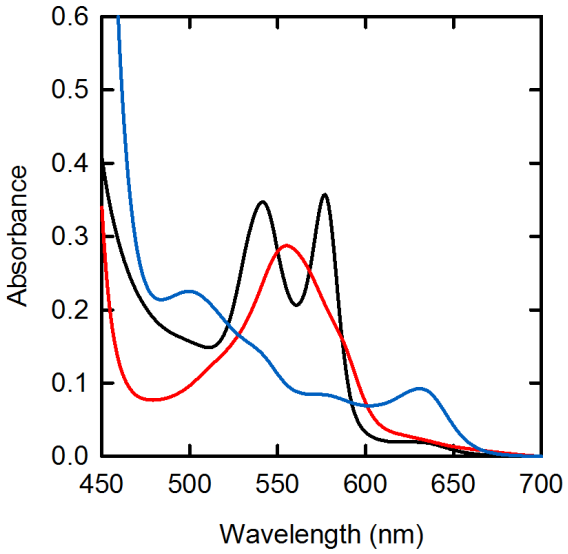

Figure 4.2: Spectra of polymerized bovine Hb. The spectrum of oxygenated Hb is in black, the spectrum of deoxygenated Hb is in red, and spectrum of methemoglobin is in blue.

Oxygen binding curve of polymerized bHb

The oxygen binding curves for bHb and polymerized bHb are shown in Figure 4.3. The p50s and Hill coefficients are reported in Table 1. The measured p50 (19.82 torr) and Hill coefficient (2.7 torr) for unmodified bHb were in the range reported in the literature (Fronticelli & Bucci, 1994; Julie H et al, 2004). The p50 of polymerized bHb decreased to 8.2 torr and lost cooperativity. The reason for the decrease in the p50 can be explained by the shift of the T-R equilibrium towards the R form or by a decrease in sensitivity to Cl^-. The increase in oxygen affinity was expected

as it was also reported in other works (Julie H et al, 2004). As mentioned in the introduction, a higher affinity is not negative per se, as it was shown that high-affinity HBOCs tend to better deliver oxygen to hypoxic tissues (Fontes et al, 2015).

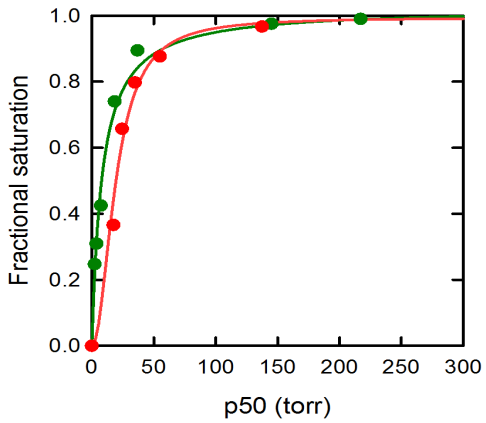

Figure 4.3: Oxygen binding curves of bHb (red) and polymerized bHb (green). The dots are experimental data and the lines represent the fit to the Hill equation. The oxygen-binding curves were measured at 25 °C in the presence of the Hayashi reducing system.

	HbA	bHb	Polymerized bHb
p50 (Torr)	2.61 ± 0.05	19.3 ± 0.3	8 ± 1
n	2.36 ± 0.06	2.1 ± 0.2	1.0 ± 0.1

Table 4.1. Oxygen binding parameters of unmodified bHb and polymerized bHb.

4.4 Conclusions

Normothermic reperfusion is a recently introduced technique to preserve organs, restore their functionality and recover marginal organs. As organs require adequate oxygenation, HBOCs are a promising component of perfusion solutions. Polymerization can be used to engineer HBOCs with the required oxygen binding properties, but the role of these modifications in altering the allosteric properties is not clearly understood. The processing of several liters of blood\Hb solutions for these applications was efficiently processed through a combination of large-volume centrifuges, homogenizers for cell disruption and tangential flow systems for buffer exchange. The polymerized bHb was characterized in terms of oxygen binding and cooperativity, showing an increase in oxygen affinity in comparison with unmodified bHb. Preliminary experiments show that the product can be used in a perfusion machine as a provider of oxygen with no apparent damage to organs.

Part II: Recombinant human alpha 1-antitrypsin

Chapter 5: Recombinant human alpha 1-antitrypsin, expression, purification, PEGylation and formulation as powder

5.1 Introduction

Alpha-1 antitrypsin (AAT) is glycosylated protein of 394 amino acids mostly produced by the liver (Kurachi et al., 1981; Travis, 1988). It is also synthesized in small quantities by circulating monocytes and alveolar macrophages in the lungs, intestinal tissue, and kidneys. It is one of the main protein components of plasma, with a concentration of 1.5 - 3.5 g/L. It has a circulatory half-life of 4-5 days, strongly affected by the degree of glycosylation (Zhang et al., 2003; Chung et al., 2016; Dunlea et al., 2016, Lomas & Parfrey, 2004, Hazari et al, 2017). Indeed, carbohydrate chains are N-linked to Asn46, Asn83, and Asn247, resulting in an apparent molecular weight of 52 kDa. A healthy person produces around 34 mg/kg/day of AAT, which increases in acute phase responses in many conditions such as inflammation, pregnancy, and trauma. According to the World Health Organization, the required minimum protective serum concentration of AAT is 11 μM. AAT has been found to have higher concentrations in serum compared to tissues (Gadek et al, 1981) (Ward et al, 1985) (1997).

AAT belongs to superfamily of serpins, structurally conserved proteins that inhibit several proteases through a covalent inactivation mechanism. AAT has nine α-helices and three β-sheets. The exposed

mobile reactive center loop (RCL) of AAT works as pesudosubstrate for proteases and contains a Met358 residue crucial for activity. Specifically, the unstructured reactive loop of serpins binds near the active site of the target protease, inducing a large conformational change that permanently inactivates the enzyme (Huntington et al., 2000). AAT inhibits neutrophil elastase (EC 3.4.21.37), a serine protease secreted by neutrophils during inflammation and capable of destroying tissues through the proteolysis of elastin, among other substrates (Travis, 1988; Barnes et al., 2003). When expressed aberrantly or when its action is not counterbalanced by AAT, neutrophil elastase can cause emphysema by breaking down the lung structure (Barnes et al., 2003), inducing pulmonary emphysema and bronchiectasis. Moreover, these proteins form polymers that work as chemotactic signals to recruit immunity cells (Gadek et al, 1981; Hazari et al, 2017; Moraga & Janciauskiene, 2000; Parmar et al, 2002).

Alpha-1 antitrypsin deficiency (AATD) is a genetic recessive disorder inherited in an autosomal codominant pattern caused by hereditary mutations of the highly polymorphic SERPINA1 gene, which encodes for AAT (Stoller and Aboussouan, 2012). More than 100 mutations have been recognized, some leading to a shortage of AAT, others to poorly active forms. Some mutants of AAT were shown to exhibit an altered conformation in which the RCL forms a beta strand, macking the protein inactive (Figure 5.1) (Law et al, 2006, Huntington et al, 2000, Haq et al, 2016, Hazari et al, 2017; Janciauskiene, 2001). Other mutants encode a

deficient variant which is 35% less concentrated than normal and the null alleles result in undetectable plasma levels (Baraldo et al, 2016). Most AATD forms result in lung damage, with symptoms ranging from shortness of breath to asthma-like symptoms and emphysema (de Serres and Blanco, 2014; Greene et al., 2016). A subset of AATD patients also suffers from reduced liver function (Lomas et al., 1992). Several animal models have been proposed for the investigation of AATD and to test investigational drugs (Ni et al., 2016). Particularly, the so-called pallid mouse (Martorana et al., 1993) is a strain with low levels of AAT that spontaneously develops emphysema.

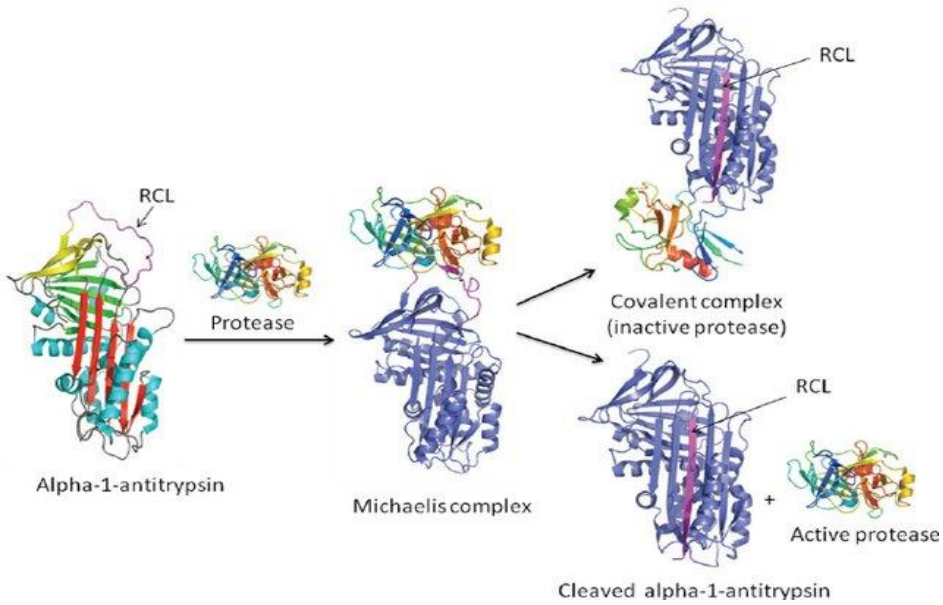

Figure 5.1: Alpha1-Antitrypsin structure and its reaction with protease (Law et al, 2006).

The management of AATD currently consists in an augmentation therapy with weekly infusions of AAT purified from plasma (60 mg/kg body weight) to slow down the progression of emphysema. This therapy has been approved in several countries for the treatment of lung-affected AATD patients (Wewers et al., 1987; Mohanka et al., 2012). An anti-inflammatory effect independent of elastase inhibition was also observed (Jonigk et al., 2013). However, the weekly intravenous administration has the obvious limitation of being invasive. Moreover, AAT purified from plasma is costly, its availability is limited by blood donations and, as all blood derivatives, is amenable to pathogen transmission (Stoller & Aboussouan, 2004). Finally, only 3% of AAT reaches the lungs (Turner, 2013), where most of the damages of AATD are observed and which is the only organ that benefits from AAT augmentation therapy (Mohanka et al., 2012). The liver manifestations of AATD do not benefit from it (Fairbanks and Tavill, 2008).

Administration of AAT through the airways could be a non-invasive alternative to address the lung tissue damage by delivering sufficient AAT to the alveoli compared to the infusion route. This route of administration is currently under investigation (Griese and Scheuch, 2016). However, it has potential issues regarding the penetration of the droplets in the airways, which was shown to be crucial for the therapeutic effect (Griese and Scheuch, 2016). Adherence is also problematic and some commercial preparations might contain traces of IgA, causing anaphylaxis. Additionally, AAT purified from plasma is very expensive and the source

availability poses a further challenge. Aerosolized human AAT is still in the clinical trial phase (Griese & Scheuch, 2016).

As an alternative to AAT purified from plasma, recombinant AAT (rAAT) expressed in bacteria has been proposed (Hazari et al, 2017) for the infusion therapy.

The goals of this project were:

1. Producing tagged recombinant AAT (rAAT) expressed in *E. coli* at high yields to reduce the dependence of AAT availability on blood donation. Expression of rAAT in *E.coli* has a drawback that the protein is not glycosylated, and this could affect the protein folding and functionality and increase the clearance *in vivo* (Hazari et al, 2017; Wang et al, 2013).

2. Introducing PEGylation of cysteine 232 to modulate both the formulation properties and the pharmacokinetics properties of rAAT in terms of lung persistence, systemic absorption, and plasma half-life. PEGylation is the only chemical modification that has so far allowed to improve the pharmacokinetic profiles of protein therapeutics, with several PEGylated products already on the market (Harris and Chess, 2003; Swierczewska et al., 2015). Indeed, PEGylation allows mimicking protein glycosylation, which is not carried out by bacterial cells but that is associated with a longer half-life of AAT (Chung et al., 2016). Moreover, many pieces of evidence have been provided that inhaled PEGylated-proteins exhibit longer retention, decreased systemic absorption and increases mucus adhesion within the lungs (D'Souza A & Shegokar, 2016).

3. Formulating PEGylated rATT as a respirable powder using a spray drying technology in collaboration with prof. Bettini's group of our Department, allowing easy pulmonary administration. The goal is the construction of microparticles for the direct deposition of the drug on the damaged surface, providing higher local concentrations with lower doses compared to systemic administration.

4. Testing the powder and the protein in solution in a mouse model in collaboration with Prof. Barocelli's group in our Department.

5.2 Materials and methods

5.2.1 Materials

All chemicals and materials were purchased from Sigma-Aldrich (St. Louis, MO, USA), unless otherwise stated. Filters with 0.20 µm cutoff were purchased from Sarstedt. The Nichel-Sepharose resin for IMAC chromatography was purchased from Merck (Darmstadt, Germany). Centrifugal filters for the Amicon concentration system (30 kD cutoff) were from Merk Millipore (Cork, Ireland). The endotoxin removal capsule Sartobind Q STIC PA (4 mm) were from Sartorius.

5.2.2 Expression of recombinant human AAT

The synthetic human α-1-antitrypsin gene was cloned in a pET-28a (+) vector fused to the gene encoding an N-terminal hexa-histidine tag. The pET-28a (+) gene confers kanamycin resistance. BL21(DE3) *E. coli* cells were transformed with the vector through electroporation and a glycerol

stock of the cells was stored at -80 °C.

5.2.3 rAAT culture

Preliminary expression trials in a small laboratory scale were carried out to determine the best expression conditions before the scale-up. Single colonies of transformed BL21(DE3) *E. coli* cells were inoculated in 5 mL of LB medium and grown overnight. The culture was then inoculated in 1 L of LB medium contained in a 5 L flask. Kanamycin was added at a final concentration of 50 µg/ mL to the LB medium.

5.2.4 Expression rAAT in fed-batch culture

A high cell density culture (HCDC) protocol was used for growing *E. coli* cells in a 10 L SARTORIUS BIOSTAT C plus fermenter. The medium (HDCF1) contained all the nutrients necessary for bacterial growth.

6 L of the medium were prepared by mixing:

- 60 mL of trace elements solution. 1 L of this solution contained 6 g of $CaCl_2$ * 2 H_2O, 6 g of $FeSO_4$ * 7 H_2O, 1.15 g of $MnCl_2$ * 4 H_2O, 0.8 g of $CoCl_2$ * 6 H_2O, 0.7 g of $ZnSO_4$ * 7 H_2O, 0.3 g of $CuCl_2$ *2 H_2O, 0.02 g of H_3BO_3 and 0.25 g of $(NH4)_6Mo_7O_{24}$ * 4 H_2O, 5 g of ethylenediaminetetraacetic acid (EDTA). The components were dissolved in the minimum amount of HCl and added to water containing EDTA. The solution was autoclaved and stored in the dark at 4 °C.
- 60 mL of $MgCl_2$ 1 M, sterilized through 0.20 µm filters

- 12 g of yeast extract
- 60 mL glycerol
- 60 g of K_2HPO_4,
- 60 g of KH_2PO_4,
- 545 g of Na_2HPO_4 *2 H_2O,
- 6.6 g of NH_4Cl,
- 22.2 g of KCl
- 39,6 g of $(NH_4)_2SO_4$

The resulting solution was autoclaved directly in the fermenter.

The fermenter was connected with pumps supplying the culture with

i) a 20% NH_3 solution to adjust the pH

ii) a 20% sterilized antifoam solution

iii) a solution composed of trace elements solution (70 mL per liter), $MgCl_2$ 1 M (20 mL per liter) and glycerol (710 mL per liter).

The target pH was set at 6.8 and the target pO_2 was set at 30% (with respect to air pressure).

A cell pre-culture of 50 mL was grown overnight and added to the sterilized medium directly in the fermenter, along with kanamycin. The culture was left to grow for 10 h at 37 °C. After 10 h, the temperature was lowered to 20 °C and the expression was induced with 2 mM isopropyl β-D-thiogalactoside (IPTG). Nutrients were provided with the profile described in Table 5.1.

Step	Time	SetPoint	Pump flow rate
Step 1	0:00 h	0%	0 ml/min
Step 2	2:00 h	0%	0 ml/min
Step 3	2:05 h	5%	0,25 ml/min
Step 4	5:00 h	5%	0,25 ml/min
Step 5	5:05 h	10%	0,10 ml/min
Step 6	10:00 h	10%	0,10 ml/min
Step 7	10:05 h	15%	0,75 ml/min
Step 8	15:00 h	15%	0,75 ml/min
Step 9	15:05 h	18%	0,9 ml/min
Step 10	18:00 h	20%	1 ml/min

Table 5.1: Profile of nutrition supply during fermentation.

Cells were collected after 10 h from induction and were washed three times with a Tris-HCl buffer at pH.8 by using an Eppendorf® 5920 centrifuge cooled at 4°C. The final cell pellet was stored at -80 °C.

5.2.5 Cell processing

Cells were resuspended in a buffer containing 20 mM KH_2PO_4 and 0.2 M NaCl, pH.8 (35 g of cell paste/ 100 mL of buffer). A mixture of protease inhibitors was added to the resuspended cells (0.2 mM PMSF, 0.2 mM benzamidine, 1 mM pepstatine). Cells were then broken using a PandaPlus 200 (GEA) homogenizer by applying a pressure of 500 torr in one cycle. The cell lysate was centrifuged for 45 min at 20000 x g at 4 °C to remove cell debris. The supernatant containing soluble rAAT was first added with $(NH_4)_2SO_4$ at 35%, and, after the removal of the pellet, added with more $(NH_4)_2SO_4$ to reach a final concentration of 75%. AAT was recovered in the pellet after the second precipitation step.

5.2.6 Protein purification

The pellet was resuspended with 30 mL of a solution containing 20 mM Tris, 0.5 NaCl and 5 mM imidazole, at pH 8. The resuspended protein solution was loaded on a nickel IMAC column (5 mL of slurry) previously washed with 2% NaOH to remove lipopolysaccharides (LPS). Once the protein was loaded, the resin was washed several times with a solution containing 20 mM Tris, 0.5 M NaCl, and 20 mM imidazole at pH 8. The protein was eluted by the addition of 50 mL of a solution containing 20 mM Tris, 0.5 NaCl and 250 mM imidazole at pH 8. The eluted protein was collected and dialyzed against PBS (137 mM NaCl, 10 mM phosphate and 2.7 mM KCl, at pH 7.4) at 4°C. EDTA (1 mM final concentration) was added to the protein solution immediately after elution. The resulting solution

was flash frozen and stored at -80°C.

5.2.7 Purity and quantification of rAAT

Coomassie-stained SDS-PAGE gels were used to assess protein purity and to quantify the yield from every purification step and after dialysis. Bradford assays were carried out to assess the concentration.

5.2.8 Endotoxin removal and protein preparation

The protein solution was sterilized using 0.2 µm filters. It was then passed 3 times through the endotoxin removal capsules to remove LPS. Endotoxin removal was assessed in the final preparation by prof. Nicoletta Ronda of our Department using a cell-based assay.

5.2.9 Powder formulation

The protein powder was formulated in the Laboratory of Pharmaceutical Technology of Parma University using a B-290 mini spray-dryer (Buchi, Switzerland). For the formulation, mannitol was added to the PBS solution in a 50:50 ratio with respect to rAAT.

5.2.10 AAT activity assay

An enzyme assay was designed to determine the activity of the purified protein as an inhibitor of elastase, knowing that AAT inhibits porcine pancreatic elastase in 1:1 stoichiometry. The assay was carried out by incubating 10 nM of elastase with 5 nM of purified rAAT in a solution containing 0.1 M HEPES, 0.5 M NaCl and 0.05% Triton, pH 7.4.

The incubation was carried out at 37°C. The residual elastase activity was determined by following the hydrolysis of the substrate N-succinyl-Ala-Ala-Ala-*p*-nitroanilide to form p-nitroaniline, which absorbs at 410 nm. The assay was followed for 5 min in a Cary 4000 UV-Vis spectrophotometer. A control of non-inhibited elastase was used as a reference. All the measurements were done in replicate. As elastase is double the concentration of rAAT in the incubation mixture, a 50% inhibition is expected if rAAT is totally active. The excess residual activity of elastase over 50% is inversely proportional to rATT activity.

5.2.11 Stability assay of protein in solution

To assess the stability of the protein solution aliquots were stored at -80 °C, - 20 °C, +4 °C and + 25°C and their activity was followed over time using the assay described in 5.2.10.

5.2.12 Stability assay of the powder

The quantity of rAAT in the powder was determined for every formulation by resuspending the powder in PBS and running an aliquot in SDS-PAGE. The stability was assessed by measuring the residual activity of AAT with the same assay described in 5.2.10.

5.2.13 PEGylation of rAAT

AAT in a PBS solution was reacted with 20 kDa maleimide-PEG in a 5-fold molar excess for two hours under continuous stirring, in the dark. The

reaction was carried out at both 37°C and 20°C to determine the best condition. The reaction was quenched by addition 2ml of 4 M lysine solution. At the end of the reaction, the PEGylation yield was assessed by using two SDS-PAGE gels, one gel stained with Coomassie blue and the second stained with an iodine-based stain specific for PEG groups. To determine whether conjugation affected the capacity to inhibit the protease, the activity assay carried out after the reaction. PEGylated rAAT at + 20°C was stored at - 20°C and + 4°C to follow the stability over time, using the same assay described in 5.2.10.

5.2.14 Administration of rAAT to mice

AAT was administered to mice by Prof. Barocell's group in our Department. Male mice were grouped according to the administration route. The first group was administered 120 µl of a sterile LPS-free rAAT (1 mg /mL) intravenously. Plasma samples were collected from the mice before administration and then at different time intervals (2h, 4h, 8h and 24 h). The second group was administered 0.9 mg of powder, containing 63 µg of rAAT. The powder was administered intratracheally under anesthesia using a Penn-Century dry powder insufflator. Bronchoalveolar lavages (BALs) were collected twice after administration by using a 0.9% NaCl solution, then after 2 h and after 4 h. After 4 h of administration, mice were sacrificed and the lungs and trachea were recovered. Some mice were sacrificed directly after powder administration to follow the powder deposition in the respiratory system. Lungs and BALs were

collected from all groups.

5.2.15 Presence of rAAT in plasma

The presence of rAAT in plasma over time was assessed and compared to the basal AAT activity associated with the murine endogenous protein. Assuming a physiological concentration in mice plasma around 140 μM, samples with an unknown concentration of AAT were diluted 3 times in PBS to reach a concentration of less than 10 nM. Diluted plasma samples were incubated with 10 nm elastase for 1 h. The assay in 5.2.10 was carried out.

5.2.16 Presence of rAAT in lower respiratory of mice

Lungs were thawed in ice and ground cryogenically with mortar and pestle in the presence of liquid nitrogen. The lung tissue powder was resuspended in lysis buffer in the presence of a mixture of protease inhibitors. An optimized assay was optimized and a calibration curve was preliminarily measured by preparing serial dilutions of rAAT (1 mg/mL) in 10 μl of lung lysates from control mice. 1 μl from each solution was tested for anti elastase activity as described in 5.2.9 (160 μl final volume). Lung lysate samples from treated mice were then tested in the same assay and the elastase inhibition values were compared with the calibration curve.

The presence of rAAT in BAL samples was assessed by using these samples directly in the inhibition assay described in 5.2.9.

5.3 Results and discussion

5.3.1 Expression yield and protein purity

The fermentation protocol described in Materials and Methods yielded around 1 kg of cell paste from 7 L of medium. Purification led to 93% purity (Figure 5.2a). The purification protocol was scaled up, showing that 450 g of cells could be processed at one time without losing protein (Figure 5.2b). Overall, 400 mg of purified AAT could be obtained from a single 7 L fermentation.

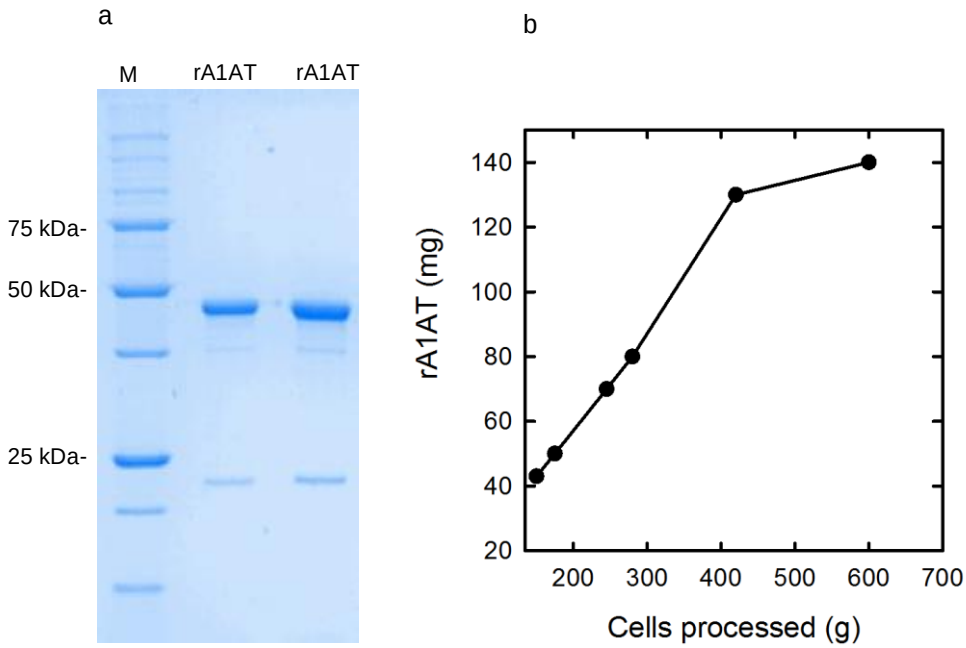

Figure 5.2: (a) Coomassie blue-stained SDS-PAGE gels of purified rAAT (in replicate). **(b)** protein yield vs the processed amount of bacterial paste (in weight).

5.3.2 Protein stability in solution

The stability of rAAT stored at different temperatures in a PBS solution was tested. rAAT stored at -80 °C maintained full activity over time; at -20 °C, the loss of activity was minimal over several weeks; at 4°C, 50% of activity was maintained within three weeks. The stability was lost within a few days for the solution stored at +25°C (Figure 5.3a). The SDS-PAGE of two samples stored for 4 weeks at +4 °C showed a small band around 40 kDa, possibly indicating a partial proteolytic degradation (Figure 5.3.b). However, most of the protein remained intact, hinting at different mechanisms of inactivation, including oxidation of Met358 and Met351. The two residues are known to oxidize irreversibly to form methionine sulphoxide (Taggart et al, 2000, Moraga et al, 2000).

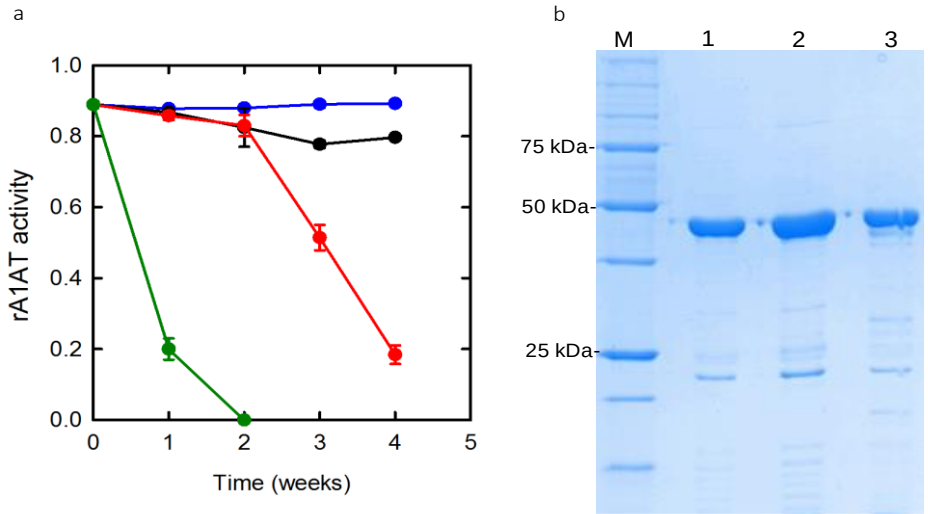

Figure 5.3: (a) Activity of rAAT stored in solution at -80 °C (blue), at -20 °C (black), at +4 °C (red) and at 25°C (green). Data are shown as mean ± SE. **(b)** SDS-PAGE of rAAT after 4 weeks when stored at -80°C (lanes 1 and 2) and + 4 °C (lane 3).

5.3.3 Protein Powder stability

The formulation of rAAT as a powder was carried out using the spray-drying technology, which might be stressful for the protein, possibly inducing aggregation or oxidation. For this reason, after every step of the formulation, the activity of the protein was assessed by comparing it with the starting solution, confirming that no step was responsible for any significant loss in activity (data not shown).

The stability of the formulated powders was then followed over an extended period of time, upon storage in the absence and presence of oxygen and at different temperatures. In the absence of oxygen, the powder stored at -20 °C was stable over weeks, but the protein activity was lost dramatically after 5 months (Figure 5.4a). The powder stored at +25 °C lost 80% of the activity after two months. At +4 °C, only 20% of activity was retained after 3 months (Figure 5.4a). The powder exposed to oxygen lost activity much faster at all temperatures (Figure 5.4b).

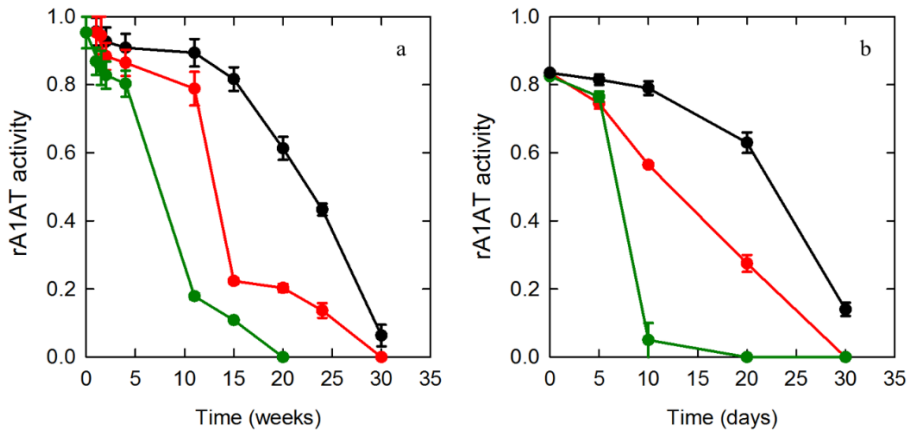

Figure 5.4: (a) Stability of rAAT powder stored in the absence of oxygen **(a)** and in the absence of oxygen **(b)** at -20 °C (black), +4 °C (red) and + 25°C (green). Data are shown as mean ± SE.

5.3.4 PEGylation of rAAT

The site-specific conjugation with MAL-PEG was carried out at +37°C and +20°C. The resulting yield of PEGylation was 52% for both reactions. The apparent molecular weight increased from 48 kDa to around 100 kDa (Figure 5.5). A band at 70 kDa was also observed (Figure 5.5). The iodine-stained gel confirmed the attribution of the 100 kDa bands to PEGylated rAAT (figure 5.5b). The large band around 50 kDa is non-reacted MAL-PEG. PEGylation at 20°C did not affect protein activity in comparison to non-PEGylated rAAT, but around 50% of the activity was lost when PEGylation was carried out at +37°C (Figure 5.6a).

The stability assay of PEGylated rAAT at 20°C showed that PEG rAAT lost its activity within one month at + 4°C and within two months at - 20°C

(Figure 5.6b), indicating that PEGylation affects stability in a negative fashion. It could be that the hydrophilicity of PEG polymers makes water molecules closer to the protein molecules as a layer of hydration (Dimitrov, 2012). Further work has to be done to formulate the PEGylated protein solution and to enhance its stability over time.

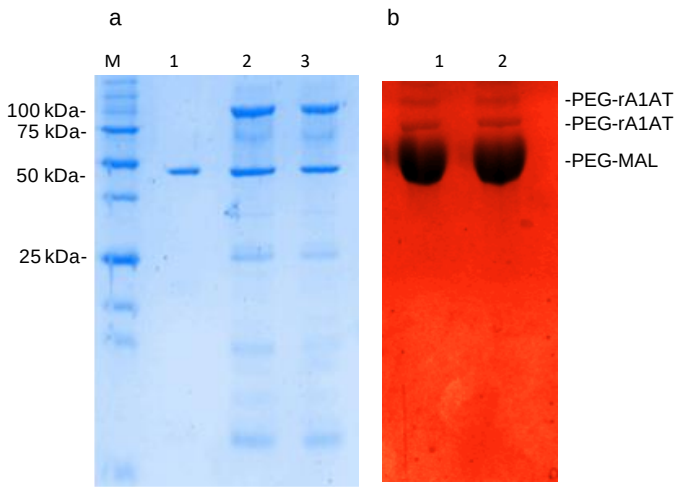

Figure 5.5: **(a)** Comassie blue-stained SDS-PAGE gels of not-PEGylated rAAT (lane 1), PEG-rAAT obtained at +20°C (lane 2) and PEG-rAAT obtained at +37°C (lane 3), **(b)** SDS-PAGE gel stained using a iodine-based staining protocol with PEG-rAAT PEG obtained at +20°C (lane 1) and at +37°C (lane 2).

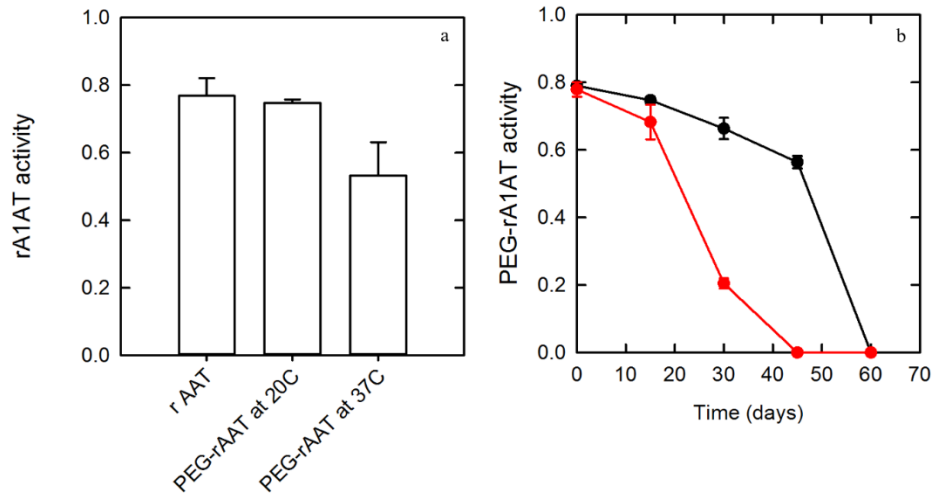

Figure 5.6: **(a)** Stability of PEGylated rAAT after the PEGylation reaction carried out at two different temperatures (20 and 37°C), **(b)** Stability of PEG-rAAT produced at 20°C and stored at -20°C (black) and at + 4°C (red). Data are shown as mean ± SE.

5.3.5 The presence of rAAT in mice treated IV

The activity of rAAT in plasma after IV administration was assessed and compared to the basal AAT activity associated with that of the murine endogenous protein. After two hours, a significant peak in AAT activity indicated that rAAT was in the bloodstream, validating the activity assay as a future strategy to monitor rAAT pharmacokinetics (Figure 5.7). After 4 h, AAT activity returned to the basal values, suggesting a limited half-life of rAAT. The same result was obtained by Western blot (data not shown).

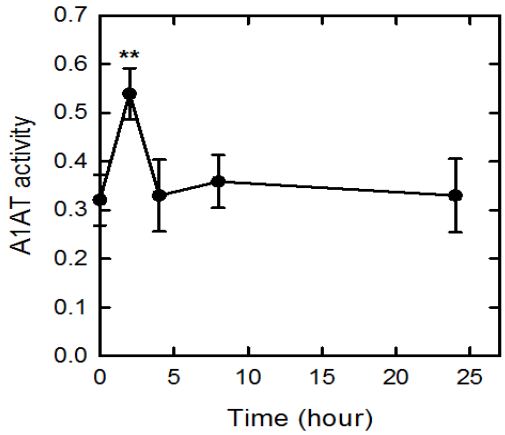

Figure 5.7: AAT activity in plasma following IV administration. Data are shown as mean ± SD. Statistical analysis: Ordinary one-way ANOVA followed by Tukey's multiple comparisons test, ** $p<0.001$.

5.3.6 Detection of rAAT in the lower respiratory tract

The assessment of the rAAT activity in BAL did not show any difference between treated and non-treated mice (data not shown) and AAT activity could not be detected in lung lysates (Figure 5.8, red dot). To rule out any bias associated with the enzyme assay applied to tissue lysates, we tested AAT activity of lung lysate samples spiked with different amounts of the AAT solution. The assay yielded a linear response (Figure 5.8), confirming that it can be applied to lung lysates and that the absence of AAT activity probably reflects the poor delivery of the powder to the lungs.

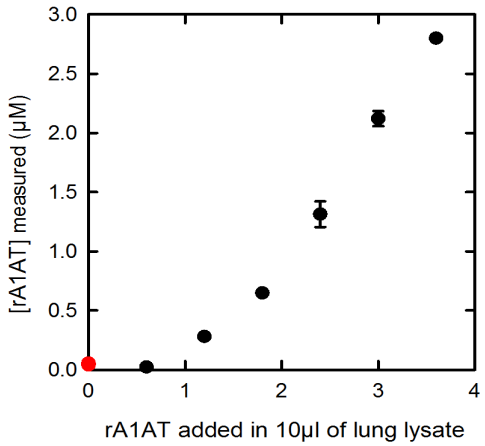

Figure 5.8: AAT concentration in lung lysates as determined by activity assays. The red dot corresponds to the value measured in the lung lysate of an animal treated with the AAT powder intratracheally. The black points constitute a calibration curve obtained by spiking lung lysates with known concentrations of ATT. Data are shown as mean ± SE.

Western blots were performed to investigate the presence of rAAT in plasma, lung and trachea lysates in treated mice. Inhaled rAAT was not detectable neither in plasma nor in lung lysates, but two mice had detectable rAAT in the trachea (Figure 5.9). The sensitivity of the assay for the anti-rAAT antibodies was confirmed in control samples spiked with rAAT (Figure 5.9). These results were consistent with the activity assay, confirming that the powder did not reach the lungs.

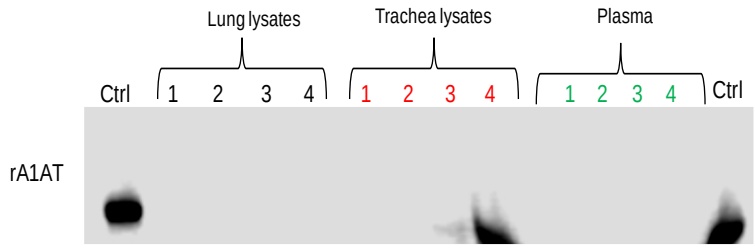

Figure 5.9: Western blot of lung lysates, trachea lysates and plasma from mice treated with rAAT powder. Control samples of rAAT solution were used (Ctrl). Numbers 1 to 4 refer to individual mice.

5.4 Conclusions

Recombinant AAT could be produced at yields high enough for its formulation as powder and for preliminary *in vivo* experiments. The protein was fully active at inhibiting elastase and maintained its activity upon formulation. The stability of the resulting powder was assessed, defining a possible shelf-life and storage conditions. PEGylation did not affect protein activity but lowered its stability in solution. The protein was not deposited in the lung of mice with the protocol that was used. Future work will be aimed at improving the powder formulation to enhance its capability to reach the lungs.

References

Aburawi MM, Fontan FM, Karimian N, Eymard C, Cronin S, Pendexter C, Nagpal S, Banik P, Ozer S, Mahboub P, Delmonico FL, Yeh H, Uygun K, Markmann JF (2019) Synthetic hemoglobin-based oxygen carriers are an acceptable alternative for packed red blood cells in normothermic kidney perfusion. American journal of transplantation: official journal of the American Society of Transplantation and the American Society of Transplant Surgeons

Alayash AI (2011) Haptoglobin: old protein with new functions. Clin Chim Acta 412: 493-498

Alayash AI (2014) Blood substitutes: why haven't we been more successful? Trends in biotechnology 32: 177-185

Alayash AI (2017) Mechanisms of Toxicity and Modulation of Hemoglobin-Based Oxygen Carriers (HBOCs). Shock (Augusta, Ga)

Alayash AI (2019) Mechanisms of Toxicity and Modulation of Hemoglobin-based Oxygen Carriers. Shock (Augusta, Ga) 52: 41-49

Alayash AI, D'Agnillo F, Buehler PW (2007) First-generation blood substitutes: what have we learned? Biochemical and physiological perspectives. Expert Opin Biol Ther 7: 665-675

Antonini E, Brunori A (1971) Hemoglobin and Myoglobin in Their Reactions with Ligands, Amsterdam: North-Holland.

Arnone A (1972) X-ray diffraction study of binding of 2,3-diphosphoglycerate to human deoxyhaemoglobin. Nature 237: 146-149

Ayala A, Munoz MF, Arguelles S (2014) Lipid peroxidation: production, metabolism, and signaling mechanisms of malondialdehyde and 4-hydroxy-2-nonenal. Oxidative medicine and cellular longevity 2014: 360438

Babusiak M, Man P, Sutak R, Petrak J, Vyoral D (2005) Identification of heme binding protein complexes in murine erythroleukemic cells: study by a novel two-dimensional native separation -- liquid chromatography and electrophoresis.
5: 340-350

Baek JH, Zhou Y, Harris DR, Schaer DJ, Palmer AF, Buehler PW (2012) Down selection of polymerized bovine hemoglobins for use as oxygen releasing therapeutics in a guinea pig model. Toxicol Sci 127: 567-581

Baldwin J, Chothia C (1979) Haemoglobin: the structural changes related to ligand binding and its allosteric mechanism. J Mol Biol 129: 175-220

Baraldo S, Balestro E, Bazzan E, Tine ME, Biondini D, Turato G, Cosio MG, Saetta M (2016) Alpha-1 Antitrypsin Deficiency Today: New Insights in the Immunological Pathways. Respiration 91: 380-385

Belcher DA, Banerjee U, Baehr CM, Richardson KE, Cabrales P, Berthiaume F, Palmer AF (2017) Mixtures of tense and relaxed state polymerized human hemoglobin regulate oxygen affinity and tissue construct oxygenation. PLoS ONE 12: e0185988

Belcher DA, Ju JA, Baek JH, Yalamanoglu A, Buehler PW, Gilkes DM, Palmer AF (2018) The quaternary state of polymerized human hemoglobin regulates oxygenation of breast cancer solid tumors: A theoretical and experimental study. PLoS ONE 13: e0191275-e0191275

Bellelli A, Brunori M, Miele AE, Panetta G, Vallone B (2006) The allosteric properties of hemoglobin: insights from natural and site-directed mutants. Curr Protein Pept Sci 7: 17-45

Benesch R, Benesch RE (1967) The effect of organic phosphates from the human erythrocyte on the allosteric properties of hemoglobin. Biochem Biophys Res Commun 26: 162-167

Benitez Cardenas AS, Samuel PP, Olson JS (2019) Current Challenges in the Development of Acellular Hemoglobin Oxygen Carriers by Protein Engineering. Shock (Augusta, Ga) 52: 28-40

Bian Y, Rong Z, Chang TM (2011) Polyhemoglobin-superoxide dismutase-catalase-carbonic anhydrase: a novel biotechnology-based blood substitute that transports both oxygen and carbon dioxide and also acts as an antioxidant. Artif Cells Blood Substit Immobil Biotechnol 39: 127-136

Birukou I, Schweers RL, Olson JS (2010) Distal histidine stabilizes bound O2 and acts as a gate for ligand entry in both subunits of adult human hemoglobin. J Biol Chem 285: 8840-8854

Bobofchak KM, Mito T, Texel SJ, Bellelli A, Nemoto M, Traystman RJ, Koehler RC, Brinigar WS, Fronticelli C (2003) A recombinant polymeric hemoglobin with conformational, functional, and physiological characteristics of an in vivo O2 transporter. Am J Physiol Heart Circ Physiol 285: H549-561

Boretti FS, Buehler PW, D'Agnillo F, Kluge K, Glaus T, Butt OI, Jia Y, Goede J, Pereira CP, Maggiorini M, Schoedon G, Alayash AI, Schaer DJ (2009) Sequestration of extracellular hemoglobin within a haptoglobin complex decreases its hypertensive and oxidative effects in dogs and guinea pigs. The Journal of clinical investigation 119: 2271-2280

Bruno S, Ronda L, Bettati S, Mozzarelli A (2007) Trapping hemoglobin in rigid matrices: fine-tuning of oxygen binding properties by modulation of encapsulation protocols. Artif Cells Blood Substit Immobil Biotechnol 35: 69-79

Buehler PW, Alayash AI (2004) Toxicities of hemoglobin solutions: in search of in-vitro and in-vivo model systems. Transfusion 44: 1516-1530

Buehler PW, D'Agnillo F, Schaer DJ (2010a) Hemoglobin-based oxygen carriers: From mechanisms of toxicity and clearance to rational drug design. Trends Mol Med 16: 447-457

Buehler PW, Zhou Y, Cabrales P, Jia Y, Sun G, Harris DR, Tsai AG, Intaglietta M, Palmer AF (2010b) Synthesis, biophysical properties and pharmacokinetics of ultrahigh molecular weight tense and relaxed state polymerized bovine hemoglobins. Biomaterials 31: 3723-3735

Butt OI, Buehler PW, D'Agnillo F (2011) Blood-brain barrier disruption and oxidative stress in Guinea pig after systemic exposure to modified cell-free hemoglobin. The American journal of pathology 178: 1316-1328

Caccia D, Ronda L, Frassi R, Perrella M, Del Favero E, Bruno S, Pioselli B, Abbruzzetti S, Viappiani C, Mozzarelli A (2009) PEGylation promotes hemoglobin tetramer dissociation. Bioconjugate chemistry 20: 1356-1366

Canas B, Lopez-Ferrer D, Ramos-Fernandez A, Camafeita E, Calvo E (2006) Mass spectrometry technologies for proteomics. Brief Funct Genomic Proteomic 4: 295-320

Cardenas ASB, Samuel PP, Olson JS (2017) 2017 Military Supplement: Current Challenges in the Development of Acellular Hemoglobin Oxygen Carriers by Protein Engineering. Shock (Augusta, Ga)

Ceresa CDL, Nasralla D, Coussios CC, Friend PJ (2018) The case for normothermic machine perfusion in liver transplantation. Liver transplantation: official publication of the American Association for the Study of Liver Diseases and the International Liver Transplantation Society 24: 269-275

Chakane S, Matos T, Kettisen K, Bulow L (2017) Fetal hemoglobin is much less prone to DNA cleavage compared to the adult protein. Redox biology 12: 114-120

Chaudhuri AR, de Waal EM, Pierce A, Van Remmen H, Ward WF, Richardson A (2006) Detection of protein carbonyls in aging liver tissue: A fluorescence-based proteomic approach. Mech Ageing Dev 127: 849-861

Cooper CE, Silkstone GGA, Simons M, Rajagopal B, Syrett N, Shaik T, Gretton S, Welbourn E, Bulow L, Eriksson NL, Ronda L, Mozzarelli A, Eke A, Mathe D, Reeder BJ (2019) Engineering tyrosine residues into hemoglobin enhances heme reduction, decreases oxidative stress and increases vascular retention of a hemoglobin based blood substitute. Free Radic Biol Med 134: 106-118

D'Souza A A, Shegokar R (2016) Polyethylene glycol (PEG): a versatile polymer for pharmaceutical applications. Expert Opin Drug Deliv 13: 1257-1275

Dimitrov DS (2012) Therapeutic proteins. Methods Mol Biol 899: 1-26

Dolgin E (2017) Bioengineering: Doing without donors. Nature 549: S12-S15

Eaton WA, Henry ER, Hofrichter J, Mozzarelli A (1999) Is cooperative oxygen binding by hemoglobin really understood? Nat Struct Biol 6: 351-358

Eshmuminov D, Leoni F, Schneider MA, Becker D, Muller X, Onder C, Hefti M, Schuler MJ, Dutkowski P, Graf R, Rudolf von Rohr P, Clavien PA, Bautista Borrego L (2018) Perfusion settings and additives in liver normothermic machine perfusion with red blood cells as oxygen carrier. A systematic review of human and porcine perfusion protocols. Transplant international : official journal of the European Society for Organ Transplantation

Estep T, Bucci E, Farmer M, Greenburg G, Harrington J, Kim HW, Klein H, Mitchell P, Nemo G, Olsen K, Palmer A, Valeri CR, Winslow R (2008) Basic science focus on blood substitutes: a summary of the NHLBI Division of

Blood Diseases and Resources Working Group Workshop, March 1, 2006. Transfusion (Paris) 48: 776-782

Ferenz KB, Steinbicker AU (2019) Artificial Oxygen Carriers-Past, Present, and Future-a Review of the Most Innovative and Clinically Relevant Concepts. J Pharmacol Exp Ther 369: 300-310

Fontes P, Lopez R, van der Plaats A, Vodovotz Y, Minervini M, Scott V, Soltys K, Shiva S, Paranjpe S, Sadowsky D, Barclay D, Zamora R, Stolz D, Demetris A, Michalopoulos G, Marsh JW (2015) Liver Preservation With Machine Perfusion and a Newly Developed Cell-Free Oxygen Carrier Solution Under Subnormothermic Conditions. American Journal of Transplantation 15: 381-394

Frokjaer S, Otzen DE (2005) Protein drug stability: a formulation challenge. Nat Rev Drug Discov 4: 298-306

Fronticelli C, Koehler RC (2009) Design of recombinant hemoglobins for use in transfusion fluids. Crit Care Clin 25: 357-371, Table of Contents

Fronticelli C, Bucci E (1994) Conformational and functional characteristics of bovine hemoglobin. Methods in enzymology 231: 150-163

Frost AT, Jacobsen IH, Worberg A, Martinez JL (2018) How Synthetic Biology and Metabolic Engineering Can Boost the Generation of Artificial Blood Using Microbial Production Hosts. Frontiers in bioengineering and biotechnology 6: 186

Gadek JE, Fells GA, Zimmerman RL, Rennard SI, Crystal RG (1981) Antielastases of the human alveolar structures. Implications for the protease-antiprotease theory of emphysema. J Clin Invest 68: 889-898

Gasthuys M, Alves S, Tabet JC (2005) N-terminal adducts of bovine hemoglobin with glutaraldehyde in a hemoglobin-based oxygen carrier. Analytical chemistry 77: 3372-3378

Gould SA, Moore EE, Hoyt DB, Burch JM, Haenel JB, Garcia J, DeWoskin R, Moss GS (1998) The first randomized trial of human polymerized hemoglobin as a blood substitute in acute trauma and emergent surgery. J Am Coll Surg 187: 113-120

Graves PE, Henderson DP, Horstman MJ, Solomon BJ, Olson JS (2008) Enhancing stability and expression of recombinant human hemoglobin in E. coli: Progress in the development of a recombinant HBOC source. Biochimica et biophysica acta 1784: 1471-1479

Griese M, Scheuch G (2016) Delivery of Alpha-1 Antitrypsin to Airways. Ann Am Thorac Soc 13 Suppl 4: S346-351

Habeeb AJ, Hiramoto R (1968) Reaction of proteins with glutaraldehyde. Archives of biochemistry and biophysics 126: 16-26

Haq I, Irving JA, Saleh AD, Dron L, Regan-Mochrie GL, Motamedi-Shad N, Hurst JR, Gooptu B, Lomas DA (2016) Deficiency Mutations of Alpha-1 Antitrypsin. Effects on Folding, Function, and Polymerization. Am J Respir Cell Mol Biol 54: 71-80

Hazari YM, Bashir A, Habib M, Bashir S, Habib H, Qasim MA, Shah NN, Haq E, Teckman J, Fazili KM (2017) Alpha-1-antitrypsin deficiency: Genetic variations, clinical manifestations and therapeutic interventions. Mutat Res 773: 14-25

Henry ER, Mozzarelli A, Viappiani C, Abbruzzetti S, Bettati S, Ronda L, Bruno S, Eaton WA (2015) Experiments on Hemoglobin in Single Crystals and Silica Gels Distinguish among Allosteric Models. Biophys J 109: 1264-1272

Huntington JA, Read RJ, Carrell RW (2000) Structure of a serpin-protease complex shows inhibition by deformation. Nature 407: 923-926

Iafelice R, Cristoni S, Caccia D, Russo R, Rossi-Bernardi L, Lowe KC, Perrella M (2007) Identification of the sites of deoxyhaemoglobin PEGylation. The Biochemical journal 403: 189-196

Inayat MS, Bernard AC, Gallicchio VS, Garvy BA, Elford HL, Oakley OR (2006) Oxygen carriers: a selected review. Transfus Apher Sci 34: 25-32

Jahr JS, Akha AS, Holtby RJ (2012) Crosslinked, polymerized, and PEG-conjugated hemoglobin-based oxygen carriers: clinical safety and efficacy of recent and current products. Curr Drug Discov Technol 9: 158-165

Janciauskiene S (2001) Conformational properties of serine proteinase inhibitors (serpins) confer multiple pathophysiological roles. Biochim Biophys Acta 1535: 221-235

Julie H. Eike, Andre F. Palmer (2004) Effects of glutaraldehyde concentration on the physical properties of polymerized hemoglobin - based oxygen carriers. Biotechnology progress 20:1255-1232.

Keipert PE (2016) Clinical Evaluation of MP4CO: A Phase 1b Escalating-Dose, Safety and Tolerability Study in Stable Adult Patients with Sickle Cell Disease. Adv Exp Med Biol 923: 23-29

Kocian R, Spahn DR (2008) Haemoglobin, oxygen carriers and perioperative organ perfusion. Best Pract Res Clin Anaesthesiol 22: 63-80

Kumar SN, Konorev EA, Aggarwal D, Kalyanaraman B (2010) Analysis of proteome changes in doxorubicin-treated adult rat cardiomyocyte. Journal of proteomics 74: 683-697

Lagasse HA, Alexaki A, Simhadri VL, Katagiri NH, Jankowski W, Sauna ZE, Kimchi-Sarfaty C (2017) Recent advances in (therapeutic protein) drug development. F1000Research 6: 113

Laing RW, Bhogal RH, Wallace L, Boteon Y, Neil DAH, Smith A, Stephenson BTF, Schlegel A, Hubscher SG, Mirza DF, Afford SC, Mergental H (2017)

The Use of an Acellular Oxygen Carrier in a Human Liver Model of Normothermic Machine Perfusion. Transplantation 101: 2746-2756

Law RH, Zhang Q, McGowan S, Buckle AM, Silverman GA, Wong W, Rosado CJ, Langendorf CG, Pike RN, Bird PI, Whisstock JC (2006) An overview of the serpin superfamily. Genome Biol 7: 216

Li D, Manjula BN, Acharya AS (2006) Extension arm facilitated PEGylation of hemoglobin: correlation of the properties with the extent of PEGylation. Protein J 25: 263-274

Lind C, Gerdes R, Hamnell Y, Schuppe-Koistinen I, von Lowenhielm HB, Holmgren A, Cotgreave IA (2002) Identification of S-glutathionylated cellular proteins during oxidative stress and constitutive metabolism by affinity purification and proteomic analysis. Archives of biochemistry and biophysics 406: 229-240

Lloyd E, Mauk AG (1994) Formation of sulphmyoglobin during expression of horse heart myoglobin in Escherichia coli. FEBS Lett 340: 281-286

Lomas DA, Parfrey H (2004) Alpha1-antitrypsin deficiency. 4: Molecular pathophysiology. Thorax 59: 529-535

Lopez-Gallego F, Betancor L, Mateo C, Hidalgo A, Alonso-Morales N, Dellamora-Ortiz G, Guisan JM, Fernandez-Lafuente R (2005) Enzyme stabilization by glutaraldehyde crosslinking of adsorbed proteins on aminated supports. Journal of biotechnology 119: 70-75

Lui FE, Dong P, Kluger R (2008) Polyethylene glycol conjugation enhances the nitrite reductase activity of native and cross-linked hemoglobin. Biochemistry 47: 10773-10780

Lui FE, Kluger R (2009) Enhancing nitrite reductase activity of modified hemoglobin: bis-tetramers and their PEGylated derivatives. Biochemistry 48: 11912-11919

Manjula BN, Malavalli A, Smith PK, Chan NL, Arnone A, Friedman JM, Acharya AS (2000) Cys-93-betabeta-succinimidophenyl polyethylene glycol 2000 hemoglobin A. Intramolecular cross-bridging of hemoglobin outside the central cavity. J Biol Chem 275: 5527-5534

Manjula BN, Tsai AG, Intaglietta M, Tsai CH, Ho C, Smith PK, Perumalsamy K, Kanika ND, Friedman JM, Acharya SA (2005) Conjugation of multiple copies of polyethylene glycol to hemoglobin facilitated through thiolation: influence on hemoglobin structure and function. Protein J 24: 133-146

Marchetti M, Liuzzi A, Fermi B, Corsini R, Folli C, Speranzini V, Gandolfi F, Bettati S, Ronda L, Cendron L, Berni R, Zanotti G, Percudani R (2016) Catalysis and Structure of Zebrafish Urate Oxidase Provide Insights into the Origin of Hyperuricemia in Hominoids. Scientific reports 6: 38302

Marchetti M, Ronda L, Faggiano S, Liuzzi A, Percudani R, Bettati S (2018) Fluorescence quantification of allantoin in biological samples by cap-immobilized allantoinase/resorcinol assay. Sensors and Actuators B: Chemical 255: 2820-2828

Matton APM, Burlage LC, van Rijn R, de Vries Y, Karangwa SA, Nijsten MW, Gouw ASH, Wiersema-Buist J, Adelmeijer J, Westerkamp AC, Lisman T, Porte RJ (2018) Normothermic machine perfusion of donor livers without the need for human blood products. Liver Transpl 24: 528-538

Merlino A, Howes B, Prisco G, Verde C, Smulevich G, Mazzarella L, Vergo A (2011) Occurrence and Formation of Endogenous Histidine Hexa-Coordination in Cold-Adapted Hemoglobins. IUBMB Life 63: 295-303

Meng F, Kassa T, Jana S, Wood F, Zhang X, Jia Y, D'Agnillo F, Alayash AI (2018) Comprehensive Biochemical and Biophysical Characterization of Hemoglobin-Based Oxygen Carrier Therapeutics: All HBOCs Are Not Created Equally. Bioconjug Chem 29: 1560-1575

Moraga F, Janciauskiene S (2000) Activation of primary human monocytes by the oxidized form of alpha1-antitrypsin. J Biol Chem 275: 7693-7700

Mozzarelli A, Ronda L, Faggiano S, Bettati S, Bruno S (2010) Haemoglobin-based oxygen carriers: Research and reality towards an alternative to blood transfusions. Blood Transfusion 8

Natanson C, Kern SJ, Lurie P, Banks SM, Wolfe SM (2008) Cell-free hemoglobin-based blood substitutes and risk of myocardial infarction and death: a meta-analysis. JAMA 299: 2304-2312

Nigam PK (2007) Biochemical markers of myocardial injury. Indian J Clin Biochem 22: 10-17

Nugent WH, Jubin R, Buontempo PJ, Kazo F, Song BK (2019) Microvascular and systemic responses to novel PEGylated carboxyhaemoglobin-based oxygen carrier in a rat model of vaso-occlusive crisis. Artificial cells, nanomedicine, and biotechnology 47: 95-103

Olofsson C, Nygards EB, Ponzer S, Fagrell B, Przybelski R, Keipert PE, Winslow N, Winslow RM (2008) A randomized, single-blind, increasing dose safety trial of an oxygen-carrying plasma expander (Hemospan) administered to orthopaedic surgery patients with spinal anaesthesia. Transfus Med 18: 28-39

Parmar JS, Mahadeva R, Reed BJ, Farahi N, Cadwallader KA, Keogan MT, Bilton D, Chilvers ER, Lomas DA (2002) Polymers of alpha(1)-antitrypsin are chemotactic for human neutrophils: a new paradigm for the pathogenesis of emphysema. Am J Respir Cell Mol Biol 26: 723-730

Perutz MF (1970a) Stereochemistry of cooperative effects in haemoglobin. Nature 228: 726-739

Pilger A, Rudiger HW (2006) 8-Hydroxy-2'-deoxyguanosine as a marker of oxidative DNA damage related to occupational and environmental

exposures. International archives of occupational and environmental health 80: 1-15

Portoro I, Kocsis L, Herman P, Caccia D, Perrella M, Ronda L, Bruno S, Bettati S, Micalella C, Mozzarelli A, Varga A, Vas M, Lowe KC, Eke A (2008) Towards a novel haemoglobin-based oxygen carrier: Euro-PEG-Hb, physico-chemical properties, vasoactivity and renal filtration. Biochimica et biophysica acta 1784: 1402-1409

Rabe H (2011) Reference ranges for biochemical parameters in guinea pigs for the Vettest(R)8008 blood analyzer. Tierarztl Prax Ausg K Kleintiere Heimtiere 39: 170-175

Ratanasopa K, Cedervall T, Bulow L (2016) Possibilities of Using Fetal Hemoglobin as a Platform for Producing Hemoglobin-Based Oxygen Carriers (HBOCs). Adv Exp Med Biol 876: 445-453

Ratanasopa K, Strader MB, Alayash AI, Bulow L (2015) Dissection of the radical reactions linked to fetal hemoglobin reveals enhanced pseudoperoxidase activity. Frontiers in physiology 6: 39

Rehman K, Hamid Akash MS, Akhtar B, Tariq M, Mahmood A, Ibrahim M (2016) Delivery of Therapeutic Proteins: Challenges and Strategies. Current drug targets 17: 1172-1188

Rentsendorj O, Zhang X, Williams MC, Buehler PW, D'Agnillo F (2016) Transcriptional Suppression of Renal Antioxidant Enzyme Systems in Guinea Pigs Exposed to Polymerized Cell-Free Hemoglobin. Toxics 4

Reznick AZ, Packer L (1994) [38] Oxidative damage to proteins: Spectrophotometric method for carbonyl assay. In Methods in Enzymology Vol. 233, pp 357-363. Academic Press

Rifkind JM, Mohanty JG, Nagababu E (2014) The pathophysiology of extracellular hemoglobin associated with enhanced oxidative reactions. Frontiers in physiology 5: 500

Roberts MJ, Bentley MD, Harris JM (2002) Chemistry for peptide and protein PEGylation. Adv Drug Deliv Rev 54: 459-476

Ronda L, Bruno S, Abbruzzetti S, Viappiani C, Bettati S (2008a) Ligand reactivity and allosteric regulation of hemoglobin-based oxygen carriers. Biochimica et Biophysica Acta - Proteins and Proteomics 1784: 1365-1377

Ronda L, Bruno S, Faggiano S, Bettati S, Mozzarelli A (2008b) Oxygen binding to heme proteins in solution, encapsulated in silica gels, and in the crystalline state. Methods Enzymol 437: 311-328

Ronda L, Bruno S, Viappiani C, Abbruzzetti S, Mozzarelli A, Lowe KC, Bettati S (2006) Circular dichroism spectroscopy of tertiary and quaternary conformations of human hemoglobin entrapped in wet silica gels. Protein Sci 15: 1961-1967

Saidi RF, Hejazii Kenari SK (2014) Challenges of organ shortage for transplantation: solutions and opportunities. Int J Organ Transplant Med 5: 87-96

Sakota D, Sakamoto R, Sobajima H, Yokoyama N, Waguri S, Ohuchi K, Takatani S (2008) Mechanical damage of red blood cells by rotary blood pumps: selective destruction of aged red blood cells and subhemolytic trauma. Artificial organs 32: 785-791

Schütte-Nütgen K, Finke M, Ehlert S, Thölking G, Pavenstädt H, Suwelack B, Palmes D, Bahde R, Koch R, Reuter S (2019) Expanding the donor pool in kidney transplantation: Should organs with acute kidney injury be accepted?-A retrospective study. PloS one 14: e0213608-e0213608

Scott AV, Nagababu E, Johnson DJ, Kebaish KM, Lipsitz JA, Dwyer IM, Zuckerberg GS, Barodka VM, Berkowitz DE, Frank SM (2016) 2,3-Diphosphoglycerate Concentrations in Autologous Salvaged Versus

Stored Red Blood Cells and in Surgical Patients After Transfusion. Anesth Analg 122: 616-623

Shibayama N, Saigo S (1995) Fixation of the quaternary structures of human adult haemoglobin by encapsulation in transparent porous silica gels. J Mol Biol 251: 203-209

Simons M, Gretton S, Silkstone GGA, Rajagopal BS, Allen-Baume V, Syrett N, Shaik T, Leiva-Eriksson N, Ronda L, Mozzarelli A, Strader MB, Alayash AI, Reeder BJ, Cooper CE (2018) Comparison of the oxidative reactivity of recombinant fetal and adult human hemoglobin: implications for the design of hemoglobin-based oxygen carriers. Bioscience reports 38

Smani Y (2008) Hemospan: a hemoglobin-based oxygen carrier for potential use as a blood substitute and for the potential treatment of critical limb ischemia. Curr Opin Investig Drugs 9: 1009-1019

Smith RC, Garbutt GJ, Isaacks RE, Harkness DR (1979) Oxygen binding of fetal and adult bovine hemoglobin in the presence of organic phosphates and uric acid riboside. Hemoglobin 3: 47-55

Stoller JK, Aboussouan LS (2004) alpha1-Antitrypsin deficiency . 5: intravenous augmentation therapy: current understanding. Thorax 59: 708-712

Sun J, Steenbergen C, Murphy E (2006) S-nitrosylation: NO-related redox signaling to protect against oxidative stress. Antioxidants & redox signaling 8: 1693-1705

Taggart C, Cervantes-Laurean D, Kim G, McElvaney NG, Wehr N, Moss J, Levine RL (2000) Oxidation of either methionine 351 or methionine 358 in alpha 1-antitrypsin causes loss of anti-neutrophil elastase activity. J Biol Chem 275: 27258-27265

Tsai AG, Vandegriff KD, Intaglietta M, Winslow RM (2003) Targeted O2 delivery by low-P50 hemoglobin: a new basis for O2 therapeutics.

American journal of physiology Heart and circulatory physiology 285: H1411-1419

Turner AM (2013) Alpha-1 antitrypsin deficiency: new developments in augmentation and other therapies. BioDrugs 27: 547-558

Vandegriff KD, Malavalli A, Wooldridge J, Lohman J, Winslow RM (2003) MP4, a new nonvasoactive PEG-Hb conjugate. Transfusion 43: 509-516

Varnado CL, Mollan TL, Birukou I, Smith BJZ, Henderson DP, Olson JS (2013) Development of recombinant hemoglobin-based oxygen carriers. Antioxid Redox Signal 18: 2314-2328

Venkatesan B, Mahimainathan L, Das F, Ghosh-Choudhury N, Ghosh Choudhury G (2007) Downregulation of catalase by reactive oxygen species via PI 3 kinase/Akt signaling in mesangial cells. Journal of cellular physiology 211: 457-467

Viappiani C, Bettati S, Bruno S, Ronda L, Abbruzzetti S, Mozzarelli A, Eaton WA (2004) New insights into allosteric mechanisms from trapping unstable protein conformations in silica gels. Proc Natl Acad Sci U S A 101: 14414-14419

Walker LM, York JL, Imam SZ, Ali SF, Muldrew KL, Mayeux PR (2001) Oxidative Stress and Reactive Nitrogen Species Generation during Renal Ischemia. Toxicological Sciences 63: 143-148

Wang Y, Wang L, Yu W, Gao D, You G, Li P, Zhang S, Zhang J, Hu T, Zhao L, Zhou H (2017) A PEGylated bovine hemoglobin as a potent hemoglobin-based oxygen carrier. Biotechnology progress 33: 252-260

Wang Z, Hilder TL, van der Drift K, Sloan J, Wee K (2013) Structural characterization of recombinant alpha-1-antitrypsin expressed in a human cell line. Anal Biochem 437: 20-28

Ward AM, White PA, Wild G (1985) Reference ranges for serum alpha 1 antitrypsin. Arch Dis Child 60: 261-262

Weber D, Davies MJ, Grune T (2015) Determination of protein carbonyls in plasma, cell extracts, tissue homogenates, isolated proteins: Focus on sample preparation and derivatization conditions. Redox biology 5: 367-380

Weber D, Milkovic L, Bennett SJ, Griffiths HR, Zarkovic N, Grune T (2013) Measurement of HNE-protein adducts in human plasma and serum by ELISA-Comparison of two primary antibodies. Redox biology 1: 226-233

Winslow RM (2004) MP4, a new nonvasoactive polyethylene glycol-hemoglobin conjugate. Artif Organs 28: 800-806

Winslow RM (2006) Current status of oxygen carriers ('blood substitutes'): 2006. Vox Sang 91: 102-110

Young MA, Riddez L, Kjellstrom BT, Bursell J, Winslow F, Lohman J, Winslow RM (2005) MalPEG-hemoglobin (MP4) improves hemodynamics, acid-base status, and survival after uncontrolled hemorrhage in anesthetized swine. Crit Care Med 33: 1794-1804

Zhang N, Jia Y, Chen G, Cabrales P, Palmer AF (2011) Biophysical properties and oxygenation potential of high-molecular-weight glutaraldehyde-polymerized human hemoglobins maintained in the tense and relaxed quaternary states. Tissue engineering Part A 17: 927-940

Zhou Y, Jia Y, Buehler PW, Chen G, Cabrales P, Palmer AF (2011) Synthesis, biophysical properties, and oxygenation potential of variable molecular weight glutaraldehyde-polymerized bovine hemoglobins with low and high oxygen affinity. Biotechnol Prog 27: 1172-1184